AEROSOL AND PRECIPITATION CHEMISTRY RELATIONSHIPS IN ARIZONA DURING THE MONSOON SEASON

by

David Humberto Lopez

A Thesis Submitted to the Faculty of the

DEPARTMENT OF CHEMICAL AND ENVIRONMENTAL ENGINEERING

In Partial Fulfillment of the Requirements

For the Degree of

MASTER OF SCIENCE
WITH A MAJOR IN CHEMICAL ENGINEERING

In the Graduate College

THE UNIVERSITY OF ARIZONA

2019

THE UNIVERSITY OF ARIZONA
GRADUATE COLLEGE

As members of the Master's Committee, we certify that we have read the thesis prepared by David Humberto Lopez, titled *Aerosol and Precipitation Chemistry Relationships in Arizona During the Monsoon Season* and recommend that it be accepted as fulfilling the dissertation requirement for the Master's Degree.

Committee Chair: Dr. Armin Sorooshian — Date: 5/8/2019

Committee Member: Dr. Heidi Mansour — Date: 5/8/2019

Committee Member: Dr. Jianqin Lu — Date: 5/8/2019

Final approval and acceptance of this thesis is contingent upon the candidate's submission of the final copies of the thesis to the Graduate College.

I hereby certify that I have read this thesis prepared under my direction and recommend that it be accepted as fulfilling the Master's requirement.

Date: 5/8/2019

Dr. Armin Sorooshian, Professor
Master's Thesis Committee Chair
Department of Chemical & Environmental Engineering

ACKNOWLEDGEMENTS

First, I would like to thank Dr. Armin Sorooshian for his extreme patience and guidance during my graduate career. I am grateful for your recommendations to help me fund my graduate career. Despite my weaknesses and hardships, you helped push me towards reaching my goals. I am in great debt and am extremely proud of having you as my advisor.

I would like to thank Dr. Jim Field and the National Science Foundation Bridge to the Doctorate program. I am grateful for Dr. Field's guidance during my Master's career and for the funding I received from the fellowship program. I will do my best to complete a PhD.

I would like to extend my deepest thanks to Dr. Heidi Mansour for her guidance, time, and recommendations during my graduate career. I appreciate the opportunities you gave me to enter the area of Pharmaceutical Sciences and my experience as a TA has led me to desire a position in academia.

I would like to thank Ting Chun (Leo) Chiu for helping me to write PYTHON programs to analyze the data. I have learned about the benefits of programming from you and hope to become a master as you are.

I would like to thank Dr. Tax and the IMSD program for funding my graduate career. I am very lucky to have received this fellowship and it has helped me greatly.

I would like to thank Dr. Srini Raghavan for accepting me as his future PhD student. I am ready to start a new chapter in my life.

I would like to express my upmost gratitude to Dr. Cham Kim from DGIST who has provided me invaluable research opportunities. You have helped re-gain motivation during the hardest of times.

I am thankful for the lectures and time given to me from professors from previous courses I took such as Dr. Roberto Guzman and Dr. Samuel Yalkowsky.

I am thankful for the support of my friends Seojin Park, Yenhsun Chang, Wen Xie, Monem Aldahif, Zhengjie Xu, Thomas Foss, Takeshi Miyauchi, and Jerry Gayin Chen.

Last but not least, I express my thanks to my beloved family, Gloria and David and brothers Christian and Diego. During my graduate career, I was supported by the greatest family. The emotional support, the warm delicious food, the time you all took to pick me up from school and drop me off… there are an infinite amount of things you have all done for me. I am a step closer to realizing my goals and hope to give back to you all soon.

DEDICATION

Dedicated to my mother (Gloria), father (David),
brothers (Christian and Diego), family,
friends, and my future

TABLE OF CONTENTS

TABLE OF CONTENTS- Continued

LIST OF FIGURES

LIST OF TABLES

LIST OF TABLES- Continued

DEFINITIONS/NOMENCLATURE

NAM- North American Monsoon
CCN- Cloud Condensation Nuclei
IN- Ice Nuclei
IMPROVE- Interagency Monitoring of Protected Visual Environments
NADP NTN- The National Atmospheric Deposition Program National Trends Network
HYSPLIT- Hybrid Single- Particle Lagrangian Integrated Trajectory Model
PM_{10} (MT)- particulate matter 10 micrometers or less in diameter
$PM_{2.5}$ (MF)- particulate matter 2.5 micrometers or less in diameter
Coarse Mass (CM)- particulate matter between 10 and 2.5 micrometers in diameter
Fine soil (SOILf)- calculated aerosol concentration used as dust tracer
Chir NM- Chiricahua National Monument
Organ Pipe NM- Organ Pipe National Monument
Petrified NP- Petrified National Park
Pet NP- Petrified National Park

$\mu g/m^3$- microgram per cubic meter, used for aerosol concentrations
Ca, Aerosol Ca- Calcium aerosol concentration
Mg, Aerosol Mg- Magnesium aerosol concentration
K, Aerosol K-Potassium aerosol concentration
Na, Aerosol Na- Sodium aerosol concentration
Cl^-, Aerosol Cl - Chloride aerosol concentration
SO_4^{2-}, Aerosol SO_4- Sulfate aerosol concentration
NO_3^-, Aerosol NO_3- Nitrate aerosol concentration

mg/L- milligrams per liter, used for rain concentrations
$\mu S/cm$- microsiemens per centimeter, used for rain conductivity
mm- millimeters, used for rain accumulation
Ca^{2+}, Rain Ca - Calcium rain concentration
Mg^{2+}, Rain Mg- Magnesium rain concentration
K^+, Rain K- Potassium rain concentration
Na^+, Rain Na- Sodium rain concentration
Cl^-, Rain Cl- Chloride rain concentration
SO_4^{2-}, Rain SO_4- Sulfate rain concentration
NO_3^-, Rain NO_3- Nitrate rain concentration

Ca frac, Aerosol Ca frac- Calcium aerosol mass fraction
Mg frac, Aerosol Mg frac- Magnesium aerosol mass fraction
K frac, Aerosol K frac- Potassium aerosol mass fraction
Na frac, Aerosol Na frac- Sodium aerosol mass fraction
Cl frac, Aerosol Cl frac- Chloride aerosol mass fraction
SO_4 frac, Aerosol SO_4 frac- Sulfate aerosol mass fraction
NO_3 frac, Aerosol NO_3 frac- Nitrate aerosol mass fraction

Rain Ca frac- Calcium rain mass fraction

DEFINITIONS/NOMENCLATURE- Continued

Rain Mg frac- Magnesium rain mass fraction
Rain K frac- Potassium rain mass fraction
Rain Na frac- Sodium rain mass fraction
Rain Cl frac- Chloride rain mass fraction
Rain SO_4 frac- Sulfate rain mass fraction
Rain NO_3 frac- Nitrate rain mass fraction

Ca-moles- moles of Calcium in rain
Mg-moles- moles of Magnesium in rain
K-moles- moles of Potassium in rain
Na-moles- moles of Sodium in rain
Cl-moles- moles of Chloride in rain
SO_4- moles- moles of Sulfate in rain
NO_3- moles- moles of Nitrate in rain

Abstract

This study identified the relationships between aerosol and precipitation chemistry during the monsoon season (June 15- September 15) in Arizona by using four co-located IMPROVE and NADP NTN sites: Chiricahua National Monument (Chir NM), Grand Canyon, Organ Pipe National Monument (Organ Pipe NM), and Petrified National Park (Petrified NP). Relationships between 1999 and 2014 were determined by using the using a two-tailed student's t-test (95% confidence).

In Chir NM and Grand Canyon, decreasing significant annual trends of sulfate aerosol fractions coincided with increasing significant annual trends of rain pH. This result suggests that in Chir NM and Grand Canyon, the decrease in sulfate aerosol concentrations result in more alkaline pH. Aerosol and rain interrelationships in all sites showed that calcium (Ca), magnesium (Mg), and potassium (K) were highly related to each other suggesting their origin from common dust sources. Similarly based on these interrelationships, sodium (Na) and chloride (Cl^-) were related to sea salt in all sites. At all sites, the highest correlation values between aerosol and precipitation concentration correlations were found for Ca, K, Mg, and Na (in decreasing order), suggesting the role of dust and sea salt as cloud condensation nuclei (CCN) or ice nuclei (IN).

The highest grand average of rain accumulation was found in Chir NM and this coincided with the most acidic pH and lowest rain concentrations. In Chir NM, the highest mass fractions and amount of moles in rain of Sulfate and Nitrate were found which justify the acidic pH. The opposite trends are found in Petrified NP, which has the lowest grand annual average of rain accumulation, most alkaline pH, highest rain concentrations, and lowest mass fractions and moles in rain of nitrate and sulfate. The use of rain concentrations are misleading due to the dilution of rain which does not provide information on the absolute amount and abundance of certain ions. Hence it is necessary to

analyze the amount of moles and mass fractions in rain of acidic anions to determine the effect on rain pH.

At all sites, the significant correlations between rain accumulation and aerosol and rain concentrations were negative, suggesting that the monsoon rain acts as a sink. However, the significant correlations between rain accumulation and amount of moles in rain were positive for all species in all sites. The positive relationships are justified by the uptake of aerosol concentrations by rain by cloud seeding and scavenging. Of these relationships, sulfate and nitrate exhibited the highest correlated values (r-values) where sulfate and nitrate gaseous precursors are capable of directly entering rain drops.

Inverse relationships between air and rain mass fractions of nitrate were found with respect to pH where nitrate was more alkaline in the air and more acidic in the rain. The result suggests that in the air, precursor forms of nitrate which can react with dust emissions are found, and the product of this reaction (highly water soluble) serves as cloud condensation nuclei where the presence of nitrate in rain is acidic. In addition, the slope of the correlation value for air or rain mass fraction can be used as a proxy to determine whether it is acidic or alkaline. Acidic mass fractions would exhibit positive values with respect to sulfate air mass fractions and rain accumulation and negative values for all other aerosol and precipitation data.

To determine the effects of moisture source on aerosol and precipitation chemistry, it was necessary to choose one site that had sources of moisture from the Gulf of California and compare this to another site that had moisture sources from the Gulf of Mexico. The Kruskal Wallis test was applied to aerosol concentrations to determine if sites shared similar air mass sources. The results of this test indicate that Chir NM, Grand Canyon, and Petrified NP share similar air mass sources while Organ Pipe NM did not share any similarities. Next, based on these results and previous studies, Chir NM and Organ Pipe NM were chosen to determine the effects of air mass source on the aerosol and

precipitation chemistry. Air mass back trajectories revealed that Chir NM and Organ Pipe NM shared similar moisture sources from the Gulf of California and few dates were found where they differed. Future work will seek to compare sites in western Arizona (Organ Pipe NM) to other co-located NADP and IMPROVE sites in New Mexico.

The results of this work suggest that the reactions between dust and precursors of nitrate and sulfate are commonly found in Arizona. During the monsoon period, higher rain accumulation is observed which uptakes more dust containing acidic ions and acidic precursor gases via scavenging, resulting in increasingly acidic rain pH. Therefore, the aquatic and terrestrial ecosystems found in the area are exposed to acidic rain during the monsoon season. However, in 1999 to 2014, the reduction of sulfate aerosol concentrations due to air regulations has possibly led to an increase in alkalinity of rain pH.

1. Introduction

The North American Monsoon (NAM) impacts the southwestern United States, in particular Arizona, in significant ways owing to the importance of precipitation in this semi-arid region (Adams and Comrie 1997; Higgins et al., 1997; Barlow et al., 1998; Sheppard et al., 2002; Leung et al., 2003; Vera et al., 2006). The NAM provides a range of 50-70% of annual rainfall in Southern Arizona (Douglas et al., 1993; Adams and Comrie 1997; Higgins et al., 1997; Gochis et al., 2002; Jana et al., 2018). Previous studies have projected that this region will become more arid over time, which highlights the importance of precipitation associated with the NAM (Seager et al., 2007; Westerling et al., 2008; Cayan et al., 2010; Dennison et al., 2014; Raman et al., 2014). A consequence of increasingly dry conditions in this region is more wind-blown dust in the air, which impacts air quality, public health, and clouds owing to the role of dust particles serving as both cloud condensation nuclei (CCN) and ice nuclei (IN) (Heintzenberg et al., 1996; Rosenfeld and Givati,

2006; Koehler et al., 2007; Sorooshian et al., 2013). Dust particles are sufficiently large that they can serve as IN and CCN regardless of whether they are hygroscopic or not; furthermore, dust can be coated with soluble species (e.g., sulfate, nitrate) which increases the ability of dust as CCN (Levin et al., 1996; Perry et al., 2004; Fan et al., 2004; Twohy et al., 2009) and IN (Isono and Ikebe, 1960; Kumai, 1961; Demott et al., 2003; Van den Heever et al., 2006; Koehler et al., 2007; Zimmerman et al., 2008; Wiacek et al., 2010).

The NAM has been reported to serve as a major sink that dilutes aerosol concentrations (Sorooshian et al., 2011; Youn et al., 2013; Crosbie et al., 2015). This can be explained by the interaction of aerosols and precipitation via wet scavenging and uptake of aerosols due to the role of CCN and IN (Sorooshian et al., 2011; Dadashazar et al., 2019). Previous studies confirmed that in regions of Arizona that contain mine tailings and high metal concentrations in dust, there are trace metals within the rainwater (Sorooshian et al., 2013). Not only is the composition of precipitation affected by the aerosol concentration found within the region but also by the history and trajectory of air mass (Hutchings et al., 2009). The ability of aerosols in affecting NAM precipitation through direct and indirect effects have been observed (Zhao et al., 2012; Sorooshian et al., 2013; Crosbie et al., 2015). The interaction between airborne aerosol particles, such as dust, and clouds is considered to be the largest uncertainty in estimates of global anthropogenic radiative forcing (IPCC, 2013). The uncertainties are especially high for deep convective clouds associated with NAM precipitation owing to the scarcity of in situ observations to advance knowledge of aerosol-cloud interactions in such systems.

It is important to determine the composition and acidity of rain water because of its potential effects on land and water ecosystems (Fenn et al., 1998; Baron et al., 2000; Wolfe et al., 2003; Neff et al., 2008). In Arizona, various acids such as nitrate and sulfate have been shown to react with dust emissions which can serve as CCN, resulting in potential acidification of precipitation (Matsuki et al.,

2010; Sorooshian et al., 2013). In addition, deposition of components such as mineral dust can provide nutrients (such as phosphorus) that benefit various ecosystems (Eger et al., 2013; Aciego et al., 2017). On the other hand, wet dust deposition can also transport trace metals that can act as toxic pollutants (Csavina et al., 2012). Therefore, in an area characterized by high dust emissions, it is important to examine the interrelationships between the chemistry of aerosol particles and precipitation in Arizona.

Two previous studies examined sources of pollution impacting precipitation in the southwestern United States. Hutchings et al. (2009) reported that the dust from windblown soils in northern Arizona could be found in cloud water, since they can serve as CCN and IN. Sorooshian et al. (2013) observed the same finding for Arizona and suggested that acidic gases react and partition to crustal particles or drops containing crustal constituents. Precipitation chemistry in the region is not only altered by the aerosols found in the region, but also the history and source of the air masses that provide moisture in the region (Ponette-Gonzalez et al., 2018; Jana et al., 2018). A long-term aerosol-precipitation study that focuses on the NAM which also incorporates the analysis of air pathways has not been done in this region before.

The goal of this study is to identify the relationships of aerosol and precipitation chemistry as functions of time, location, and rain accumulation during the monsoon season in Arizona from 1999 to 2014. This study is done by using statistical correlations between long-term aerosol and precipitation data as done in previous studies (Sorooshian et al., 2013; Dadashazar et al., 2019). The following questions are addressed: (i) how do aerosol and precipitation chemistry vary with respect to time and site-location?; (ii) how do aerosol and precipitation chemistry relationships vary as a function of time and site-location; (iii) how do the results in (i) and (ii) change with respect to rain accumulation?; and (iv) how does the source of air affect the aerosol and precipitation chemistry relationships?

2. Experimental Methods

The range of dates for the NAM are defined in this study between June 15 to September 15. Although the National Weather Service (NWS) defines the NAM between June 15 to September 30 (https://www.weather.gov/psr/MonsoonAwarenessWeek), Adams and Comrie (1997) state that the precipitation lasts until mid-September. Therefore, the chosen dates are from using a combination of the NWS and the Adams and Comrie (1997) definitions.

2.1 Aerosol Data

Aerosol composition is provided by the United States Environmental Protection Agency's (US EPA) Interagency Monitoring of Protected Visual Environments (IMPROVE) network, where the stations that are located in remote areas such as national parks have aerosol filter samples collected every third day for a 24 h duration. Aerosol composition data contains ions, trace metals, carbonaceous compounds such as organic carbon (OC) and elemental carbon (EC) in the fine aerosol mode ($PM_{2.5}$). PM_{10} is defined as particulate matter 10 micrometers or less in diameter and coarse mass is defined as the difference between PM_{10} and $PM_{2.5}$.

Additional information on sampling methods can be found in other references (Solomon et al., 2014; Chow et al., 2015). Fine soil concentrations used this study are calculated using the following equation (Malm et al., 1994):

$$\text{Fine Soil } (\mu g\ m^{-3}) = 2.2[Al] + 2.49[Si] + 1.63[Ca] + 2.42[Fe] + 1.94[Ti] \quad (1)$$

In this study, four IMPROVE stations that are co-located with NADP stations within Arizona are used (Figure 1) and the time range selected for the data is June 15 to September 15 with data ranging from 1999 until 2014 (Table 1).

Table 1. Summary of co-located IMPROVE and NADP sites and date ranges over which data are analyzed. Altitudes are above sea level.

Site Name	Latitude (°)	Longitude (°)	Altitude (m)	Date Range
Chiricahua (IMPROVE)	32.0994	-109.389	1554	June 15, 1999–September 15, 2014
Chiricahua (NADP)	32.0097	-109.389	1570	
Grand Canyon (IMPROVE)	35.9731	-111.9841	2267	June 15, 1999–September 15, 2014
Grand Canyon (NADP)	36.0586	-112.184	2071	
Organ Pipe (IMPROVE)	31.951	-112.802	504	June 15, 2003–September 15, 2014
Organ Pipe Cactus NM(NADP)	31.9492	-112.802	501	
Petrified National Park (IMPROVE)	35.0777	-109.7692	1766	June 15, 2003–September 15, 2014
Petrified National Park (NADP)	34.8224	-109.8925	1707	

2.2. Precipitation Data

The National Atmospheric Deposition Program (NADP) National Trends Network (NTN) (http://nadp.slh.wisc.edu) began in 1978 to monitor the effects of wet deposition on different ecosystems (Lamb and Bowersox, 2000; NADP, 2012a; NADP, 2012b; NADP, 2013; NADP, 2017). Rain gauges are used by NADP to report precipitation amounts on a weekly basis (Tuesday-

Tuesday). This is done by using an automated AeroChem Metrics Model A-31 wet-only collector that opens when rain falls and closes when rain ends. Next, operators determine the sample volume and use a volume basis of 1 L to decant the rainwater. The samples are then sent to the Central Analytical Laboratory (CAL) at the Illinois State Water Survey (ISWS) for chemical analysis. A quality assurance program is used in the dataset (NADP, 2014).

The four stations of interest in this work (Table 1 and Figure 1) report precipitation values (PptRec) once a week, as well as pH, conductivity, and concentrations of ions: calcium (Ca^{2+}), chloride (Cl^{-}), magnesium (Mg^{2+}), nitrate (NO_3^{-}), potassium (K^{+}), sodium (Na^{+}), and sulfate (SO_4^{2-}). In 2012, method detection limits (mg/L) were 0.005 for Ca^{2+}, 0.009 for Cl^{-}, 0.002 for Mg^{2+}, 0.010 for NO_3^{-}, 0.003 for K^{+}, 0.002 for Na^{+}, and 0.010 for SO_4^{2-} (NADP, 2012 c).

Data used for the trend analysis in future sections contains rain accumulation values that are non-negative, non-zero, non-blank, and non-default (i.e., 0.127 for trace values). The NADP parameter sub ppt is used for rain accumulation values, which in most cases is equal to the rain gage reading (ppt rec). For the dates with missing or invalid rain gage data, the sub ppt parameter is calculated by converting the volume of the sample in the bucket (area of 678.9 cm^2) to depth (http://nadp.slh.wisc.edu/documentation/notes-wk.html).

2.3. Air Mass Trajectory Analysis

The National Oceanic and Atmospheric Administration (NOAA) Air Resources Laboratory's (ARL) Hybrid Single- Particle Lagrangian Integrated Trajectory (HYSPLIT) model (accessed via https://www.ready.noaa.gov/HYSPLIT.php) was used for identifying air mass source origins and transport pathways (Draxler and Hess, 1997, 1998; Draxler et al., 2014; Stein et al., 2015). The model vertical velocity option was chosen for a level height of 500 m above ground level, which has been used in previous studies (Jana et al., 2018; Dadashazar et al., 2019). Trajectories were obtained

every 6 h for 168 total h using the National Centers for Environmental Prediction/National Center for Atmospheric Research (NCEP/NCAR) reanalysis data with the "model vertical velocity" method (Dadashazar et al.,2019).

3. Study Region and NAM and Sources of Moisture

3.1. Study Region

Figure 1: This map (made from Scribblemaps) shows the North American Monsoon (NAM) region, including the state of Arizona. The red markers indicate the site locations used within this study and are numbered as follows: 1. Chiricahua National Monument (NM), 2. Grand Canyon, 3. Organ Pipe National Monument (NM), 4. Petrified National Park (NP). The green circles indicate potential sources of moisture for the NAM region and are numbered as follows: 1. Northern Pacific Ocean, 2. Southern Pacific Ocean, 3. Gulf of California, 4. Gulf of Mexico.

Arizona is located in the southwestern United States (Figure 1), an area reported to have the highest dust concentrations in the entire country (Malm et al., 2004). Dust emissions can be

transported from distant areas (Lopez et al., 2016) and promoted locally by disruption of soils by human activity. In recent years, Arizona has experienced rapid population growth which results in major land use changes and aerosol emissions by agricultural activity, vehicles, construction, grazing, and mining operations (Schlesinger et al., 1990; Neff et al., 2005; Fernandez et al., 2008; Woodhouse et al., 2010; Cayan et al., 2010; Field et al., 2010; Csavina et al., 2012). Other local aerosol emissions include mine tailings which can contain high metal concentrations in dust aerosol particles (Malm and Sisler, 2000; Csavina et al., 2012, Prabhakar et al., 2014; Taylor et al., 2014; Dong et al., 2015; Youn et al., 2016). Arizona also contains one of the top five most polluted (based on particulate matter) cities (Phoenix, Arizona) in the country (Raman et al., 2016; American Lung Association). Figure 2 provides a summary of the various aerosol sources within Arizona.

Studies project that by the end of the 21st century, arid regions, including the state of Arizona, will experience increasingly warmer temperatures resulting in extreme drought conditions (Seager et al., 2007; Cayan et al., 2010). Changing to drier climate not only promotes higher dust emissions and wildfires but also shortens the duration of snow cover and melt (Harpold et al., 2012) since dust emissions (Neff et el., 2008; Field et al., 2010) affect snowpack behavior (Painter et al., 2007; Neff et al., 2008). Therefore, Arizona is experiencing rapid population growth, land use change, drought, and variability in precipitation and water availability (Woodhouse et al., 2010; Cayan et al., 2010; Seager and Vecchi, 2010), which all serve to highlight the importance of conducting aerosol studies within the region.

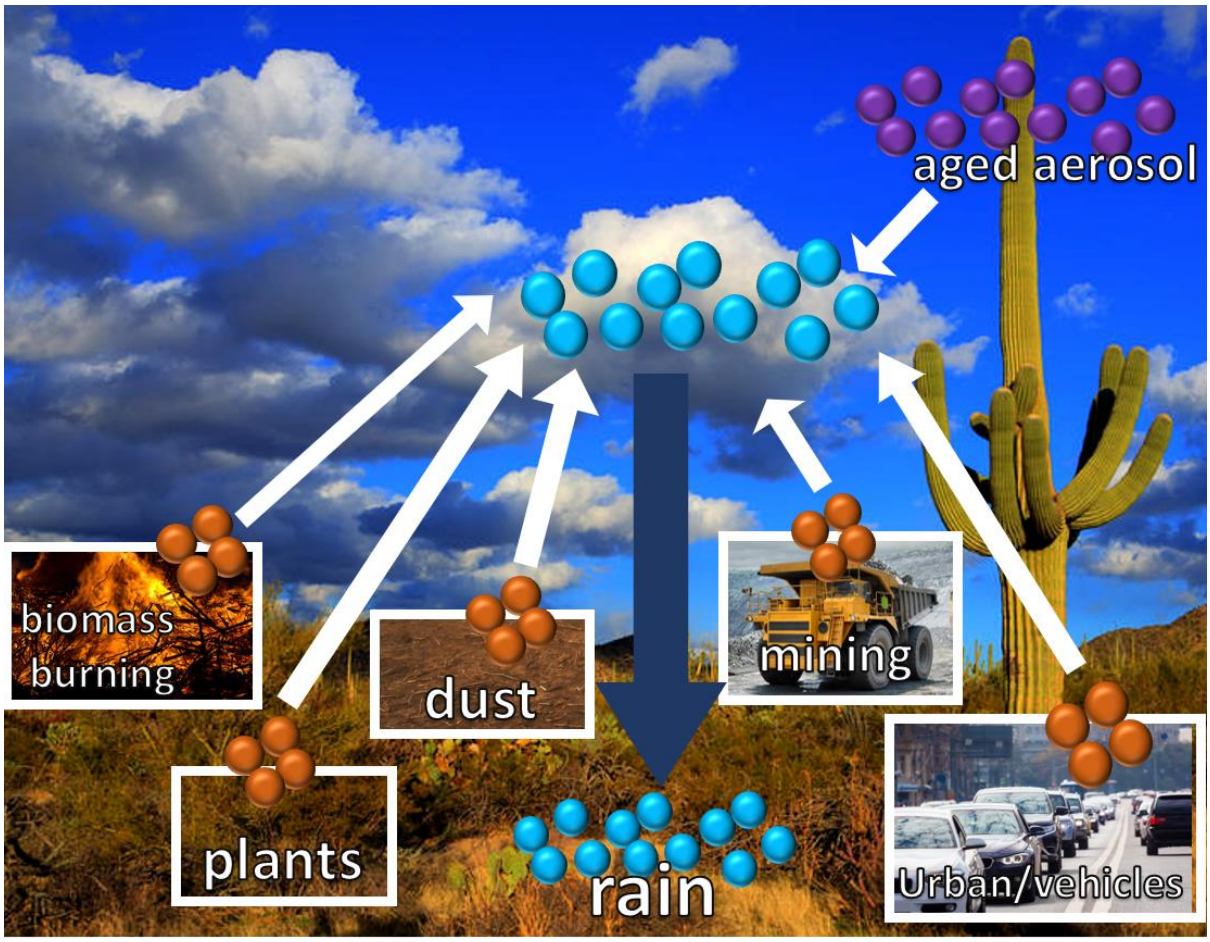

Figure 2: Schematic showing the various sources of aerosol for the sites within Arizona that can affect clouds and rainfall by serving as CCN and IN. Aged aerosol includes long range transported aerosol.

3.2. Site Descriptions

Chiricahua National Monument has Tucson as the closest major city (~150 km to the west). Major sources of pollution can come from the Wilcox playa and the Apache Power Plant, both being 45 km to the west. In comparison to the other sites within this study, Chiricahua contains the most dust sources. These dust sources include the Chihuahuan Desert and arid areas near Northern Mexico, New Mexico, and Texas. Copper smelter emissions also exist from the towns of Cananea and Nacozari (Mexican towns 140 and 180 km south of Chiricahua, respectively). Grand Canyon is

located in Northern Arizona and is removed from neighboring anthropogenic emissions. The nearest towns are Flagstaff (~133 km south with US census population ~66,145) and Tuba City (~92 km east with US 2010 census population ~8611). Organ Pipe National Monument is the southern-most site in this study, which is closest to the U.S.-Mexico border. Major sources of aerosol pollution include the town of Sonoita, Mexico (~10 km Southwest with ~10,000 population). The site is the closest to marine influences than other sites within this study. Petrified National park is located in the mid-east area of Arizona about 80 km west of the New Mexican border. The nearest town is Holbrook (42 km Southwest with US 2010 census population~5,053).

3.3. North American Monsoon (NAM) and Sources of Moisture

The NAM has been defined by previous studies to include northwestern Mexico and southwestern United States (Figure 1), including Arizona (Raman et al., 2016). The NAM radically shifts the area from dry to very humid conditions where the highest precipitation is observed in July and August (Adams and Comrie, 1997). The NAM is characterized by high ambient and soil temperatures and relative humidity especially in July and August (Sorooshian et al., 2011). This combination of meteorological conditions in addition to high influxes of moisture results in increased vegetation growth and increased photochemical reactions which result in enhanced emissions of secondary organic aerosol (SOA) and biogenic volatile organic compounds (BVOCs) (Guenther et al., 1993; Diem, 2000; Diem and Comrie, 2000; Sorooshian et al., 2011; Youn et al., 2013). In addition, high dust emissions can be observed due to accelerated wind gusts (Leinen and Sarnthein, 1989).

The source of moisture of the NAM has been intensely studied and debated. The general consensus is that the source of moisture is dependent on the altitude of the air parcel. At high altitudes above 800 hpa, moisture is transported mainly from the Gulf of Mexico (Figure 1- green

circle 4) and at lower altitudes, the moisture originates from the Gulf of California (Figure 1- green circle 3) (Adams and Comrie, 1997, Higgins et al., 1997; Dominguez et al., 2008). In addition, there can be streams of moisture originating from the northern and southern Pacific Ocean (Figure 1- green circles 1 and 2, respectively) (Jana et al., 2018; Ordoñez et al., 2019). There have been reports that the moisture from both sources mix over the Sierra Madre Occidental in Mexico before reaching the US. In early July, the monsoon anticyclone begins at the jet stream level (Carleton, 1986; Carleton et al., 1990; Erfani and Mitchell, 2014; Higgins et al., 1998, 1999; Okabe, 1995) and is followed by a high moisture influx and reversal of winds from the Gulf of California (Stensrud et al., 1997; Douglas and Leal, 2003; Adams & Stensrud, 2007; Mejia et al., 2010;). Additional streams of moisture can come from nocturnal low-level jets (Douglas, 1995; Douglas et al., 1998; Anderson et al., 2001). The origin of the source of moisture of the NAM is further complicated by a recycling process of moisture that can account for up to 13 % of the total NAM moisture (Jana et al., 2018). Convective winds, complex surges of moisture, tropical cyclones, and a vegetation-rainfall feedback causes the prediction of moisture pathways, monsoon rain and its effects to be difficult (Adams and Comrie, 1997; Dominguez et al., 2008; Jana et al., 2018).

In this study, several sites are used within the state of Arizona (Table 1 and Figure 1) and studies by Gimeno et al. (2012) and Jana et al. (2018) confirm that in eastern Arizona, (potentially in Chiricahua NM and Petrified NP), the sources of moisture originate from both the Gulf of Mexico (Figure 1- green circle 4) and Gulf of California (Figure 1-green circle 3) while in western Arizona (potentially in Organ Pipe NM), the main sources are from the Gulf of California (Figure 1- green circle 3) and Pacific Ocean (Figure 1-green circles 1 and 2).

4. Results

4.1 Yearly Profiles During the Monsoon

4.1.1 Grand Annual Mean During the Monsoon

The grand annual mean of aerosol and precipitation data for each site (Table 1) was calculated by finding the mean of the annual averages during the monsoon. Aerosol mass fractions were calculated to provide information about the abundance of the selected species. PM_{10} is defined as particulate matter 10 micrometers or less in diameter and $PM_{2.5}$ is defined as particulate matter 2.5 micrometers or less in diameter. Coarse mass is defined as the difference between PM_{10} and $PM_{2.5}$. The NADP parameter sub ppt was used for rain accumulation (in mm) because there was more data available for this parameter than for the rain gauge (ppt rec) data.

Organ Pipe exhibited the highest grand annual mean of coarse mass, PM_{10}, $PM_{2.5}$, fine soil, and all aerosol concentrations (Figures 3, 4, 5) examined (Ca, Cl^-, Mg, K, Na, SO_4^{2-}, NO_3^-) as compared to the other sites. These trends are most likely observed because Organ Pipe is the lowest station (~500 m above sea level) and is closer to dust and marine sources. These results are consistent with those found in Sorooshian et al. (2013). The lowest grand annual mean of coarse mass, PM_{10}, $PM_{2.5}$, fine soil, and all aerosol concentrations except Cl^- were found in the Grand Canyon (Figures 3, 4, 5), which is located at the highest altitude (2267 m above sea level) and is the farthest removed site from anthropogenic and marine sources.

The site with the highest grand annual mean of precipitation amount (18.82 mm) was Chiricahua (Figure 6). This was coincident with the site having the most acidic rain (Figure 7, pH = 5.39) and lowest rain concentrations (Figures 8 and 9) of Ca^{2+}, Cl^-, Mg^{2+}, NO_3^-, and Na^+. The opposite case is observed in Petrified NP, the site with the lowest grand annual average of precipitation amount (Figure 6, 10.17 mm). This site had the most alkaline rain pH (Figure 7, 5.92) including the highest rain concentrations (Figures 8 and 9) of Ca^{2+}, NO_3^-, K^+, and SO_4^{2-}. Despite Petrified NP having the highest rain concentrations (Figure 9) of NO_3^- and SO_4^{2-}, which are known to be acidic, the pH there is the most alkaline. The alkaline pH can be justified by the high rain fraction of Ca^{2+} found in

Petrified NP (Figure 10), which can reduce acidity. Hence, an inverse relationship between rain amount and rain concentrations and pH is found where more rainfall in the site caused greater dilution of species concentrations resulting in a more acidic pH and vice versa. Similar observations are also found in Dadashazar et al. (2019).

Chiricahua was the site with the lowest averaged aerosol mass fractions (Figures 12 and 13) of Ca, K, Cl^-, NO_3^-, Mg, and Na (except SO_4^{2-}). These results indicate that Chiricahua contained the lowest abundance of the listed aerosol components. In addition, Chiricahua had the lowest averaged rain fractions (Figures 10 and 11) of Ca^{2+}, Cl^-, Mg^{2+}, and Na^+. When comparing the trends in aerosol and rain fractions in Chiricahua, a relationship between aerosol and rain data can exist. Also, Chiricahua had the highest averaged precipitation amount (Figure 6) and lowest abundance of all aerosol mass fractions (except SO_4) (Figures 12 and 13). These preliminary results serve to justify the reason to perform statistical correlations between aerosol and precipitation chemistry in subsequent sections.

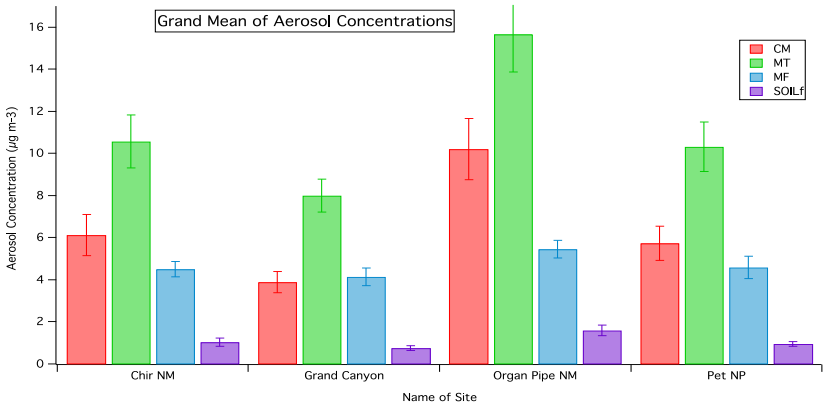

Figure 3: This bar graph exhibits the grand annual mean of coarse mass (CM), PM_{10} (MT), $PM_{2.5}$ (MF), and fine soil (SOILf) concentrations during the monsoon in $\mu g/m^3$ for Chiricahua National Monument (Chir NM), Grand Canyon, Organ Pipe National Monument (Organ Pipe NM), and Petrified National Park (Pet NP). Error bars were calculated by standard error of mean.

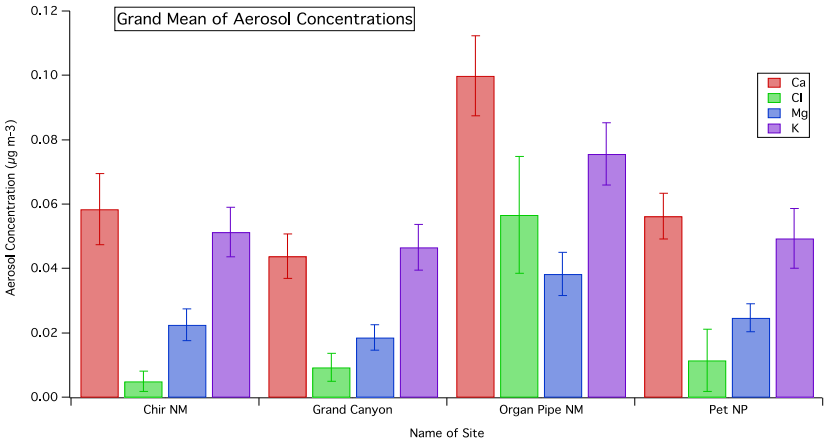

Figure 4: This bar graph exhibits the grand annual mean of calcium (Ca), chloride (Cl), magnesium (Mg), and potassium (K) aerosol concentrations during the monsoon in µg/m^3 for Chiricahua National Monument (Chir NM), Grand Canyon, Organ Pipe National Monument (Organ Pipe NM), and Petrified National Park (Pet NP). Error bars were calculated by standard error of mean.

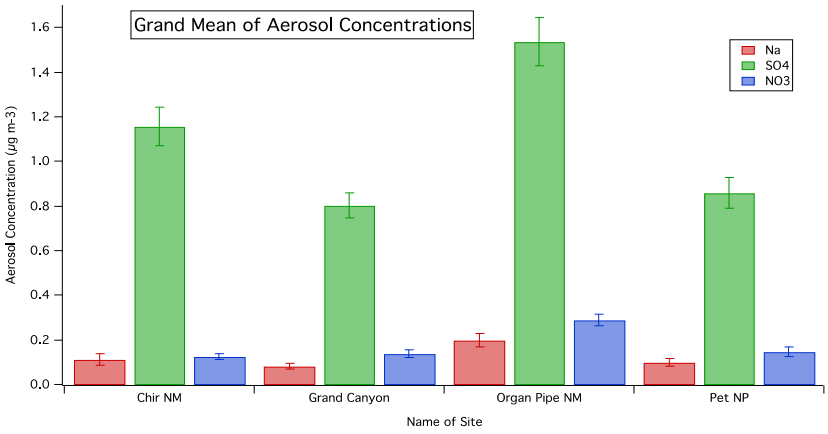

Figure 5: This bar graph exhibits the grand annual mean of sodium (Na), sulfate (SO4), and nitrate (NO3) aerosol concentrations during the monsoon in µg/m^3 for Chiricahua National Monument (Chir NM), Grand Canyon, Organ Pipe National Monument (Organ Pipe NM), and Petrified National Park (Pet NP). Error bars were calculated by standard error of mean.

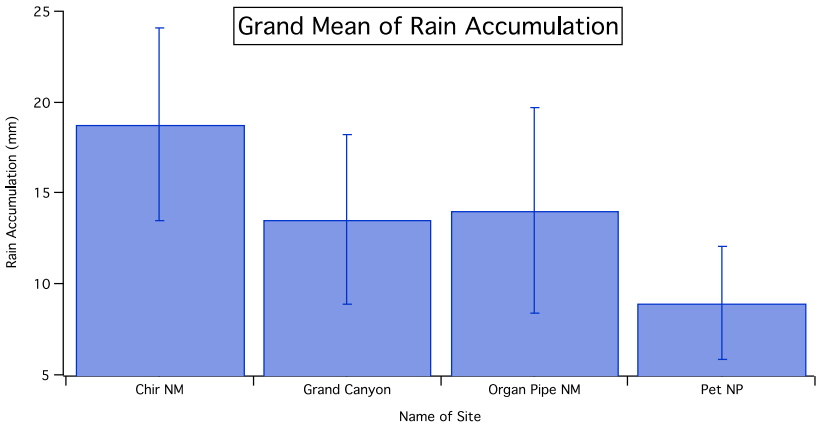

Figure 6: This bar graph exhibits the grand annual mean of rain accumulation during the monsoon in mm for Chiricahua National Monument (Chir NM), Grand Canyon, Organ Pipe National Monument (Organ Pipe NM), and Petrified National Park (Pet NP). Error bars were calculated by standard error of mean.

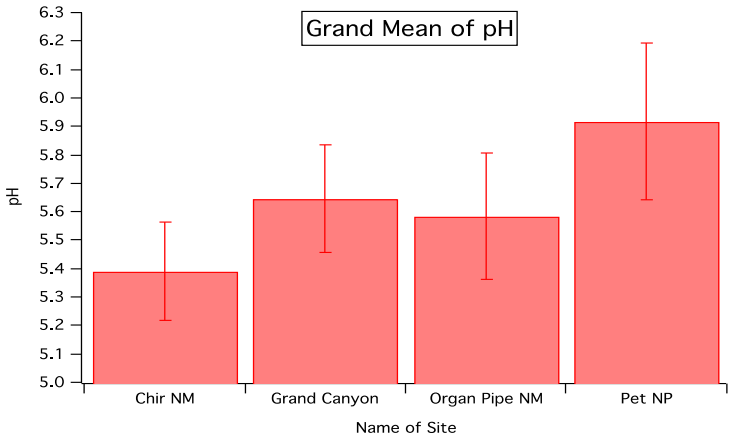

Figure 7: This bar graph exhibits the grand annual mean of rain pH during the monsoon for Chiricahua National Monument (Chir NM), Grand Canyon, Organ Pipe National Monument (Organ Pipe NM), and Petrified National Park (Pet NP). Error bars were calculated by standard error of mean.

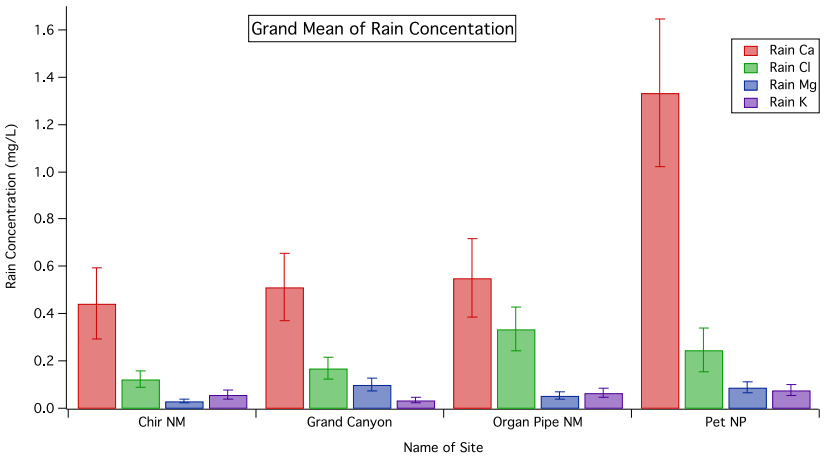

Figure 8: This bar graph exhibits the grand annual mean of rain concentrations of calcium (Rain Ca), chloride (Rain Cl), magnesium (Rain Mg), and potassium (Rain K) during the monsoon in mg/L for Chiricahua National Monument (Chir NM), Grand Canyon, Organ Pipe National Monument (Organ Pipe NM), and Petrified National Park (Pet NP). Error bars were calculated by standard error of mean.

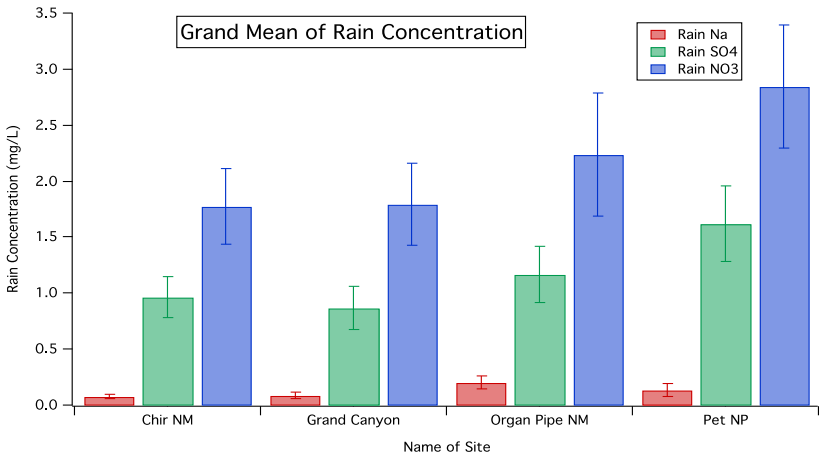

Figure 9: This bar graph exhibits the grand annual mean of rain concentrations of sodium (Rain Na), sulfate (Rain SO4), and nitrate (Rain NO3) during the monsoon in mg/L for Chiricahua National Monument (Chir NM), Grand Canyon, Organ Pipe National Monument (Organ Pipe NM), and Petrified National Park (Pet NP). Error bars were calculated by standard error of mean.

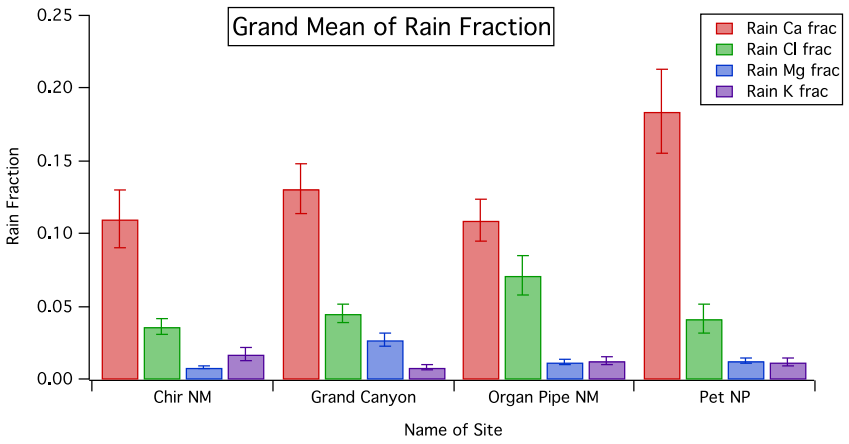

Figure 10: This bar graph exhibits the grand annual mean of rain fractions of calcium (Rain Ca frac), chloride (Rain Cl frac), magnesium (Rain Mg frac), and potassium (Rain K frac) during the monsoon for Chiricahua National Monument (Chir NM), Grand Canyon, Organ Pipe National Monument (Organ Pipe NM), and Petrified National Park (Pet NP). Error bars were calculated by standard error of mean.

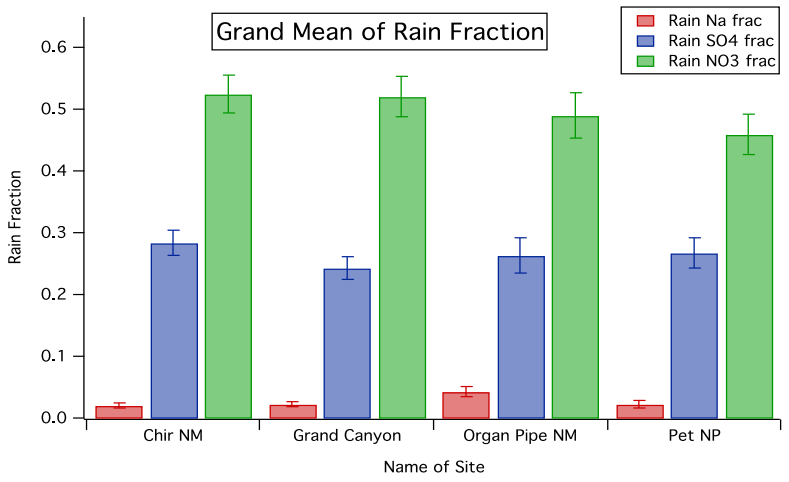

Figure 11: This bar graph exhibits the grand annual mean of rain fractions of sodium (Rain Na frac), sulfate (Rain SO4 frac), and nitrate (Rain NO3 frac) during the monsoon for Chiricahua National Monument (Chir NM), Grand Canyon, Organ Pipe National Monument (Organ Pipe NM), and Petrified National Park (Pet NP). Error bars were calculated by standard error of mean.

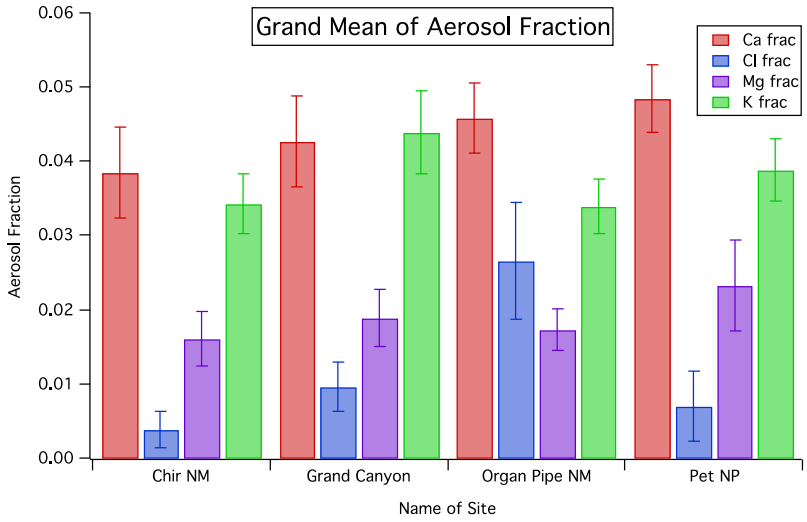

Figure 12: This bar graph exhibits the grand annual mean of aerosol fractions of calcium (Ca frac), chloride (Cl frac), magnesium (Mg frac) and potassium (K frac) during the monsoon for Chiricahua National Monument (Chir NM), Grand Canyon, Organ Pipe National Monument (Organ Pipe NM), and Petrified National Park (Pet NP). Error bars were calculated by standard error of mean.

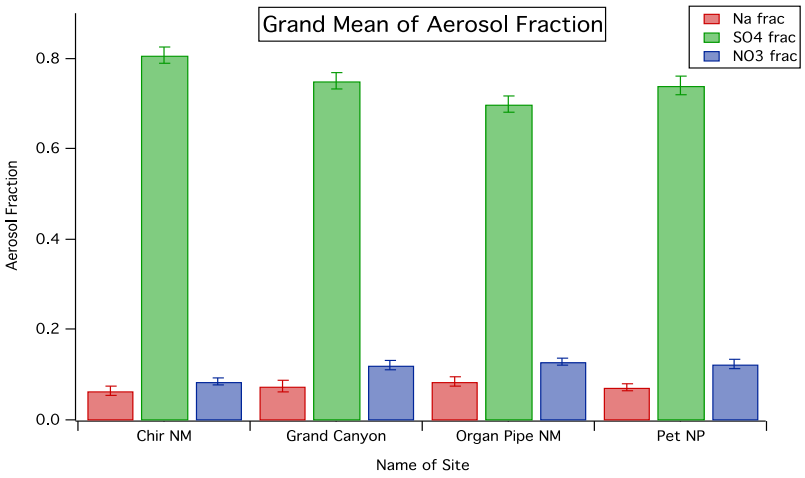

Figure 13: This bar graph exhibits the grand annual mean of aerosol fractions of sodium (Na frac), sulfate (SO4 frac), and nitrate (NO3 frac) during the monsoon for Chiricahua National Monument (Chir NM), Grand Canyon, Organ Pipe National Monument (Organ Pipe NM), and Petrified National Park (Pet NP). Error bars were calculated by standard error of mean.

4.1.2 Annual Averages During the Monsoon

In Chiricahua, 2003 was the year with the highest coarse mass, PM_{10}, $PM_{2.5}$, fine soil, and Ca, K, and Na annually averaged aerosol concentrations. Ca, K, and Na were most abundant (highest aerosol mass fractions) in 2003. Interestingly, 2003 was also the year with lowest annual precipitation amount (6.32 mm), highest yearly averaged annual conductivity (17.84 µS/cm) and highest yearly averaged rain concentrations of Ca^{2+}, Mg^{2+}, NO_3^-, and SO_4^{2-} in Chiricahua. In 2006, the highest yearly averaged precipitation amount (30.03 mm) is observed in Chiricahua, which results in high yearly averaged acidic rain pH (5.08) and the lowest yearly averaged rain concentrations of Ca^{2+}, Mg^{2+}, K^+, and Na^+, and SO_4^{2-}. The results show a relationship between concentrations of dust tracers and rain pH, where dust tracers have been noted to neutralize acid (Sorooshian et al., 2013). The lowest coarse mass, PM_{10}, $PM_{2.5}$, and fine soil aerosol concentrations are observed in 2010,

however there are no other trends observed in aerosol and rain data. These results reveal the same inverse relationship between rain amount and rain concentration found in Section 4.1.1.

In the Grand Canyon, the highest annual $PM_{2.5}$, fine soil, and Ca and K aerosol concentrations were found in 2007. The highest coarse mass and PM_{10} yearly averaged aerosol concentrations were found in 1999 which coincide with the most acidic pH (4.96) and lowest abundance of Ca^{2+}, Mg^{2+}, K^{+}, and Na^{+} .The most alkaline rain pH (6.24) and highest rain conductivity (16.4 μS/cm) found in 2004 coincided with the highest annual rain concentrations of Ca^{2+}, K^{+}, and SO_4^{2-}. The cases found in 1999 and 2004 indicate the role of dust in acid neutralization (Sorooshian et al., 2013).

In Organ Pipe, 2011 was the year with the highest coarse mass, PM_{10}, $PM_{2.5}$, fine soil, and Ca, Mg, and K yearly averaged aerosol concentrations. In addition, 2011 had the most abundance (highest mass fractions) of Ca, Mg, and K aerosol concentrations compared to other years. In regard to rain data, 2011 had the most alkaline yearly averaged rain pH (5.99) and highest abundance (rain mass fraction) of Ca^{2+}, Mg^{2+}, and K^{+}. Similar to Chiricahua, these results indicate that the presence of dust tracers in the atmosphere (fine soil, Ca, Mg, and K aerosol concentrations) and in rain (Ca^{2+}, Mg^{2+}, and K^{+}) neutralize acidity (Sorooshian et al., 2013). The highest precipitation amount (28.38 mm) was found in 2008 with the lowest yearly averaged rain conductivity (7.6 μS/cm) and the lowest yearly averaged rain concentrations of Ca^{2+}, Mg^{2+}, NO_3^{-}, K^{+}, and Na^{+}, and SO_4^{2-}. The second lowest yearly averaged precipitation amount found in 2010 (6.73 mm) was coincident with the highest yearly averaged rain concentrations of Ca^{2+}, Cl^{-}, Mg^{2+}, and Na^{+}, including the most acidic rain pH (5.12) and highest yearly averaged rain conductivity (22.68 μS/cm).

In Petrified NP, the highest coarse mass and PM_{10}, and Na yearly averaged aerosol concentrations are found in 2003. The highest annual $PM_{2.5}$ aerosol concentrations found in 2004 and 2005 do not coincide with fine soil maxima but contain the highest annual aerosol concentrations of Ca, Mg, K, SO_4^{-2}, and NO_3^{-}. The most acidic annual rain pH (5.24) was found in 2008, while the

most alkaline pH (6.97) was found in 2003. The highest coarse mass, PM_{10}, and Na yearly averaged aerosol concentrations are also found in 2003 indicating the role of acid neutralization by these aerosols. The second lowest annual precipitation amount (5.10 mm, found in 2003) occurred during the highest annual rain concentrations (all found in 2003). At the same time, the highest annual precipitation amount (14.20 mm, found in 2010) coincided with the minimum of all annual rain concentrations (found in 2013) in the same year.

Overall, when comparing the annual averages of aerosol and precipitation chemistry during the monsoon, the relationship between higher dust concentration and fraction and more alkaline pH was found. Similar results were reported where dust can serve as an acid neutralizing agent (Basak and Alagha 2004; Sorooshian et al., 2013). In addition, the relationship between the annual averages of rain amount and rain concentration demonstrated the dilution effect by higher rain amounts.

4.2 Aerosol data

4.2.1 Annual Relationships

Yearly correlations (Table 2) are done by using a two-tailed student's t-test (95% confidence) between year and annually-averaged aerosol concentrations and mass fractions (from IMPROVE) for each monsoon season (June 15- September 15). The same correlation test is used throughout the paper. Mass fractions are calculated by taking the selected species's concentration divided by the total concentration (sum of Ca, Cl^-, Mg, NO_3^-, K, Na, SO_4^{2-}). The range of data is found in Table 1.

Annual aerosol concentrations (Table 2) of PM_{10} (r=-0.59, n=12) and $PM_{2.5}$ (r=-0.59, n=12) were found to exhibit negative relationships with respect to year only in Petrified NP. Annual aerosol concentrations display negative relationships with respect to year for Chiricahua (SO_4^{2-} [r=-0.59, n=16]), Grand Canyon [Na (r=-0.67, n=16), SO_4^{2-} (r=-0.60, n=16)], and Petrified NP (NO_3^- [r=-0.75, n=12], K [r=-0.62, n=12], and Na [r=-0.64, n=12]). The trends of PM_{10} and $PM_{2.5}$ found in Petrified

NP imply that air emissions in the site have decreased with respect to year. SO_4^{2-} aerosol concentrations most likely decreased in Chiricahua and the Grand Canyon with respect to year due to air pollution regulations since SO_4^{2-} has been attributed to anthropogenic emissions (Hutchings et al., 2009; Sorooshian et al., 2013). These air regulations can also justify the decreasing trends in annual nitrate aerosol concentrations in Petrified NP, since NO_3^- sources have been described to be from the combustion of fossil fuels (Park et al., 2004). Organ pipe did not exhibit any significant aerosol concentration relationships with respect to year.

Yearly correlations between aerosol mass fractions and year (Table 2) reveal that the annual Na aerosol mass fractions exhibit decreasing trends during the monsoon season in Grand Canyon (r=-0.62, n=16) and Petrified NP (r=-0.65, n=12) with respect to year. Neither Organ Pipe nor Chiricahua showed significant annual correlations with respect to aerosol mass fraction.

All of the annual correlations between aerosol concentrations and mass fractions revealed that Organ Pipe did not have any significant species while Chiricahua, Grand Canyon, and Petrified NP had at least one. This result implies that the aerosol chemistry is different within Organ Pipe and can be influenced by a different air mass source than that of Chiricahua, Grand Canyon, and Petrified NP. To further support this statement, case studies in Section 4.9 were performed.

The two-tailed student's t-test (95% confidence) was used to perform statistical correlations in this section and subsequent sections. The main assumption in using this method is that the data follows a normal distribution. Non-parametric tests do not require that the data follows this kind of distribution. The Mann-Kendall test is a non-parametric test that can find significant trends in a time-series, regardless of significant seasonal variations and missing values in the data. This test has been previously used to determine annual trends in precipitation chemistry data (Niles and Conley, 2001; Kvaalen et al., 2002; Sicard et al., 2007). The Mann-Kendall test is applied to the same data (Table 2) as in the two-tailed student's t-test (95% confidence), to compare and contrast the results of both

methods. The Mann-Kendall test (Appendix Table 1) exhibited significance for the same aerosol concentrations and aerosol mass fractions as in the student's t-test. Overall, this finding corroborates the use of the student's t-test (95% confidence) throughout this study.

Table 2: The correlation (r value) between annually-averaged aerosol data and year in Chiricahua National Monument (Chir NM), Grand Canyon, Organ Pipe, and Petrified National Park (Pet NP). The data ranged from 1999-2014 for Chir NM and Grand Canyon and 2003-2014 for Organ Pipe and Pet NP.
Aerosol concentrations are noted as coarse mass (CM), PM_{10} (MT), $PM_{2.5}$ (MF), fine soil (SOILf), calcium (Ca), chloride (Cl), magnesium (Mg), potassium (K), sodium (Na), sulfate (SO_4), and nitrate (NO_3). Aerosol mass fractions are noted as calcium (Ca frac), magnesium (Mg frac), potassium (K frac), sodium (Na frac), sulfate (SO_4 frac), and nitrate (NO_3 frac).
Values are only shown when statistically significant with respect to a two-tailed student's t-test (95% confidence). The values in parentheses indicate the sample range used in the correlation (n-value).

	Annual Correlations- Aerosol Data			
	Chir NM	Grand Canyon	Organ Pipe NM	Pet NP
CM	-	-	-	-
MT	-	-	-	-0.59 (12)
MF	-	-	-	-0.59 (12)
SOILf	-	-	-	-
Ca	-	-	-	-
Cl	-	-	-	-
Mg	-	-	-	-
K	-	-	-	-0.62 (12)
Na	-	-0.67 (16)	-	-0.64 (12)
SO_4	-0.59 (16)	-0.60 (16)	-	-
NO_3	-	-	-	-0.75 (12)
Ca frac	-	-	-	-
Cl frac	-	-	-	-
Mg frac	-	-	-	-
K frac	-	-	-	-
Na frac	-	-0.62 (16)	-	-0.65 (12)
SO_4 frac	-	-	-	-
NO_3 frac	-	-	-	-

4.2.2 Aerosol Interrelationships

In Chiricahua, interrelationships (Table 3) revealed that coarse mass**,** PM_{10}, and $PM_{2.5}$ aerosol concentrations had the highest (based on r-value) significant correlations with fine soil, Ca, and K aerosol. This result suggests that the main pollution sources during the monsoon in Chiricahua were dust emissions, since fine soil and Ca aerosol concentrations have been used as dust tracers in previous work (Sorooshian et al., 2013). In addition, Ca was the strongest correlated aerosol concentration (Table 3) to fine soil, followed by K. Cl^- interrelationships with dust tracers were not significant or had low correlation values (based on r value). The strongest correlations to Cl^- were to coarse mass and Na, implying that Cl^- in Chiricahua is most likely not associated with dust emissions, but sea salt (Sorooshian et al., 2013). Mg was strongly linked to fine soil, Ca, and K implying that its source is from dust emissions. K was also strongly linked to dust emissions where high correlations with fine soil, $PM_{2.5}$, and Ca were found. Na aerosol concentrations had higher correlation values to Ca, K, and fine soil than Cl^-, implying that Na is more related to crustal emissions than sea salt. SO_4^{2-} was correlated best to $PM_{2.5}$ and NO_3^-. NO_3^- aerosol concentrations were better correlated to crustal emissions which are $PM_{2.5}$, K, PM_{10}, and Mg. This result implies that there are reactions in the area between dust and nitrate gaseous precursors such as HNO_3 to form particulate NO_3^- (Malm et al., 2003). This trend coincides with reductions in annual SO_4^{2-} aerosol concentrations as observed in Sorooshian et al. (2013).

As observed in Chiricahua, coarse mass and PM_{10} in Grand Canyon were highly correlated (Table 4) to fine soil, Ca, and K. However, $PM_{2.5}$ did not correlate well with fine soil and Ca, implying that in the fine mode, dust emissions were not as high. Instead $PM_{2.5}$ correlated best with K, which can have multiple source emissions such as wildfires (Schlosser et al., 2017). Ca, Mg and K correlated best with each other and fine soil which suggests their main source is from dust emissions. Cl^- and Na correlated best with each other implying that they originate mainly from sea salt emissions. SO_4^{2-} was correlated best with NO_3^- as seen in Chiricahua. NO_3^- correlated best with K and

Na suggestive of reactions between dust and sea salt and HNO_3 to form particulate NO_3^- which coincides with annual decreasing trends of SO_4^{2-} aerosol concentrations (Lee et al., 2004, 2008).

Similar to Chiricahua, Organ Pipe aerosol interrelationships (Table 5) revealed that coarse mass**,** PM_{10}, and $PM_{2.5}$ aerosol concentrations were mostly characterized by dust emissions (fine soil, Ca, K, and Mg aerosol). Ca, K, and Mg were highly related to each other and to fine soil implying that the main sources of these concentrations were from dust emissions. Cl^- correlated best with Na and vice versa (Table 5), implying that the emissions of Na and Cl^- in Organ Pipe originate from sea salt emissions. Organ Pipe is the closest site to marine emissions and a similar observation is found in Sorooshian et al. (2013). SO_4^{2-} was best correlated to NO_3^- as seen in Chiricahua. However, NO_3^- correlated best with Na and SO_4^{2-}, and not dust emissions as seen in Chiricahua. This result suggests that there are more reactions in the area between sea salt and nitrate precursors such as HNO_3 to form particulate NO_3^- (Lee et al., 2004, 2008).

In Petrified NP, coarse mass correlated best (Table 6) with Na and Mg and not fine soil or Ca. In addition, $PM_{2.5}$ was more related to K and NO_3^- than dust emissions (fine soil or Ca). PM_{10} however was best related to Ca and Na. These results imply that the main sources of pollution in the area are not mostly from dust as seen in Chiricahua, Organ Pipe and the Grand Canyon. Possible sources include sea salt which is justified by the high correlations between Na and Cl^-. K and NO_3^- were highly related to each other in this area in the fine mode, suggestive of wildfire emissions (Schlosser et al., 2017). Mg was best correlated to Ca and fine soil suggesting its profile is characteristic of dust emissions. Interestingly, SO_4^{2-} correlated best with fine soil and Na.

Interrelationships between aerosol concentrations (Tables 3-6) suggested that the main sources of pollution in Chiricahua, Organ Pipe, and the Grand Canyon are dust emissions. Petrified NP had different major pollution sources which may include coarse sea salt. Ca and Mg aerosol concentrations were found to be characteristic of dust emissions in all sites. In Chiricahua, Organ

Pipe, and the Grand Canyon, K aerosol concentrations were highly related to dust emissions but not in Petrified NP where NO_3^- provided the highest correlation (possibly biomass burning). Cl^- aerosol concentrations correlated well with Na in Organ Pipe, the Grand Canyon and Petrified NP suggesting its origin from sea salt emissions, except in Chiricahua. Na aerosol concentrations were characteristic of sea salt due to high correlations with Cl^- in all sites except in Chiricahua, where they were most likely from dust emissions. The interrelationships for NO_3^- were varied between sites where higher correlations to dust tracers were found in Chiricahua and sea salt tracers in Organ Pipe and the Grand Canyon. In Petrified NP, NO_3^- was highly correlated to K aerosol concentrations which can have various emissions such as wildfires (Schlosser et al., 2017). SO_4^{2-} was best correlated to NO_3^- in all sites except Petrified NP where fine soil and Na aerosol concentrations provided the highest correlations. Previous work has stated that both SO_4^{2-} and NO_3^- can be of similar anthropogenic nature, which can justify the results found in Chiricahua, Organ Pipe, and the Grand Canyon (Sorooshian et al., 2013).

Table 3: This table shows the correlation (r value) of the interrelationships between aerosol concentrations in Chiricahua National Monument (Chiricahua NM).
Aerosol concentrations are noted as coarse mass (CM), PM_{10} (MT), $PM_{2.5}$ (MF), fine soil (SOILf), calcium (Ca), chloride (Cl), magnesium (Mg), potassium (K), sodium (Na), sulfate (SO_4), and nitrate (NO_3).
Values are only shown when statistically significant with respect to a two-tailed student's t-test (95% confidence). The n values row indicates the sample range with a few exceptions that have sample range values in parentheses.

	Aerosol Interrelationships- Chiricahua NM										
n values	453	453	459	459	459	134	176	458	250	465	465
aerosol type	CM	MT	MF	SOILf	Ca	Cl	Mg	K	Na	SO_4	NO_3
CM	1.00	0.98	0.76	0.84	0.79	0.28	0.65	0.81	0.46	0.16	0.50
MT		1.00	0.86	0.88	0.82	0.25	0.69	0.87	0.36	0.27	0.55
MF			1.00	0.84	0.81	-	0.70	0.89	0.56	0.51	0.57
SOILf				1.00	0.94	0.21	0.80	0.92	0.60	0.16	0.46
Ca					1.00	-	0.75	0.89	0.65	0.10	0.40
Cl						1.00	0.22 (134)	0.21 (134)	0.25 (134)	-	-
Mg							1.00	0.77 (176)	0.41 (176)	-	0.49(176)
K								1.00	0.61	0.20	0.56
Na									1.00	-	0.28
SO_4										1.00	0.38
NO_3											1.00

Table 4: This table shows the correlation (r value) of the interrelationships between aerosol concentrations in Grand Canyon. Aerosol concentrations are noted as coarse mass (CM), PM_{10} (MT), $PM_{2.5}$ (MF), fine soil (SOILf), calcium (Ca), chloride (Cl), magnesium (Mg), potassium (K), sodium (Na), sulfate (SO_4), and nitrate (NO_3).
Values are only shown when statistically significant with respect to a two-tailed student's t-test (95% confidence). The sample range is found in parentheses.

	Aerosol Interrelationships- Grand Canyon										
aerosol type	CM	MT	MF	SOILf	Ca	Cl	Mg	K	Na	SO_4	NO_3
CM	1.00	0.85 (460)	0.32 (460)	0.71 (460)	0.71 (460)	0.28 (134)	0.61(199)	0.52 (460)	0.40 (291)	0.21 (460)	0.41 (460)
MT		1.00	0.77 (469)	0.71 (469)	0.74 (469)	0.17 (134)	0.53 (199)	0.66 (469)	0.40 (291)	0.36 (469)	0.56 (469)
MF			1.00	0.52 (473)	0.56 (473)	-	0.24 (199)	0.63 (473)	0.23 (491)	0.40 (469)	0.53 (475)
SOILf				1.00	0.95 (473)	-	0.76 (199)	0.79 (473)	0.39 (291)	0.24 (473)	0.45 (473)
Ca					1.00	-	0.71 (199)	0.81 (473)	0.48 (291)	0.24 (473)	0.50 (473)
Cl						1.00	0.28 (134)	-	0.62 (134)	-	0.30 (134)
Mg							1.00	0.55 (199)	0.35 (199)	0.27 (199)	0.489 (199)
K								1.00	0.50 (291)	0.32 (458)	0.63 (458)
Na									1.00	0.27 (291)	0.59 (291)
SO_4										1.00	0.4 (475)
NO_3											1.00

Table 5: This table shows the correlation (r value) of the interrelationships between aerosol concentrations in Organ Pipe National Monument (Organ Pipe NM). Aerosol concentrations are noted as coarse mass (CM), PM_{10} (MT), $PM_{2.5}$ (MF), fine soil (SOILf), calcium (Ca), chloride (Cl), magnesium (Mg), potassium (K), sodium (Na), sulfate (SO_4), and nitrate (NO_3).
Values are only shown when statistically significant with respect to a two-tailed student's t-test (95% confidence). The n values row indicates the sample range with a few exceptions that have sample range values in parentheses.

	Aerosol Interrelationships- Organ Pipe NM										
n values	355	355	355	355	355	199	232	355	294	355	354
aerosol type	CM	MT	MF	SOILf	Ca	Cl	Mg	K	Na	SO_4	NO_3
CM	1.00	0.99	0.76	0.84	0.69	-	0.75	0.81	0.26	0.21	0.25
MT		1.00	0.84	0.87	0.75	-	0.78	0.86	0.32	0.31	0.32
MF			1.00	0.84	0.81	-	0.76	0.90	0.48	0.62	0.54
SOILf				1.00	0.86	-	0.80	0.92	0.31	0.21	0.22
Ca					1.00	0.13	0.71	0.88	0.44	0.27	0.31
Cl						1.00	0.19	-	0.76 (199)	-	0.32 (199)
Mg							1.00	0.78 (232)	0.36 (232)	0.26 (232)	0.37 (232)
K								1.00	0.44	0.34	0.36
Na									1.00	0.29 (294)	0.64 (294)
SO_4										1.00	0.38
NO_3											1.00

Table 6: This table shows a correlation matrix (r value) of the interrelationships between aerosol concentrations in Petrified National Park (Petrified NP). Aerosol concentrations are noted as coarse mass (CM), PM_{10} (MT), $PM_{2.5}$ (MF), fine soil (SOILf), calcium (Ca), chloride (Cl), magnesium (Mg), potassium (K), sodium (Na), sulfate (SO_4), and nitrate (NO_3).

Values are only shown when statistically significant with respect to a two-tailed student's t-test (95% confidence). The sample range is found in parentheses.

	Aerosol Interrelationships- Petrified NP										
aerosol type	CM	MT	MF	SOILf	Ca	Cl	Mg	K	Na	SO_4	NO_3
CM	1.00	0.91 (311)	0.32 (311)	0.44 (311)	0.45 (311)	-	0.53 (177)	0.21 (311)	0.56 (199)	0.37 (311)	0.20 (311)
MT		1.00	0.69 (316)	0.59 (316)	0.67 (316)	-	0.54 (177)	0.56 (316)	0.65 (199)	0.50 (316)	0.52 (316)
MF			1.00	0.56 (322)	0.72 (322)	-	0.44 (177)	0.90 (322)	0.61 (199)	0.50 (322)	0.82 (322)
SOILf				1.00	0.88 (322)	-	0.58 (177)	0.42 (322)	0.56 (199)	0.52 (322)	0.32 (322)
Ca					1.00	0.27 (122)	0.63 (177)	0.63 (322)	0.60 (199)	0.44 (322)	0.53 (322)
Cl						1.00	0.19 (122)	-	0.81 (122)	-	0.21 (122)
Mg							1.00	0.47 (177)	0.51 (177)	0.31 (177)	0.47 (177)
K								1.00	0.53 (199)	0.29 (322)	0.89 (322)
Na									1.00	0.50 (199)	0.60 (199)
SO_4										1.00	0.32 (327)
NO_3											1.00

4.3 Precipitation data

4.3.1 Annual Relationships

Rain conductivity in Chiricahua (r=-0.58, n=16) and Petrified NP (r=-0.65, n=12) and rain pH in Chiricahua (r=0.73, n=16) and the Grand Canyon (r=0.50, n=16) exhibited significant correlations with respect to year (Table 7). Organ Pipe had no significant trends in rain pH and rain conductivity. In addition, rain accumulation (sub ppt) in all sites did not exhibit significant trends with respect to year.

Correlations of annually averaged rain concentrations with respect to year (Table 7) were only found in Petrified NP. It was found that Ca^{2+} (r=-0.62, n=12), Mg^{2+} (r=-0.60, n=12), NO_3^- (r=-0.64, n=12), K^+ (r=-0.72, n=12), and SO_4^{2-} (r=-0.80, n=12) exhibit decreasing concentrations over time. The results in Section 4.2.1 found in Petrified NP for decreasing NO_3^- and K^+ aerosol concentrations, coincide with the decreasing trends of rain concentrations of NO_3^- and K^+ with respect to year. This observation provides insight into potential aerosol and precipitation chemistry relationships (subsequent Section 4.4).

The correlation between rain mass fraction and year (Table 7) result in positive relationships of Mg^{2+} for Chiricahua (r=0.55, n=16) and the Grand Canyon (r=0.67, n=16). Sources of Mg^{2+} in rain

samples are due to the interaction of trace metals such as Mg aerosol concentrations from mine tailings and dust which can serve as CCN or IN, and thus resulting in the observation of trace metals in deposition (Sorooshian et al., 2013; Prabhakar et al., 2014; Taylor et al., 2014). Neither Chiricahua or Organ Pipe show significant annual correlations with respect to rain mass fraction.

Table 7: This table shows the correlation (r value) between yearly averaged rain data and year in Chiricahua National Monument (Chir NM), Grand Canyon, Organ Pipe National Monument (Organ Pipe NM), and Petrified National Park (Pet NP). The data ranged from 1999-2014 for Chir NM and Grand Canyon and 2003-2014 for Organ Pipe and Pet NP.
Rain conductivity, rain pH and rain concentrations are noted as Rain Ca for Ca^{2+}, Rain Cl for Cl^-, Rain Mg for Mg^{2+}, Rain K for K^+, Rain Na for Na^+, Rain SO_4 for SO_4^{2-} and Rain NO_3 for NO_3^-. Rain mass fractions are noted as Rain Ca frac, Rain Mg frac, Rain K frac, Rain Na frac, Rain SO_4 frac, and Rain NO_3 frac.
Values are only shown when statistically significant with respect to a two-tailed student's t-test (95% confidence). The values in parentheses indicate the sample range used in the correlation (n-value).

	Annual Correlations- Rain Data			
	Chir NM	Grand Canyon	Organ Pipe NM	Pet NP
Rain accumulation	-	-	-	-
Rain conductivity	-0.58 (16)	-	-	-0.65 (12)
Rain pH	0.73 (16)	0.50 (16)	-	-
Rain Ca	-	-	-	-0.62 (12)
Rain Cl	-	-	-	-
Rain Mg	-	-	-	-0.60 (12)
Rain K	-	-	-	-0.72 (12)
Rain Na	-	-	-	-
Rain SO_4	-	-	-	-0.80 (12)
Rain NO_3	-	-	-	-0.64 (12)
Rain Ca frac	-	-	-	-
Rain Cl frac	-	-	-	-
Rain Mg frac	0.55 (16)	0.67 (16)	-	-
Rain K frac	-	-	-	-
Rain Na frac	-	-	-	-
Rain SO_4 frac	-	-	-	-
Rain NO_3 frac	-	-	-	-

4.3.2 Rain Interrelationships

In Chiricahua (Table 8) rain conductivity was best correlated to SO_4^{2-} and NO_3^- which have higher ionic strengths in solution. pH had the highest positive correlations with Ca^{2+} and Mg^{2+} suggesting that crustal particles (aerosol concentrations of Ca and Mg) neutralize acidic pH. Rain accumulation correlations with the precipitation data are reported in Section 4.5. Ca^{2+} and Mg^{2+} were highly correlated to each other. Cl^- was best correlated with Na^+ and vice versa and this observation is also found in the aerosol concentration interrelationship (Section 4.2.2). K^+ was more related to Cl^-. NO_3^- and SO_4^{2-} were best correlated to each other and this observation is also found in aerosol concentrations (Section 4.2.2).

In the Grand Canyon (Table 9), rain conductivity was best correlated to SO_4^{2-}, Ca^{2+}, and then NO_3^- (shown in decreasing order). Ca^{2+} and Cl^- have higher correlations to rain conductivity than in Chiricahua and Organ Pipe. Similar to Organ Pipe, pH is best correlated with Ca^{2+} and K^+ and Ca^{2+}, Mg^{2+}, and K^+ were highly correlated to each other which is similar to the observation found in the aerosol concentration interrelationship (Section 4.2.2). Similar to Chiricahua, Cl^- was best correlated with Na^+ and vice versa and this observation is also found in the aerosol concentration interrelationship (Section 4.2.2). NO_3^- was best correlated SO_4^{2-}. However, SO_4^{2-} was best correlated to Ca^{2+} and Cl^-.

In Organ Pipe (Table 10), rain conductivity was best correlated to NO_3^- and SO_4^{2-}. Rain pH correlated best to Ca^{2+} and K^+. Ca^{2+}, Mg^{2+}, and K^+ were highly correlated to each other which is similar to the observation found in the aerosol concentration interrelationship (Section 4.2.2). Cl^- was best correlated with Na^+ and vice versa and this observation is also found in the aerosol concentration interrelationship (Section 4.2.2). NO_3^- was best correlated to $Ca^{2+}$and then SO_4^{2-}. NO_3^- and SO_4^{2-} were best correlated to each other and this observation is also found in aerosol concentrations (Section 4.2.2). SO_4^{2-} best correlated to Ca^{2+} and then NO_3^-.

In Petrified NP (Table 11), rain conductivity was best correlated to NO_3^- and SO_4^{2-} which follows the results of the Chiricahua. The correlations of rain conductivity with Ca^{2+},Mg^{2+}, and Cl^- were not as high as in other sites. As observed in other sites, pH correlated best with $Ca^{2+}$and Mg^{2+} and Ca^{2+} and Mg^{2+} correlated the best with each other. Similar to Chiricahua, Organ Pipe, and the Grand Canyon, Cl^- was best correlated with Na^+ and vice versa and this observation is also found in the interrelationships of aerosol concentrations (Section 4.2.2). K^+ was best correlated to Mg^{2+}. Consistent with the results in Chiricahua and Organ Pipe, NO_3^- and SO_4^{2-} were best correlated to each other.

The interrelationships between rain concentrations (Tables 8-11) revealed that in all sites, rain conductivity values were best correlated to SO_4^{2-} and NO_3^-. In addition, in all sites pH correlated best with Ca^{2+}which represents the acid neutralization effect by crustal emissions (Sorooshian et al., 2013.) In all sites, Ca^{2+}, Mg^{2+}, and K^+ were highly correlated to each other and this result is similar to the observations found between aerosol interrelationships (Section 4.2.2), implying that they originate from dust emissions. In all sites Cl^- and Na^+ were best correlated to each other, consistent with the results found in the aerosol interrelationships which imply that they originate from sea salt emissions. Another observation is that NO_3^- is best correlated with SO_4^{2-} in all sites and this is also found in Section 4.2.2. Therefore, some of the trends found in rain concentration interrelationships are also found in aerosol interrelationships. These observations provide justification to analyze the correlations between aerosol and precipitation chemistry.

Table 8: This table shows the correlation (r value) of the interrelationships between rain pH, conductivity, and rain concentrations in Chiricahua National Monument (Chiricahua NM).
Rain concentrations are noted as Rain Ca for Ca^{2+}, Rain Cl for Cl^-, Rain Mg for Mg^{2+}, Rain K for K^+, Rain Na for Na^+, Rain SO_4 for SO_4^{2-} and Rain NO_3 for NO_3^-.
Values are only shown when statistically significant with respect to a two-tailed student's t-test (95% confidence). The n values row indicates the sample range with a few exceptions that have sample range values in parentheses.

	Rain Interrelationships- Chiricahua NM								
n values	154	154	153	154	154	154	154	154	154
	Rain Conductivity	Rain pH	Rain Ca	Rain Cl	Rain Mg	Rain K	Rain Na	Rain SO_4	Rain NO_3
Rain Conductivity	1.00	-	0.67	0.69	0.71	0.31	0.68	0.90	0.87
Rain pH		1.00	0.40	-	0.29	0.20	0.20	-	-
Rain Ca			1.00	0.64 (153)	0.93 (153)	0.44 (153)	0.71 (153)	0.70 (153)	0.64 (153)
Rain Cl				1.00	0.79	0.64	0.87	0.72	0.61
Rain Mg					1.00	0.50	0.85	0.76	0.68
Rain K						1.00	0.41	0.31	0.26
Rain Na							1.00	0.74	0.65
Rain SO_4								1.00	0.80
Rain NO_3									1.00

Table 9: This table shows the correlation (r value) of the interrelationships between rain pH, conductivity, and rain concentrations in Grand Canyon.
Rain concentrations are noted as Rain Ca for Ca^{2+}, Rain Cl for Cl^-, Rain Mg for Mg^{2+}, Rain K for K^+, Rain Na for Na^+, Rain SO_4 for SO_4^{2-} and Rain NO_3 for NO_3^-.
Values are only shown when statistically significant with respect to a two-tailed student's t-test (95% confidence). The n values row indicates the sample range with a few exceptions that have sample range values in parentheses.

	Rain Interrelationships- Grand Canyon								
n values	124	124	122	123	122	123	122	123	123
	Rain Conductivity	Rain pH	Rain Ca	Rain Cl	Rain Mg	Rain K	Rain Na	Rain SO_4	Rain NO_3
Rain Conductivity	1.00	0.19	0.89	0.85	0.68	0.78	0.78	0.92	0.89
Rain pH		1.00	0.55	0.44	0.53	0.22	0.46	0.34	0.22
Rain Ca			1.00	0.85 (122)	0.84	0.88 (122)	0.76	0.85 (122)	0.78 (122)
Rain Cl				1.00	0.69	0.80	0.97	0.84	0.73
Rain Mg					1.00	0.77 (122)	0.58	0.67 (123)	0.47 (123)
Rain K						1.00	0.68	0.75	0.61
Rain Na							1.00	0.79 (122)	0.69 (122)
Rain SO_4								1.00	0.83
Rain NO_3									1.00

Table 10: This table shows the correlation (r value) of the interrelationships between rain pH, conductivity, and rain concentrations in Organ Pipe National Monument (Organ Pipe NM). Rain

concentrations are noted as Rain Ca for Ca^{2+}, Rain Cl for Cl^-, Rain Mg for Mg^{2+}, Rain K for K^+, Rain Na for Na^+, Rain SO_4 for SO_4^{2-} and Rain NO_3 for NO_3^-.
Values are only shown when statistically significant with respect to a two-tailed student's t-test (95% confidence). The n values row indicates the sample range with a few exceptions that have sample range values in parentheses.

	Rain Interrelationships- Organ Pipe NM								
n values	71	71	70	69	70	70	70	70	70
	Rain Conductivity	Rain pH	Rain Ca	Rain Cl	Rain Mg	Rain K	Rain Na	Rain SO_4	Rain NO_3
Rain Conductivity	1.00	-	0.85	0.75	0.84	0.74	0.73	0.88	0.94
Rain pH		1.00	0.30	-	-	0.36	-	-	-
Rain Ca			1.00	0.74	0.96	0.91	0.74	0.82	0.82
Rain Cl				1.00	0.86 (69)	0.71 (69)	0.98 (69)	0.61 (69)	0.71 (69)
Rain Mg					1.00	0.89	0.86	0.78	0.80
Rain K						1.00	0.72	0.70	0.72
Rain Na							1.00	0.61	0.69
Rain SO_4								1.00	0.81
Rain NO_3									1.00

Table 11: This table shows the correlation (r value) of the interrelationships between rain pH, conductivity, and rain concentrations in Petrified National Park (Petrified NP). Rain concentrations are noted as Rain Ca for Ca^{2+}, Rain Cl for Cl^-, Rain Mg for Mg^{2+}, Rain K for K^+, Rain Na for Na^+, Rain SO_4 for SO_4^{2-} and Rain NO_3 for NO_3^-.
Values are only shown when statistically significant with respect to a two-tailed student's t-test (95% confidence). The n values row indicates the sample range with a few exceptions that have sample range values in parentheses.

	Rain Interrelationships- Petrified NP								
n values	93	93	93	93	93	92	93	93	93
	Rain Conductivity	Rain pH	Rain Ca	Rain Cl	Rain Mg	Rain K	Rain Na	Rain SO_4	Rain NO_3
Rain Conductivity	1.00	-	0.73	0.62	0.76	0.66	0.55	0.85	0.89
Rain pH		1.00	0.58	-	0.52	0.40	-	-	-
Rain Ca			1.00	0.53	0.95	0.61	0.51	0.77	0.72
Rain Cl				1.00	0.64	0.57	0.93	0.56	0.49
Rain Mg					1.00	0.67	0.62	0.75	0.73
Rain K						1.00	0.46 (92)	0.63 (92)	0.63 (92)
Rain Na							1.00	0.50	0.42
Rain SO_4								1.00	0.86
Rain NO_3									1.00

4.4 Aerosol and Precipitation Relationships

Due to the nature of the IMPROVE dataset which reports concentrations every third day and NADP dataset which reports weekly measurements, weekly trends were observed to correlate the

relationships between aerosol and rain concentrations. The IMPROVE data set was averaged to correlate the same week between both datasets.

4.4.1: Aerosol vs Precipitation Concentrations

Weekly averaged K aerosol concentrations correlated significantly (Table 12) with weekly averaged K^+ rain concentrations in all sites. Ca from aerosol and Ca^{2+} from rain had the highest correlation value (based on r-value) of all sites (found in Chiricahua). Ca, Cl^-, K, and NO_3^- aerosol concentrations correlated significantly with rain concentrations of Ca^{2+}, Cl^-, K^+, and NO_3^-, respectively in Chiricahua, Grand Canyon, and Petrified NP. In these sites, Ca in the aerosol phase was determined to be characteristic of dust emissions (based on Section 4.2.2). K was associated with dust emissions in Chiricahua and the Grand Canyon, except in Petrified NP where it was speculated that there were other sources involved such as wildfires. These results suggest that Ca and K potentially served as aerosol cloud seeds within those sites due to the significant correlations observed between aerosol and rain concentrations. The significant correlation of NO_3^- can be justified by previous studies that have reported that dust and other hygroscopic particles containing NO_3^- ions can serve as cloud seeds (Adams, Seinfeld, & Koch, 1999). Cl^- can originate from sea salt emissions (based on interrelationships Sections 4.2.2 and 4.3.2) which can also serve as CCN.

4.4.2: Aerosol vs Precipitation Fractions

Aerosol and rain mass fractions were calculated to provide information about the abundance of each species. The correlation between weekly averaged aerosol and rain mass fractions in Chiricahua (Table 12) revealed that the highest correlation value was Cl^- in Petrified NP. Aerosol concentrations of Ca, K, and SO_4^{2-} were significantly correlated to their respective ionized form in rain in three out of four sites. Based on the interrelationships of aerosol concentrations (Section 4.2.2), the highest contribution to the pollution in Chiricahua was dust emissions. The combination of these results

indicates the potential role of dust as cloud seeds in the form of Ca. In the Grand Canyon, aerosol mass fractions of K shared the highest significant correlations with its respective ionized form, K^+. By using the results of aerosol interrelationships in the Grand Canyon, (Section 4.2.2), K was most likely linked to dust emissions, indicating its role in cloud seeding.

In Organ Pipe, Na and Cl^- aerosol mass fractions were better linked to their ionized form in rain. The site location (closest to marine emissions) and interrelationships results, indicate the presence of sea salt in the area. Hence, sea salt in Organ Pipe can be a potential cloud seed as it has a significant correlation between its aerosol and ionized form in rain. In Petrified National Park, aerosol mass fractions of Cl^- and Mg had the highest significant correlation values to their respective ionized forms in rain. In this area, the presence of sea salt and dust were determined (section 4.2.2) to be abundant and cloud seeds in the form of Cl^- and Mg are very likely.

4.4.3: Coarse Mass, PM_{10}, $PM_{2.5}$, and Fine Soil vs Rain Data

The correlation between coarse mass against rain concentrations (Table 13) resulted in the highest correlation value (r-value) for Ca^{2+} and Mg^{2+} in all sites except the Grand Canyon (Na^+ and Cl^- were the highest). The statistical test between coarse mass and rain mass fractions resulted in similar results for Ca^{2+} and Mg^{2+} and no significant correlations in the Grand Canyon. Based on Section 4.2.2, coarse mass is mainly characterized by crustal emissions (Ca and Mg aerosol), indicating that these emissions were most likely found in precipitation.

All rain concentrations were significantly correlated to PM_{10} in Chiricahua (Table 13). Among them, Ca^{2+} and Mg^{2+} exhibited the highest correlation values in most sites for rain concentrations and rain mass fractions. Similar results are found in the correlations (Table 13) of $PM_{2.5}$ and fine soil to rain data. PM_{10} and $PM_{2.5}$, are mostly characterized by crustal emissions (Section 4.2.2), implying that dust particles within the PM_{10} mode acted as CCN.

Correlations between fine soil aerosol concentrations and rain concentrations (Table 13) exhibited the highest correlation values with respect to Ca^{2+} in all sites except Organ Pipe where no significant correlations were observed. In addition, fine soil aerosol concentrations correlated significantly with all weekly averaged rain concentrations within Chiricahua and Grand Canyon. In these sites, the weekly averaged fine soil aerosol concentrations exhibited significant correlations with weekly averaged SO_4^{2-}, NO_3^-, and Cl^- rain concentrations which suggests that acidic gases reacted with crustal particles (Matsuki et al., 2010; Sorooshian et al., 2013). Similar to coarse mass, PM_{10}, $PM_{2.5}$, and fine soil correlated best with Ca^{2+} and Mg^{2+} rain concentrations and mass fractions in most sites. The results suggest that Ca^{2+} and Mg^{2+} in rain is related to dust emissions in all sites.

4.4.4: Rain Conductivity and pH vs Aerosol Data

To assess which aerosol concentration or mass fraction had the highest contribution to rain conductivity, the correlation (Table 14) was applied between conductivity and aerosol data. Cl^- in the Grand Canyon and Na^+ rain mass fraction in Petrified NP had the highest correlation values. Surprisingly, SO_4^{2-} and NO_3^- did not exhibit the highest correlations (as found in Section 4.3.2). All aerosol concentrations in Chiricahua NM except SO_4^{2-} exhibited significant increasing trends. The aerosol fractions and concentrations in Organ Pipe NM did not exhibit any significant trends.

The correlation between rain pH and rain concentrations (Table 14) resulted in the highest correlation values for Cl^- in Chiricahua NM, K in the Grand Canyon, and Mg in Organ Pipe NM and Petrified NP. Regarding aerosol mass fractions, the highest r-values are found for SO_4^{2-} in Chiricahua, Grand Canyon, and Petrified NP (tied with Mg aerosol mass fraction) and Mg^{2+} in Organ Pipe NM and Petrified NP (tied with SO_4^{-2} aerosol mass fraction). Dust emissions have been reported to increase the alkalinity within rain pH (Sorooshian et al., 2013) and this effect is found in Table 14,

where crustal emissions in the form of Ca, Mg, K and Na in addition to fine soil all exhibit positive correlation values with respect to rain pH.

It is interesting to note that the significant trends between SO_4^{2-} aerosol mass fraction and rain pH were all negative, indicating its acidic nature where more SO_4^{2-} will cause lower pH (acidic). In addition, the highest r-value for SO_4^{2-} is found in Chiricahua, which had the highest aerosol mass fraction of SO_4^{2-} and most acidic rain pH of 5.39 compared to all sites (Section 4.1.1). SO_4^{-2} has been reported to contribute the most to rain acidity in Brazil and Colorado found in the United States (Teixeira et al., 2008; Sorooshian et al., 2013). Therefore, the results in this section suggest that rain pH is affected by the balance between aerosol fractions of SO_4^{2-} (provide acidity) and dust emissions (provide alkalinity). But, there is also the effect of rain accumulation which can dilute rain concentrations and increase pH (based on the results of Section 4.1.1 and 4.1.2).

Table 12: This table shows the correlation (r value) of the relationships between aerosol and rain data in Chiricahua National Monument (Chir NM), Grand Canyon, Organ Pipe National Monument (Organ Pipe NM), and Petrified National Park (Pet NP).
The data ranged from 1999-2014 for Chir NM and Grand Canyon and 2003-2014 for Organ Pipe and Pet NP.
Aerosol concentrations are noted as calcium (Aerosol Ca), chloride (Aerosol Cl), magnesium (Aerosol Mg), potassium (Aerosol K), sodium (Aerosol Na), sulfate (Aerosol SO_4), and nitrate (Aerosol NO_3).
Rain concentrations are noted as Rain Ca for Ca^{2+}, Rain Cl for Cl^-, Rain Mg for Mg^{2+}, Rain K for K^+, Rain Na for Na^+, Rain SO_4 for SO_4^{2-} and Rain NO_3 for NO_3^-.
Aerosol mass fractions are noted as calcium (Aerosol Ca frac), chloride (Aerosol Cl frac), magnesium (Aerosol Mg frac), potassium (Aerosol K frac), sodium (Aerosol Na frac), sulfate (Aerosol SO_4 frac), and nitrate (Aerosol NO_3 frac).
Rain mass fractions are noted as Rain Ca frac, Rain Mg frac, Rain K frac, Rain Na frac, Rain SO_4 frac, and Rain NO_3 frac.
Values are only shown when statistically significant with respect to a two-tailed student's t-test (95% confidence). The values in parentheses indicate the sample range.

	Aerosol vs Precipitation Chemistry			
	Chir NM	Grand Canyon	Organ Pipe NM	Pet NP
Aerosol Ca vs Rain Ca	0.58 (171)	0.32 (152)	-	0.44 (112)
Aerosol Cl vs Rain Cl	0.40 (24)	0.46 (71)	-	0.39 (73)
Aerosol Mg vs Rain Mg	0.24 (66)	-	-	0.44 (96)
Aerosol K vs Rain K	0.25 (172)	0.48 (153)	0.28 (93)	0.28 (111)
Aerosol Na vs Rain Na	0.18 (119)	0.25 (153)	0.21 (93)	-
Aerosol SO_4 vs Rain SO_4	-	0.17 (153)	-	-
Aerosol NO_3 vs Rain NO_3	0.24 (172)	0.16 (153)	-	0.21 (112)
Aerosol Ca frac vs Rain Ca frac	0.44 (171)	0.18 (152)	0.20 (93)	-
Aerosol Cl frac vs Rain Cl frac	-	-	0.31 (93)	0.58 (113)
Aerosol Mg frac vs Rain Mg frac	-	-	-	0.31 (97)
Aerosol K frac vs Rain K frac	0.19 (172)	0.31 (153)	-	0.20 (112)
Aerosol Na frac vs Rain Na frac	-	-	0.30 (93)	-
Aerosol SO_4 frac vs Rain SO_4 frac	0.40 (172)	0.19 (153)	-	0.22 (113)
Aerosol NO_3 frac vs Rain NO_3 frac	-	-0.20 (153)	-	-

Table 13: This table shows the correlation (r value) of the relationships of coarse mass (CM), PM_{10} , $PM_{2.5}$, and fine soil concentrations against rain conductivity, rain pH, rain concentrations, and rain mass fractions in Chiricahua National Monument (Chir NM), Grand Canyon, Organ Pipe National Monument (Organ Pipe NM), and Petrified National Park (Pet NP).
Rain concentrations are noted as Rain Ca for Ca^{2+}, Rain Cl for Cl^-, Rain Mg for Mg^{2+}, Rain K for K^+, Rain Na for Na^+, Rain SO_4 for SO_4^{2-} and Rain NO_3 for NO_3^-.
Rain mass fractions are noted as Rain Ca frac, Rain Mg frac, Rain K frac, Rain Na frac, Rain SO_4 frac, and Rain NO_3 frac.
Values are only shown when statistically significant with respect to a two-tailed student's t-test (95% confidence). The values in parentheses indicate the sample range.

	Coarse Mass (CM)				PM_{10} (MT)				$PM_{2.5}$ (MF)				Fine Soil (Soilf)			
	Chir NM	Grand Canyon	Organ Pipe NM	Pet NP	Chir NM	Grand Canyon	Organ Pipe NM	Pet NP	Chir NM	Grand Canyon	Organ Pipe NM	Pet NP	Chir NM	Grand Canyon	Organ Pipe NM	Pet NP
Rain Conductivity	0.20 (172)	0.27 (153)	-	0.28 (112)	0.23 (172)	0.24 (153)	-	0.25 (112)	0.22 (172)	-	-	-	0.27 (172)	0.25 (153)	-	0.19 (112)
Rain pH	0.41 (172)	-	0.24 (94)	0.34 (112)	0.39 (172)	-	0.27 (94)	0.34 (112)	0.26(172)	0.19 (153)	0.32 (94)	0.30 (112)	0.43 (172)	0.20 (153)	0.21 (94)	0.26 (112)
Rain Ca	0.38 (171)	0.22 (152)	0.25 (93)	0.44 (112)	0.41 (171)	0.22 (152)	0.26 (93)	0.40 (112)	0.40 (171)	-	0.22 (93)	0.31 (112)	0.50 (171)	0.27 (152)	-	0.38 (112)
Rain Cl	0.23 (172)	0.25 (152)	-	-	0.22 (172)	0.24 (152)	-	-	0.16 (172)	-	-	-	0.25 (172)	0.28 (152)	-	-
Rain Mg	0.36 (172)	-	0.24 (93)	0.45 (112)	0.37 (172)	-	0.24 (93)	0.42 (112)	0.33 (172)	-	-	0.32 (112)	0.43 (172)	0.17 (152)	-	0.41 (112)
Rain K	0.22 (172)	0.20 (152)	0.31 (93)	0.32 (111)	0.20 (172)	0.16 (152)	0.32 (93)	0.29 (111)	-	-	0.26 (93)	0.20 (111)	0.24 (172)	0.25 (152)	-	0.26 (111)
Rain Na	0.25 (172)	0.23 (152)	-	-	0.26 (172)	0.22 (152)	-	-	0.23 (172)	-	-	-	0.30 (172)	0.27 (152)	-	-
Rain SO_4	-	0.20 (152)	-	0.26 (112)	0.18 (172)	0.21 (152)	-	0.23 (112)	0.25 (172)	-	-	-	0.25 (172)	0.21 (152)	-	0.22 (112)
Rain NO_3	0.17 (172)	0.19 (152)	-	0.27 (112)	0.20 (172)	0.19 (152)	-	0.25 (112)	0.22 (172)	-	-	-	0.28 (172)	0.22 (152)	-	0.19 (112)
Rain Ca frac	0.41 (171)	-	0.47 (93)	0.35 (112)	0.42 (171)	0.18 (152)	0.46 (93)	0.33 (112)	0.36 (171)	-	0.32 (93)	0.28 (112)	0.42 (171)	-	0.34 (93)	0.29 (112)
Rain Cl frac	-	-	-	-	-	-	0.12 (93)	-	-	-	0.33 (93)	-	-	-	-	-
Rain Mg frac	0.42 (172)	-	0.47 (93)	0.40 (112)	0.40 (172)	-	0.46 (93)	0.37 (112)	0.25 (172)	-	-	0.28 (112)	0.35 (172)	-	0.32 (93)	0.36 (112)
Rain K frac	-	-	0.39 (93)	-	-	-	0.39 (93)	-	-	-	0.28 (93)	-	-	0.24 (152)	0.22 (93)	-
Rain Na frac	0.22 (172)	-	-	-	0.22 (172)	-	-	-	0.16 (172)	-	0.31 (93)	-	0.24 (172)	-	-	-
Rain SO_4 frac	-0.30 (172)	-	-	-	-0.28 (172)	-	-	-	-	-	-	-	-0.28 (172)	-	-	-
Rainf NO_3 frac	-0.17 (172)	-	-	-0.27 (112)	-0.17 (172)	-	-	-0.25 (112)	-	-	-	-	-0.17 (172)	-	-	-0.25 (112)

Table 14: This table shows the correlation (r value) of the relationships of rain conductivity and rain pH against aerosol concentrations and mass fractions in Chiricahua National Monument (Chir NM), Grand Canyon, Organ Pipe National Monument (Organ Pipe NM), and Petrified National Park (Pet NP). The data ranged from 1999-2014 for Chir NM and Grand Canyon and 2003-2014 for Organ Pipe and Pet NP.
Aerosol concentrations are noted as coarse mass (CM), PM_{10} (MT), $PM_{2.5}$ (MF), fine soil (SOILf), calcium (Aerosol Ca), chloride (Aerosol Cl), magnesium (Aerosol Mg), potassium (Aerosol K), sodium (Aerosol Na), sulfate (Aerosol SO_4), and nitrate (Aerosol NO_3).
Aerosol mass fractions are noted as calcium (Ca frac), chloride (Cl frac), magnesium (Mg frac), potassium (K frac), sodium (Na frac), sulfate (SO_4 frac), and nitrate (NO_3 frac).
Values are only shown when statistically significant with respect to a two-tailed student's t-test (95% confidence). The values in parentheses indicate the sample range.

	Rain Conductivity				Rain pH			
	Chir NM	Grand Canyon	Organ Pipe NM	Pet NP	Chir NM	Grand Canyon	Organ Pipe NM	Pet NP
CM	0.20 (172)	0.27 (148)	-	0.28 (110)	0.41 (172)	-	0.24 (94)	0.34 (112)
MT	0.23 (172)	0.24 (148)	-	0.25 (110)	0.39 (172)	-	0.27 (94)	0.34 (112)
MF	0.22 (172)	-	-	-	0.26(172)	0.19 (148)	0.32 (94)	0.30 (112)
SOILf	0.27 (172)	0.25 (148)	-	0.19 (11)	0.43 (172)	0.20 (148)	0.21 (94)	0.26 (112)
Ca	0.33 (172)	0.29 (148)	-	0.28 (110)	0.40 (172)	0.21 (148	0.23 (94)	0.33 (112)
Cl	0.38 (24)	0.48 (71)	-	-	0.57 (24)	-	0.21 (94)	-
Mg	0.40 (66)	-	-	-	0.28 (66)	-	0.42 (94)	0.47 (96)
K	0.31 (172)	0.36 (148)	-	0.20 (110)	0.41 (172)	0.34 (148)	0.33 (94)	0.37 (112)
Na	0.24 (119)	0.33 (148)	-	0.37 (109)	-	-	0.21 (94)	0.31 (112)
SO_4	-	-	-	-	-	0.28 (148)	-	0.20 (112)
NO_3	0.17 (172)	0.28 (148)	-	0.23 (110)	0.33 (172)	0.30 (148)	0.23 (94)	0.35 (112)
Ca frac	0.34 (172)	-	-	-	0.39 (172)	-	-	0.22 (112)
Cl frac	-	0.34 (71)	-	-	0.33 (67)	-	-	-
Mg frac	0.24 (99)	-	-	-	-	-	0.35 (94)	0.35 (97)
K frac	0.27 (172)	-	-	-	0.49 (99)	0.24 (153)	0.25 (94)	0.34 (112)
Na frac	0.29 (138)	-	-	0.39 (110)	0.20 (138)	-	-	0.28 (112)
SO_4 frac	-0.29 (172)	-0.28 (148)	-	-	-0.56 (172)	-0.36 (153)	-0.28 (94)	-0.35 (112)
NO_3 frac	-	0.18 (148)	-	-	0.44 (172)	0.30 (153)	-	-

4.5 Rain Accumulation

The relationships between aerosol and precipitation chemistry can be altered by various meteorological processes, where wind and moisture can provide favorable conditions for cloud seeding. Precipitation droplets in clouds, which contain aerosol concentrations from cloud seeding, can also attract other aerosol particles (based on hygroscopicity), in the air as rain drops fall during precipitation events. This process is known as aerosol scavenging and can affect the correlations in

section 4.4. In addition, an increase in rain accumulation results in the dilution of rain concentrations which was observed to increase the acidity of rain pH (Sections 4.1.1 and 4.1.2). It is proposed to correlate the amount of rainfall (in mm) to aerosol and precipitation chemistry data to provide insight about the effects of rain accumulation during the monsoon season in Arizona.

The NADP parameter sub ppt was used for rain accumulation (in mm). To correlate rain accumulation to aerosol and precipitation data, weekly averages were calculated as in section 4.4.

4.5.1 Rain Accumulation and Aerosol Chemistry Relationships

All significant correlations except SO_4^{2-} mass fractions exhibited decreasing trends in all sites (Table 15), implying that rain can serve as a sink for aerosol concentrations (Raman et al., 2016). The correlation between rain accumulation (Table 15) and coarse mass, PM_{10}, $PM_{2.5}$, and fine soil were found significant only in Chiricahua. In Chiricahua, the highest correlation values were found for Ca aerosol concentrations and Na aerosol mass fractions. In Grand Canyon, the highest correlated aerosol concentrations were Na and NO_3^- and SO_4^{2-} aerosol mass fractions. In Organ Pipe, the best correlated aerosol concentrations were Ca and K and Ca aerosol mass fractions. In Petrified NP, Mg and Na aerosol concentrations showed negative decreasing trends and there were no significant trends for aerosol mass fractions.

Overall, the correlation between rain accumulation and aerosol concentrations and aerosol mass fractions exhibited significant decreasing trends. These results suggest that there is a dilution effect by rain accumulation on aerosol concentrations. The only exception is found for SO_4^{2-} aerosol mass fraction (positive) in Chiricahua, Grand Canyon, and Organ Pipe. The increase in SO_4^{2-} is most likely due to the uptake of precursor gases of SO_4^{2-} which are very hygroscopic by cloud seeding and aerosol scavenging. This result can lead to a more acidic rain pH. In Section 4.1, high rain

accumulation coincided with more acidic pH. It is necessary to correlate rain accumulation to rain data to deduce whether rain accumulation or SO_4^{2-} aerosol mass fraction impacts rain pH the most.

Table 15: This table shows the correlation (r value) of the relationships between rain amount (in mm) and aerosol concentrations and fractions in Chiricahua National Monument (Chir NM), Grand Canyon, Organ Pipe National Monument (Organ Pipe NM), and Petrified National Park (Petrified NP). The data ranged from 1999-2014 for Chir NM and Grand Canyon and 2003-2014 for Organ Pipe and Pet NP.
Aerosol concentrations are noted in as Coarse mass (CM), PM_{10} (MT), $PM_{2.5}$ (MF), fine soil (SOILf), calcium (Ca), chloride (Cl), magnesium (Mg), potassium (K), sodium (Na), sulfate (SO_4), and nitrate (NO_3). Aerosol mass fractions are noted as calcium (Ca frac), magnesium (Mg frac), potassium (K frac), sodium (Na frac), sulfate (SO_4 frac), and nitrate (NO_3 frac).
Values are only shown when statistically significant with respect to a two-tailed student's t-test (95% confidence). The sample range is reported in parentheses.

	Rain Accumulation Correlations- Aerosol Data			
	Chir NM	Grand Canyon	Organ Pipe NM	Pet NP
CM	-0.18 (189)	-	-	-
MT	-0.18 (189)	-	-	-
MF	-0.16 (189)	-	-	-
SOILf	-0.22 (189)	-	-	-
Ca	-0.23 (189)	-	-0.21 (112)	-
Cl	-	-	-	-
Mg	-	-	-	-0.21 (96)
K	-0.20 (189)	-0.17 (176)	-	-
Na	-0.20 (119)	-0.26 (153)	-	-0.19 (114)
SO_4	-	-	-	-
NO_3	-	-0.25 (176)	-	-
Ca frac	-0.28 (189)	-	-0.25 (112)	-
Cl frac	-	-	-	-
Mg frac	-0.20 (99)	-	-	-
K frac	-0.22 (189)	-	-0.23 (112)	-
Na frac	- 0.30 (119)	-	-0.20 (112)	-
SO_4 frac	0.24 (189)	0.27 (176)	0.22 (112)	-
NO_3 frac	-	-0.21 (176)	-	-

4.5.2 Rain Accumulation and Precipitation Chemistry Relationships

In all sites, the correlation between rain accumulation and pH (Table 16) was not significant. Instead, significant decreasing trends are observed in all sites for rain conductivity. All of the significant correlations with the exception of rain mass fractions of SO_4^{2-} and NO_3^-, exhibited negative trends. This result shows the dilution effect by rain accumulation on rain data (similar to results in Section 4.5.1).

In Chiricahua, the highest correlated rain concentrations (based on r-value) were SO_4^{2-} and NO_3^-. Mg^{2+} and NO_3^- rain fractions exhibited the most significant relationships with rain accumulation. In Organ Pipe, NO_3^- and Mg^{2+} rain concentrations and Ca^{2+} and Na^{2+} rain mass fractions showed the highest correlation values. In addition, the decreasing trend in Ca^{2+} coincides with decreasing Ca aerosol concentrations (found in Section 4.5.1). In the Grand Canyon, the highest correlation values for rain concentrations were Cl^- and Na^+ and Na^+ and Cl^- for rain mass fractions. The rain species that were significant in Grand Canyon with respect to rain accumulation do not match those found in the aerosol concentrations (Section 4.5.1). In Petrified NP, NO_3^- and Mg^{2+} rain concentrations, and Mg^{2+} and SO_4^{2-} rain mass fractions exhibited the highest correlation values. The significant negative correlation found for Mg^{2+} rain concentration coincided with that of Mg aerosol concentration (Section 4.5.1). Also, it was found that concentrations of Mg^{2+} in rain and Mg in aerosol in Petrified NP were significantly related (Section 4.4-Table 13). Therefore, in addition to the dilution effect by rain accumulation, rain concentrations can be further diluted by the reduction of aerosol concentration in the atmosphere.

Overall, the correlations between rain accumulation and lab rain conductivity, rain concentrations, and rain mass fractions were all negative with the exception of rain mass fractions of SO_4^{2-} and NO_3^-. The decreasing trends found in Table 16 are similar to those found in section 4.5.1. At higher rain accumulation, the abundance of SO_4^{2-} and NO_3^- in rain increases in Chiricahua NM,

Grand Canyon and Petrified NP and this coincides with a higher abundance of SO_4^{2-} in the atmosphere. These increasing trends of SO_4^{2-} and NO_3^- are most likely due to the hygroscopicity of acidic precursors which facilitate their uptake via cloud seeding and scavenging. Based on Table 15, for the case of the Grand Canyon shows that the abundance of NO_3^- in the air decreases with respect to rain accumulation. It is important to note the results in Table 13 for the Grand Canyon, where the significant correlation between aerosol and rain mass fractions of NO_3^- are negative. Combining these results suggests that the NO_3^- aerosol mass fractions are inversely related to the NO_3^- rain mass fractions.

Table 16: This table shows the correlation (r value) of the relationships between rain amount (in mm) and rain data in Chiricahua National Monument (Chir NM), Grand Canyon, Organ Pipe National Monument (Organ Pipe NM), and Petrified National Park (Petrified NP). The data ranged from 1999-2014 for Chir NM and Grand Canyon and 2003-2014 for Organ Pipe and Pet NP.
Rain concentrations are noted as Rain Ca for Ca^{2+}, Rain Cl for Cl^-, Rain Mg for Mg^{2+}, Rain K for K^+, Rain Na for Na^+, Rain SO_4 for SO_4^{2-} and Rain NO_3 for NO_3^-.
Rain mass fractions are noted as Rain Ca frac, Rain Mg frac, Rain K frac, Rain Na frac, Rain SO_4 frac, and Rain NO_3 frac.
Values are only shown when statistically significant with respect to a two-tailed student's t-test (95% confidence). The sample range is reported in parentheses.

	Rain Accumulation Correlations- Rain Data			
	Chir NM	Grand Canyon	Organ Pipe NM	Pet NP
Rain Conductivity	-0.51 (172)	-0.41 (153)	-0.43 (94)	-0.45 (112)
Rain pH	-	-	-	-
Rain Ca	-0.40 (171)	-0.39 (152)	-0.40 (93)	-0.33 (112)
Rain Cl	-0.45 (172)	-0.43 (153)	-0.32 (93)	-0.37 (112)
Rain Mg	-0.44 (172)	-0.35 (153)	-0.42 (93)	-0.39 (112)
Rain K	-0.34 (172)	-0.26 (153)	-0.23 (93)	-0.35 (112)
Rain Na	-0.36 (172)	-0.42 (153)	-0.30 (93)	-0.33 (112)
Rain SO_4	-0.52 (172)	-0.39 (153)	-0.37 (93)	-0.35 (112)
Rain NO_3	-0.48 (172)	-0.35 (153)	-0.44 (93)	-0.41 (112)
Rain Ca frac	-0.30 (171)	-0.27 (152)	-0.40 (93)	-
Rain Cl frac	-0.16 (172)	-0.25 (153)	-	-0.21 (113)
Rain Mg frac	-0.37 (172)	-0.22 (153)	-0.33 (93)	-0.29 (112)
Rain K frac	-0.15 (172)	-	-0.31 (93)	-0.25 (112)
Rain Na frac	-	-0.27 (153)	-0.25 (93)	-0.20 (112)
Rain SO_4 frac	-	-	-	0.28 (113)
Rain NO_3 frac	0.32 (172)	0.23 (153)	-	-

4.6: The Inverse Relationships Between NO_3^- Aerosol and Rain Mass Fractions: Aerosol and Rain Mass Fractions as Proxies for Acidity and Alkalinity

Based on the results of Section 4.5.2 (Table 16), the abundance of SO_4^{2-} and NO_3^- in rain, exhibit a direct relationship with rain accumulation. Combining the results of Table 13 and 15, suggests that the NO_3^- aerosol mass fractions are inversely related to the NO_3^- rain mass fractions. In addition, based on the results of Section 4.3.2, rain concentrations of SO_4^{2-} and NO_3^- correlated best with each other. To further investigate the meaning of this inverse trend and high intercorrelation, SO_4^{2-} and NO_3^- aerosol and rain mass fractions were correlated with respect to rain conductivity, rain pH, and all other aerosol and rain mass fractions.

The results from Table 17 show that the correlations between aerosol mass fractions and rain conductivity all follow positive trends except for SO_4^{2-} (negative). On the other hand, the correlations of SO_4^{2-} and NO_3^- rain mass fractions exhibit negative trends while the other rain mass fractions exhibit positive correlation values. Similar observations are found when regarding rain pH

correlations with respect to aerosol and rain mass fractions. All aerosol mass fractions (including NO_3^-) except SO_4^{2-} exhibit positive trends while SO_4^{2-} and NO_3^- rain mass fractions have negative correlation values and all rain fractions are positive. In the context of pH, this result indicates that NO_3^- aerosol mass fractions are alkaline and acidic in the rain mass fraction state. SO_4^{2-} has an acidic effect on pH regardless of its state as aerosol or rain fraction.

To further confirm this finding, correlations between NO_3^- aerosol mass fractions and aerosol and precipitation data were done (Table 18). Positive correlation values were found for all aerosol mass fractions except SO_4^{2-}. When comparing rain mass fractions, in the Grand Canyon a negative correlation was found for NO_3^- and SO_4^{2-}, while other rain fractions were positive. Coarse mass, PM_{10}, $PM_{2.5}$, and fine soil which were found to be characteristic of dust emissions (Section 4.2.2) all had positive relationships with NO_3^-. The positive relationship with pH in Chiricahua NM and the Grand Canyon suggest that NO_3^- aerosol mass fractions are alkaline. In addition, its positive relationships with dust emissions suggest that NO_3^- aerosol mass fractions can be characteristic of dust emissions, since dust has been shown to have alkaline effects on rain water (Sorooshian et al., 2013). Rain accumulation exhibited a negative trend in the Grand Canyon, suggesting that the abundance of NO_3^- in the atmosphere decreases with respect to higher amount of rain.

NO_3^- rain mass fractions exhibited the opposite trends (Table 18) as in the aerosol mass fraction state. First, correlations with other aerosol mass fractions were all negative except with respect to SO_4^{2-}. Next, correlations with other rain mass fractions were all negative including SO_4^{2-}. A possible reason for this is that there is a balance between alkaline (Ca^{2+}, Cl^-, Mg^{2+}, K^+, Na^+) and acidic (SO_4^{2-} and NO_3^-) rain mass fractions which exhibited negative correlation values with respect to pH. Rain accumulation showed a positive trend with respect to the abundance of NO_3^- in rain water. Therefore, when comparing the results of Tables 18 inverse relationships are observed between NO_3^- air and rain mass fractions mostly due to differences in pH. NO_3^- aerosol mass

fractions can be alkaline due to the reactions between crustal emissions and HNO_3 which were reported to be common in desert-like areas with high dust influence (Karydis et al., 2016). This is further proven by the results that NO_3^- aerosol mass fractions exhibit higher correlation values to aerosols derived from crustal emissions (Table 18) such as Ca, Mg, Na, and K. The salts produced by mineral dust and NO_3^- aerosol in the atmosphere are highly soluble in water and can serve as cloud seeds. Once in water, the ions separate providing mineral cations to the rain water as well as NO_3^- which has been noted to be highly acidic (Minoura and Iwasaka, 1996), which results in the acidic profile found for NO_3^- rain mass fractions (Table 17 and 18).

To further confirm the inverse trends observed in the case of NO_3^-, Tables 19 and 20 were created. First, the correlations between NO_3^- aerosol mass fractions and aerosol and precipitation data were compared to those of SO_4^{2-} (Table 18). Closer inspection reveals that inverse trends (based on sign) are found and NO_3^- aerosol mass fractions are confirmed to be alkaline while SO_4^{2-} aerosol mass fractions are acidic in nature. However, when comparing the results in Table 19, NO_3^- and SO_4^{2-} rain mass fractions are both acidic and do not follow positive relationships with crustal- derived rain species. Based on these findings the correlation results of aerosol and rain mass fractions can possibly be used as proxies for acidity and alkalinity of rain pH. The correlation values for acidic mass fractions would be positive with respect to SO_4^{2-} air mass fractions and rain accumulation and negative for all other aerosol and precipitation data (Tables 18, 19, 20). Alkaline mass fractions would exhibit negative correlations with SO_4^{2-} air mass fractions and rain accumulation and positive trends for all other aerosol and precipitation data.

An interesting result (Tables 18, 19, 20) is that as rain accumulation increases, the most acidic rain mass fractions NO_3^- and SO_4^{2-} increase as well, while others decrease. The increase of NO_3^- and SO_4^{2-} rain mass fractions can be justified by the uptake of acidic precursor gases via cloud seeding and scavenging. The site with the most acidic pH (Section 4.1.1) was Chiricahua and it coincided

with the highest rain amount, lowest rain concentrations as well as highest SO_4^{2-} rain mass fractions. Rain accumulation and NO_3^- and SO_4^{2-} rain mass fractions both contribute to determine rain pH, however based on the work presented it is difficult to determine which has a higher effect. Therefore, it is necessary to determine the absolute amount of species in rain.

Table 17: This table shows the correlation (r value) of the relationships of rain conductivity and rain pH against aerosol and rain mass fractions in Chiricahua National Monument (Chir NM), Grand Canyon, Organ Pipe National Monument (Organ Pipe NM), and Petrified National Park (Pet NP). The data ranged from 1999-2014 for Chir NM and Grand Canyon and 2003-2014 for Organ Pipe and Pet NP.
Aerosol mass fractions are noted as calcium (Ca frac), chloride (Cl frac), magnesium (Mg frac), potassium (K frac), sodium (Na frac), sulfate (SO_4 frac), and nitrate (NO_3 frac).
Rain mass fractions are noted as Rain Ca frac, Rain Cl frac, Rain Mg frac, Rain K frac, Rain Na frac, Rain SO_4 frac, and Rain NO_3 frac.
Values are only shown when statistically significant with respect to a two-tailed student's t-test (95% confidence). The values in parentheses indicate the sample range.

	Rain Conductivity				Rain pH			
	Chir NM	Grand Canyon	Organ Pipe NM	Pet NP	Chir NM	Grand Canyon	Organ Pipe NM	Pet NP
Ca frac	0.34 (172)	-	-	-	0.39 (172)	-	-	0.22 (112)
Cl frac	-	0.34 (71)	-	-	0.33 (67)	-	-	-
Mg frac	0.24 (99)	-	-	-	-	-	0.35 (94)	0.35 (97)
K frac	0.27 (172)	-	-	-	0.49 (99)	0.24 (153)	0.25 (94)	0.34 (112)
Na frac	0.29 (138)	-	-	0.39 (110)	0.20 (138)	-	-	0.28 (112)
SO_4 frac	-0.29 (172)	-0.28 (148)	-	-	-0.56 (172)	-0.36 (153)	-0.28 (94)	-0.35 (112)
NO_3 frac	-	0.18 (148)	-	-	0.44 (172)	0.30 (153)	-	-
Rain Ca frac	0.30 (171)	0.39 (147)	0.31 (90)	0.24 (110)	0.61 (171)	0.77 (152)	0.36 (93)	0.79 (112)
Rain Cl frac	-	0.14 (148)	-	-	-	0.19 (153)	-	-
Rain Mg frac	0.26 (172)	0.22 (148)	0.24 (90)	0.29 (110)	0.54 (172)	0.57 (153)	0.29 (93)	0.36 (112)
Rain K frac	-	0.39 (148)	-	-	-	0.55 (153)	0.43 (93)	-
Rain Na frac	0.20 (172)	0.17 (148)	-	-	0.24 (172)	0.28 (153)	-	-
Rain SO_4 frac	-	-	-	-0.20 (110)	-0.34 (172)	-	-0.36 (93)	-
Rain NO_3 frac	-0.19 (172)	-0.35 (148)	-	-	-0.26 (172)	-0.58 (153)	-	-0.25 (113)

Table 18: This table shows the correlation (r value) of the relationships of NO_3^- aerosol and rain mass fractions with respect to other aerosol and rain mass fractions, aerosol concentrations, rain accumulation, rain conductivity and rain pH in Chiricahua National Monument (Chir NM), Grand Canyon, Organ Pipe National Monument (Organ Pipe NM), and Petrified National Park (Pet NP). The data ranged from 1999-2014 for Chir NM and Grand Canyon and 2003-2014 for Organ Pipe and Pet NP.
Aerosol mass fractions are noted as calcium (Ca frac), chloride (Cl frac), magnesium (Mg frac), potassium (K frac), sodium (Na frac), sulfate (SO_4 frac), and nitrate (NO_3 frac).
Aerosol concentrations are noted as coarse mass (CM), PM_{10} (MT), $PM_{2.5}$ (MF), fine soil (SOILf).
Rain mass fractions are noted as Rain Ca frac, Rain Cl frac, Rain Mg frac, Rain K frac, Rain Na frac, Rain SO_4 frac, and Rain NO_3 frac.
Values are only shown when statistically significant with respect to a two-tailed student's t-test (95% confidence). The values in parentheses indicate the sample range.

	NO3 Aerosol Mass Frac				NO3 Rain Mass Frac			
	Chir NM	Grand Canyon	Organ Pipe NM	Pet NP	Chir NM	Grand Canyon	Organ Pipe NM	Pet NP
Ca frac	0.35 (192)	0.16 (193)	-	0.29 (141)	-0.20 (172)	-	-	-0.22 (113)
Cl frac	-	0.28 (71)	-	-	-0.29 (67)	-0.43 (71)	-	-0.22 (72)
Mg frac	0.28 (99)	0.21 (113)	-	-	-0.22 (99)	-	-	-0.36 (97)
K frac	0.48 (192)	0.20 (193)	-	0.57 (141)	-0.16 (172)	-0.17 (153)	-	-
Na frac	0.22 (138)	-	0.23 (133)	0.18 (115)	-	-	-	-0.42 (113)
SO_4 frac	-0.75 (193)	-0.77 (194)	-0.47(146)	-0.71 (142)	0.15 (172)	0.32 (153)	0.22 (93)	0.18 (113)
NO_3 frac	1.00	1.00	1.00	1.00	-	-0.20 (153)	-	-
Rain Ca frac	0.16 (171)	0.30 (152)	-	-	-0.61 (171)	-0.76 (152)	-0.51 (93)	-0.64 (113)
Rain Cl frac	-	0.28 (153)	-	-	-0.40 (172)	-0.50 (153)	-0.46 (93)	-0.45 (113)
Rain Mg frac	0.24 (172)	0.16 (153)	-	-	-0.47 (172)	-0.66 (153)	-0.61 (93)	-0.56 (113)
Rain K frac	-	0.20 (153)	-	-	-0.39 (172)	-0.60 (153)	-0.49 (93)	-0.26 (112)
Rain Na frac	0.33 (172)	0.29 (153)	-	-	-0.30 (172)	-0.46 (153)	-0.45 (93)	-0.50 (113)
Rain SO_4 frac	-0.34 (172)	-0.19 (153)	-	-	-0.46 (172)	-0.46 (153)	-0.50 (93)	-
Rain NO_3 frac	-	-0.20 (153)	-	-	1.00	1.00	1.00	1.00
CM	0.42 (189)	0.24 (191)	-	-	-0.17 (172)	-	-0.33 (93)	-0.27 (113)
MT	0.40 (191)	0.33 (193)	-	-	-0.17 (172)	-	-0.30 (93)	-0.25 (113)
MF	0.38 (191)	0.31 (194)	-	0.17 (139)	-	-	-	-
f SOIL	0.49 (191)	0.22 (193)	-	-	-0.17 (172)	-	-	-0.25 (113)
Rain Accumulation	-	-0.21 (153)	-	-	0.32 (172)	0.23 (153)	-	-
Rain pH	0.44 (172)	0.30 (153)	-	-	-0.26 (172)	-0.57 (153)	-	-0.43 (112)
Rain Conductivity	-	0.18 (153)	-	-	-0.19 (172)	-0.35(153)	-	-

Table 19: This table shows the correlation (r value) of the relationships of NO_3^- aerosol and SO_4^{2-} rain mass fractions with respect to other aerosol and rain mass fractions, aerosol concentrations, rain accumulation, rain conductivity and rain pH in Chiricahua National Monument (Chir NM), Grand

Canyon, Organ Pipe National Monument (Organ Pipe NM), and Petrified National Park (Pet NP). The data ranged from 1999-2014 for Chir NM and Grand Canyon and 2003-2014 for Organ Pipe and Pet NP.
Aerosol mass fractions are noted as calcium (Ca frac), chloride (Cl frac), magnesium (Mg frac), potassium (K frac), sodium (Na frac), sulfate (SO_4 frac), and nitrate (NO_3 frac).
Aerosol concentrations are noted as coarse mass (CM), PM_{10} (MT), $PM_{2.5}$ (MF), fine soil (SOILf).
Rain mass fractions are noted as Rain Ca frac, Rain Cl frac, Rain Mg frac, Rain K frac, Rain Na frac, Rain SO_4 frac, and Rain NO_3 frac.
Values are only shown when statistically significant with respect to a two-tailed student's t-test (95% confidence). The values in parentheses indicate the sample range.

	NO3 Aerosol Mass Frac				SO4 Aerosol Mass Frac			
	Chir NM	Grand Canyon	Organ Pipe NM	Pet NP	Chir NM	Grand Canyon	Organ Pipe NM	Pet NP
Ca frac	0.35 (192)	0.16 (193)	-	0.29 (141)	-0.76 (192)	-0.34 (193)	-0.53 (146)	-0.67 (141)
Cl frac	-	0.28 (71)	-	-	-0.39 (67)	-0.58 (71)	-0.67 (102)	-0.41 (72)
Mg frac	0.28 (99)	0.21 (113)	-	-	-0.51 (99)	-0.32 (113)	-0.44 (114)	-0.39 (97)
K frac	0.48 (192)	0.20 (193)	-	0.57 (141)	-0.80 (192)	-0.36 (193)	-0.42 (146)	-0.71 (141)
Na frac	0.22 (138)	-	0.23 (133)	0.18 (115)	-0.58 (138)	-0.25 (153)	-0.77 (133)	-0.46 (115)
SO_4 frac	-0.75 (193)	-0.77 (194)	-0.47(146)	-0.71 (142)	1.00	1.00	1.00	1.00
NO_3 frac	1.00	1.00	1.00	1.00	-0.75 (193)	-0.77 (194)	-0.47 (146)	-0.71 (142)
Rain Ca frac	0.16 (171)	0.30 (152)	-	-	-0.42 (171)	-0.43(152)	-	-0.28 (113)
Rain Cl frac	-	0.28 (153)	-	-	-	-0.32 (153)	-0.41 (93)	-
Rain Mg frac	0.24 (172)	0.16 (153)	-	-	-0.48 (172)	-0.33 (153)	-0.22 (93)	-0.28 (113)
Rain K frac	-	0.20 (153)	-	-	-0.18 (172)	-0.38 (153)	-	-0.27 (112)
Rain Na frac	0.33 (172)	0.29 (153)	-	-	-0.30 (172)	-0.27 (153)	-0.36 (93)	-
Rain SO_4 frac	-0.34 (172)	-0.19 (153)	-	-	0.40 (172)	0.19 (153)	-	0.22 (113)
Rain NO_3 frac	-	-0.20 (153)	-	-	0.15 (172)	0.32 (153)	0.22 (93)	-
CM	0.42 (189)	0.24 (191)	-	-	-0.67 (189)	-0.44 (191)	-0.28 (146)	-0.25 (135)
MT	0.40 (191)	0.33 (193)	-	-	-0.67 (191)	-0.45 (193)	-0.27 (146)	-0.30 (136)
MF	0.38 (191)	0.31 (194)	-	0.17 (139)	-0.54 (191)	-0.28 (194)	-0.16 (146)	-0.30 (139)
f SOIL	0.49 (191)	0.22 (193)	-	-	-0.75 (191)	-0.45 (193)	-0.30 (146)	-0.32 (139)
Rain Accumulation	-	-0.21 (153)	-	-	0.24 (189)	0.27 (153)	0.22 (112)	-
Rain pH	0.44 (172)	0.30 (153)	-	-	-0.56 (172)	-0.36 (153)	-0.28 (94)	-0.35 (112)
Rain Conductivity	-	0.18 (153)	-	-	-0.29 (172)	-0.28 (153)	-	-

Table 20: This table shows the correlation (r value) of the relationships of NO_3^- and SO_4^{2-} rain mass fractions with respect to other aerosol and rain mass fractions, aerosol concentrations, rain accumulation, rain conductivity and rain pH in Chiricahua National Monument (Chir NM), Grand Canyon, Organ Pipe National Monument (Organ Pipe NM), and Petrified National Park (Pet NP). The data ranged from 1999-2014 for Chir NM and Grand Canyon and 2003-2014 for Organ Pipe and Pet NP.
Aerosol mass fractions are noted as calcium (Ca frac), chloride (Cl frac), magnesium (Mg frac), potassium (K frac), sodium (Na frac), sulfate (SO_4 frac), and nitrate (NO_3 frac).
Aerosol concentrations are noted as coarse mass (CM), PM_{10} (MT), $PM_{2.5}$ (MF), fine soil (SOILf).
Rain mass fractions are noted as Rain Ca frac, Rain Cl frac, Rain Mg frac, Rain K frac, Rain Na frac, Rain SO_4 frac, and Rain NO_3 frac.

Values are only shown when statistically significant with respect to a two-tailed student's t-test (95% confidence). The values in parentheses indicate the sample range.

	NO3 Rain Mass Frac				SO4 Rain Mass Frac			
	Chir NM	Grand Canyon	Organ Pipe NM	Pet NP	Chir NM	Grand Canyon	Organ Pipe NM	Pet NP
Ca frac	-0.20 (172)	-	-	-0.22 (113)	-0.26 (172)	-	-	-
Cl frac	-0.29 (67)	-0.43 (71)	-	-0.22 (72)	0.41 (67)	-0.27 (71)	-	-
Mg frac	-0.22 (99)	-	-	-0.36 (97)	-0.27 (99)	-0.20 (113)	-	-0.26 (97)
K frac	-0.16 (172)	-0.17 (153)	-	-	-0.36 (172)	-	-0.22 (193)	-
Na frac	-	-	-	-0.42 (113)	-0.25 (138)	-	-	-
SO_4 frac	0.15 (172)	0.32 (153)	0.22 (93)	0.18 (113)	0.40 (172)	0.19 (153)	-	0.22 (113)
NO_3 frac	-	-0.20 (153)	-	-	-0.34 (172)	-0.19 (153)	-	-
Rain Ca frac	-0.61 (171)	-0.76 (152)	-0.51 (93)	-0.64 (113)	-0.16 (171)	-	-	-0.46 (113)
Rain Cl frac	-0.40 (172)	-0.50 (153)	-0.46 (93)	-0.45 (113)	-	-	-0.29 (93)	-0.29(112)
Rain Mg frac	-0.47 (172)	-0.66 (153)	-0.61 (93)	-0.56 (113)	-0.27 (172)	-	-0.23 (93)	-0.61 (113)
Rain K frac	-0.39 (172)	-0.60 (153)	-0.49 (93)	-0.26 (112)	-0.21 (172)	-	0.23 (94)	-0.23 (112)
Rain Na frac	-0.30 (172)	-0.46 (153)	-0.45 (93)	-0.50 (113)	-0.20 (172)	-	-0.30 (93)	-0.32 (113)
Rain SO4 frac	-0.46 (172)	-0.46 (153)	-0.50 (93)	-	1.00	1.00	1.00	1.00
Rain NO3 frac	1.00	1.00	1.00	1.00	-0.46 (172)	-0.46 (153)	-0.50 (93)	-
CM	-0.17 (172)	-	-0.33 (93)	-0.27 (113)	-0.30 (172)	-	-	-
MT	-0.17 (172)	-	-0.30 (93)	-0.25 (113)	-0.28 (172)	-	-	-
MF	-	-	-	-	-	-	-	-
f SOIL	-0.17 (172)	-	-	-0.25 (113)	-0.28 (172)	-	-	-
Rain Accumulation	0.32 (172)	0.23 (153)	-	-	-	-	-	0.28 (132)
Rain pH	-0.26 (172)	-0.57 (153)	-	-0.43 (112)	-0.34 (172)	-	-0.36 (94)	-0.38 (112)
Rain Conductivity	-0.19 (172)	-0.35(153)	-	-	-	-	-	-0.20 (112)

4.7: Amount of Moles in Rain Data

Due to the dilution of rain concentrations by rain accumulation, it is difficult to determine whether the amount of a certain rain species is higher with respect to an increase in rainfall. The positive relationships (Section 4.6-Tables 19 and 20) found between NO_3^- and SO_4^{2-} rain mass fractions indicated that the abundance of NO_3^- and SO_4^{2-} increase, while all others decrease. However, it is not possible to determine if the amount of rain species increase or decrease (the absolute amount) due to the high volume of water in samples by precipitation (dilution). NADP reports the sample volume in mL (Svol), and by converting the Svol to L and then multiplying the rain concentrations (mg/L) by the sample volume, then the amount of rain species in moles can be found. This value can provide information on the absolute amount of rain species. It is expected that by correlating the moles found in rain water to aerosol and rain data (as done in previous sections),

the aerosol and precipitation relationships will change. Similar to Section 4.4, the weekly averages were calculated to correlate aerosol data.

4.7.1: Grand Annual Mean of Moles in Rain

Similar to Section 4.1.1, the grand annual mean of moles in rain during the monsoon were calculated. Comparing all sites, in Chiricahua, the highest absolute amounts of NO_3^-, SO_4^{2-}, and total species were found (Figure 15). Based on results of Section 4.1.1, this site had the most acidic pH (Figure 7, pH=5.39). There are several results that can be used to justify the observations of most acidic pH. First based on Section 4.1.1, Chiricahua contained the highest SO_4^{2-} air mass fraction (Figure 12) and lowest Ca and K air mass fractions in all sites (Figures 12 and 13). Based on Section 4.6, higher SO_4^{2-} aerosol mass fraction (acidic) compared to Ca and K air mass fractions (alkaline) results in more acidic pH. Second, Chiricahua had the highest rain accumulation (Figure 6) which resulted (by dilution) in the lowest rain concentrations (Figures 8 and 9, except K and SO_4^{2-}). However, the rain mass fractions of NO_3^- and SO_4^{2-} were highest in Chiricahua (Figure 11). As found in Sections 4.5.2 and 4.6, the highest abundance of NO_3^- and SO_4^{2-} in rain not only coincides with the highest rain accumulation, but also the most acidic pH. The result of highest amount of moles of NO_3^- and SO_4^{2-} in rain (Figure 15), which are acidic also serves to justify the observation of most acidic pH in Chiricahua.

The opposite case is found in Petrified NP where the most alkaline pH is observed (Figure7, pH=5.92). In Petrified NP, the lowest mole amounts of NO_3^- and SO_4^{2-} (Figures 14, 15 ,16, including Cl^-, K^+, Na^+ and total amount of moles) and highest Ca^{2+} mole amounts are found. This means that there are less acidic species (NO_3^- and SO_4^{2-}) and more alkaline ones (Ca^{2+}), resulting in a more alkaline pH. In addition, the lowest rain accumulation is found (Figure 6) which coincides with higher rain concentrations (Figures 8 and 9, all except Cl^- and Mg^{2+}), however the highest Ca^{2+} and lowest NO_3^- rain mass fractions are observed (Figures 10 and 11). Although the rain concentrations

of many rain species are high, the abundance and amount of moles of the more alkaline ones (Ca^{2+}) are higher and the more acidic species (NO_3^- and SO_4^{2-}) are lower. This balance of ions favors a more alkaline pH, justifying the observations found in Petrified NP. When comparing the amount, abundance, and concentration in rain, NO_3^- was greatest in all sites (Figures 5, 13, 15). Similar observations of NO_3^- being the most dominant anion in rain have been noted in studies by Hutchings et al. (2009) and Sorooshian et al. (2013). The next highest mole amount was SO_4^{2-} in all sites except in Petrified NP where in some years Ca^{2+} would be greater than SO_4^- (as seen in Section 4.1.2). The high absolute amount of Ca^{2+} in Petrified NP can also be used to justify the observation of the most alkaline pH.

Based on the analysis of grand annual averages, it would appear that the trends in rain concentration are misleading due to dilution by rain. Despite the appearance of low concentrations which is due to a high amount of water, there can still be a high absolute amount (moles) and abundance (mass fraction) of other rain ions as observed in Chiricahua and Petrified NP.

Annual correlations with respect to moles in rain only showed significance (although not shown in tables) for K^+ in Petrified NP (r= -0.58, n=12).

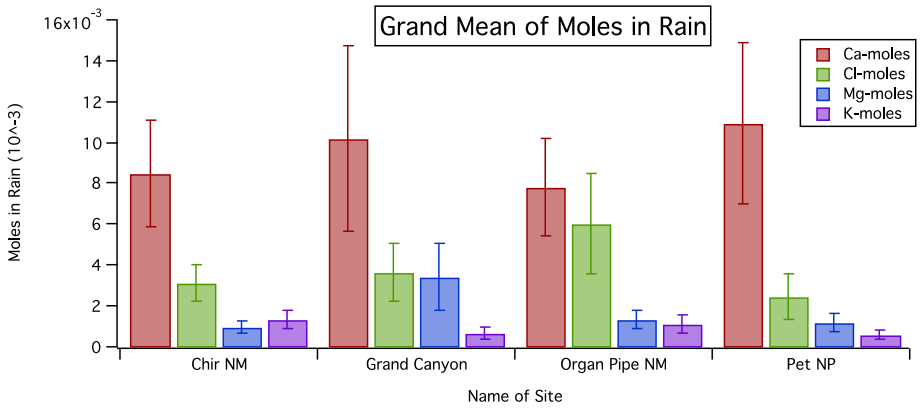

Figure 14: This bar graph exhibits the grand annual mean of amount of moles in rain of calcium (Ca-moles), chloride (Cl-moles), magnesium (Mg-moles), and potassium (K-moles) for Chiricahua

National Monument (Chir NM), Grand Canyon, Organ Pipe National Monument (Organ Pipe NM), and Petrified National Park (Pet NP). Error bars were calculated by standard error of mean.

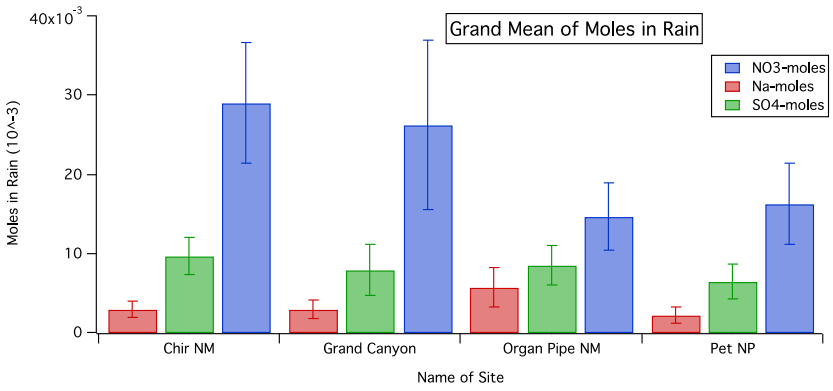

Figure 15: This bar graph exhibits the grand annual mean of amount of moles in rain of sodium (Na-moles), nitrate (NO3-moles), and sulfate (SO4-moles) for Chiricahua National Monument (Chir NM), Grand Canyon, Organ Pipe National Monument (Organ Pipe NM), and Petrified National Park (Pet NP). Error bars were calculated by standard error of mean.

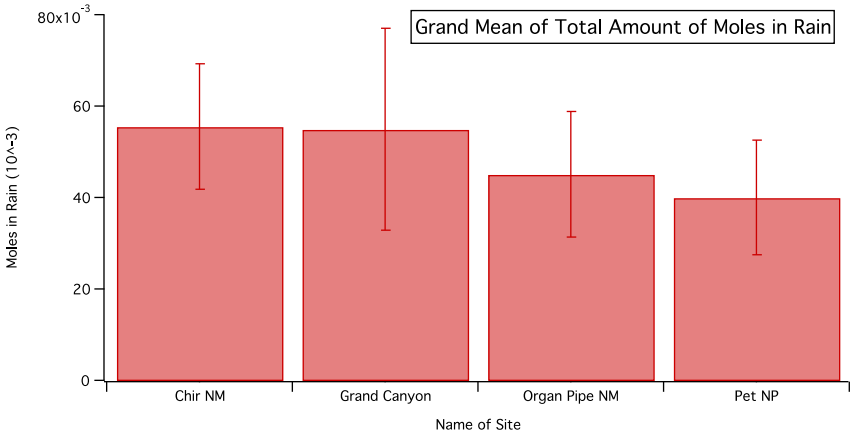

Figure 16: This bar graph exhibits the grand annual mean of total amount of moles in rain for Chiricahua National Monument (Chir NM), Grand Canyon, Organ Pipe National Monument (Organ

Pipe NM), and Petrified National Park (Pet NP). Error bars were calculated by standard error of mean.

4.7.2: Moles in Rain vs Aerosol and Precipitation Data

The correlation between aerosol concentrations and moles in rain (Table 21) showed positive relationships for all correlations except Cl^-. This indicates that as aerosol concentrations increase so does the amount of its respective rain species. Similar to the results for NO_3^- and SO_4^{2-} rain mass fractions (Table 13), the moles of NO_3^- and SO_4^{2-} in rain exhibited negative relationships (Table 22) with respect to coarse mass, PM_{10}, $PM_{2.5}$ and fine soil. In most cases, the amount of moles in rain correlated significantly better with rain mass fractions than rain concentrations (Table 23). This result is possibly due to the role of precipitation, where dilution of rain concentrations can cause lower correlations to amount of rain species.

4.7.3: Moles in Rain vs Rain Accumulation

The correlation with respect to rain accumulation (Table 24) revealed that all rain species contained positive significant correlations. The total number of moles (calculated by adding up all the rain species) also showed high positive correlations. These results contrast with those in Table 16 where all rain concentrations and all rain mass fractions (except NO_3^- and SO_4^{2-}) exhibit negative trends with respect to rain accumulation. The positive relationships observed in Table 24, mean that at higher rain accumulation the absolute amount of rain species increases. This is likely due to the uptake of aerosol by cloud seeding and scavenging where decreasing correlations with respect to aerosol concentrations are found (Section 4.5.1- Table 15).

In all sites, the highest correlated species were NO_3^- and SO_4^{2-} (Table 24) in Chiricahua NM there is a tie between NO_3^- and K^+). This result is similar to the results found for SO_4^{2-} and NO_3^- rain mass fractions (Section 4.5.2- Table 16). These results further prove that the absolute amount and

abundance of NO_3^- and SO_4^{2-} is enhanced by an increase in rain accumulation. This is most likely due to the high hygroscopicity and abundance in air of acidic precursor gases of NO_3^- and SO_4^{2-}.

The positive correlations with respect to the moles in rain of alkaline species such as Ca^{2+} and Mg^{2+} indicate that despite the dilution of alkaline rain concentrations by higher rain accumulation, there is an increase in the absolute amount of alkaline rain species in water (Table 24). However, the amount of acidic components, NO_3^- and SO_4^{2-} in rain increase greater than the alkaline components. Therefore, as rain accumulation increases, the acidity in rain pH is more driven by the increase of NO_3^- and SO_4^{2-} in rain water (both contribute to acidity) than the dilution of alkaline rain concentrations. The high influence of NO_3^- and SO_4^{2-} on rain water is further explained by the interrelationships between moles in rain (Appendix Tables 2-5). These results revealed that the total amount of moles in rain was more characteristic of NO_3^- and SO_4^{2-} in all sites (higher correlation values).

Table 21: This table shows the correlation (r value) of the relationships between amount of moles in rain and aerosol data in Chiricahua National Monument (Chir NM), Grand Canyon, Organ Pipe National Monument (Organ Pipe NM), and Petrified National Park (Pet NP). The data ranged from 1999-2014 for Chir NM and Grand Canyon and 2003-2014 for Organ Pipe and Pet NP.
Amount of moles in rain are noted as Rain Ca-moles, Rain Cl-moles, Rain Mg-moles, Rain K-moles, Rain Na-moles, Rain SO_4-moles, and Rain NO_3-moles.
Aerosol concentrations are noted as calcium (Aerosol Ca), chloride (Aerosol Cl), magnesium (Aerosol Mg), potassium (Aerosol K), sodium (Aerosol Na), sulfate (Aerosol SO_4), and nitrate (Aerosol NO_3).
Aerosol mass fractions are noted as calcium (Aerosol Ca frac), chloride (Aerosol Cl frac), magnesium (Aerosol Mg frac), potassium (Aerosol K frac), sodium (Aerosol Na frac), sulfate (Aerosol SO_4 frac), and nitrate (Aerosol NO_3 frac).
Values are only shown when statistically significant with respect to a two-tailed student's t-test (95% confidence). The values in parentheses indicate the sample range.

	Rain (moles) vs Aerosol Data			
	Chir NM	Grand Canyon	Organ Pipe NM	Pet NP
Rain Ca- moles vs Aerosol Ca	0.19 (171)	-	-	-
Rain Cl-moles vs Aerosol Cl	-0.20 (172)	-	-	-
Rain Mg-moles vs Aerosol Mg	-	-	-	-
Rain K-moles vs Aerosol K	0.15 (172)	0.26 (147)	-	0.17 (139)
Rain Na-moles vs Aerosol Na	0.20 (154)	-	-	-
Rain SO_4 -moles vs Aerosol SO_4	0.17 (172)	0.20 (147)	-	-
Rain NO_3 -moles vs Aerosol NO_3	0.18 (172)	-	-	-
Rain Ca- moles vs Aerosol Ca frac	0.18 (171)	-	-	-
Rain Cl-moles vs Aerosol Cl frac	-	-	-	-
Rain Mg-moles vs Aerosol Mg frac	0.19 (172)	-	-	-
Rain K-moles vs Aerosol K frac	0.24 (172)	-	-	0.29 (139)
Rain Na-moles vs Aerosol Na frac	-	-	-	-
Rain SO4 -moles vs Aerosol SO_4 frac	-	0.29 (147)	0.21 (146)	-
Rain NO3 -moles vs Aerosolf NO_3 frac	0.23 (171)	-	-	-

Table 22: This table shows the correlation (r value) of the relationships between amount of moles in rain and aerosol data in Chiricahua National Monument (Chir NM), Grand Canyon, Organ Pipe National Monument (Organ Pipe NM), and Petrified National Park (Pet NP). The data ranged from 1999-2014 for Chir NM and Grand Canyon and 2003-2014 for Organ Pipe and Pet NP.
Amount of moles in rain are noted as Rain Ca-moles, Rain Cl-moles, Rain Mg-moles, Rain K-moles, Rain Na-moles, Rain SO_4-moles, and Rain NO_3-moles.
Aerosol concentrations are noted as coarse mass (CM), PM_{10} (MT), $PM_{2.5}$ (MF), fine soil (SOILf).
Values are only shown when statistically significant with respect to a two-tailed student's t-test (95% confidence). The values in parentheses indicate the sample range.

	Coarse Mass (CM)				PM_{10} (MT)				$PM_{2.5}$ (MF)				Fine Soil (Soilf)			
	Chir NM	Grand Canyon	Organ Pipe NM	Pet NP	Chir NM	Grand Canyon	Organ Pipe NM	Pet NP	Chir NM	Grand Canyon	Organ Pipe NM	Pet NP	Chir NM	Grand Canyon	Organ Pipe NM	Pet NP
Rain Ca- moles	0.22 (171)	-	-	-	0.22 (171)	-	-	-	0.19 (171)	-	-	-	0.21 (171)	-	-	-
Rain Cl- moles	-	-	-	-	-	-	-	-	-	-	-	-	-	-	-	-
Rain Mg- moles	0.24 (172)	-	-	-	0.24 (171)	-	-	-	0.21 (172)	-	-	-	0.21 (172)	-	-	-
Rain K- moles	-	-	-	-	-	-	-	-	-	-	-	-	-	-	-	-
Rain Na- moles	0.18 (172)	-	-	-	0.18 (172)	-	-	-	-	-	-	-	0.17 (172)	-	-	-
Rain SO_4- moles	-	-	-0.21 (146)	-	-	-	-0.21 (146)	-	-	-	-0.17 (146)	-	-	-	-0.23 (146)	-
Rain NO_3- moles	-	-	-0.23 (146)	-	-	-	-0.22 (146)	-	-	-	-	-	-	-	-0.20 (146)	-

Table 23: This table shows the correlation (r value) of the relationships between amount of moles in rain and rain data in Chiricahua National Monument (Chir NM), Grand Canyon, Organ Pipe National

Monument (Organ Pipe NM), and Petrified National Park (Pet NP). The data ranged from 1999-2014 for Chir NM and Grand Canyon and 2003-2014 for Organ Pipe and Pet NP.
Amount of moles in rain are noted as Rain Ca-moles, Rain Cl-moles, Rain Mg-moles, Rain K-moles, Rain Na-moles, Rain SO_4-moles, and Rain NO_3-moles.
Rain concentrations are noted as Rain Ca for Ca^{2+}, Rain Cl for Cl^-, Rain Mg for Mg^{2+}, Rain K for K^+, Rain Na for Na^+, Rain SO_4 for SO_4^{2-} and Rain NO_3 for NO_3^-.
Rain mass fractions are noted as Rain Ca frac, Rain Cl frac, Rain Mg frac, Rain K frac, Rain Na frac, Rain SO_4 frac, and Rain NO_3 frac.
Values are only shown when statistically significant with respect to a two-tailed student's t-test (95% confidence). The values in parentheses indicate the sample range.

	Rain (moles) vs Rain Data			
	Chir NM	Grand Canyon	Organ Pipe NM	Pet NP
Rain Ca- moles vs Rain Ca	0.20 (153)	-	-	0.25 (93)
Rain Cl-moles vs Rain Cl	-	-	-	0.59 (93)
Rain Mg-moles vs Rain Mg	-	-	-	0.30 (93)
Rain K-moles vs Rain K	0.25 (154)	0.19 (119)	-	0.30 (92)
Rain Na-moles vs Rain Na	0.20 (154)	-	-	0.53 (93)
Rain SO_4 -moles vs Rain SO_4	-	-	-	-
Rain NO_3 -moles vs Rain NO_3	-	-	-	-
Rain Ca- moles vs Rain Ca frac	0.41 (153)	0.22 (119)	0.38 (70)	0.45 (93)
Rain Cl-moles vs Rain Cl frac	-0.24 (154)	-	0.59 (69)	-
Rain Mg-moles vs Rain Mg frac	0.23 (154)	0.22 (119)	0.33 (70)	0.44 (93)
Rain K-moles vs Rain K frac	0.44 (154)	0.45 (119)	0.69 (70)	0.37 (92)
Rain Na-moles vs Rain Na frac	0.65 (153)	0.34 (118)	0.62 (70)	-
Rain SO4 -moles vs Rain SO_4 frac	-	0.32(118)	0.42 (70)	0.32 (93)
Rain NO3 -moles vs Rain NO_3 frac	0.38 (154)	-	-	-

Table 24: This table shows the correlation (r value) of the relationships between rain accumulation and amount of moles in rain in Chiricahua National Monument (Chir NM), Grand Canyon, Organ Pipe National Monument (Organ Pipe NM), and Petrified National Park (Pet NP). The data ranged from 1999-2014 for Chir NM and Grand Canyon and 2003-2014 for Organ Pipe and Pet NP.
Amount of moles in rain are noted as Rain Ca-moles, Rain Cl-moles, Rain Mg-moles, Rain K-moles, Rain Na- moles, Rain SO_4-moles, and Rain NO_3-moles.
The Total-moles row corresponds to the sum of all moles in rain.
Values are only shown when statistically significant with respect to a two-tailed student's t-test (95% confidence). The values in parentheses indicate the sample range.

	Rain Accumulation Correlations- Rain Data			
	Chir NM	Grand Canyon	Organ Pipe NM	Pet NP
Rain Ca- moles	0.51 (153)	0.68 (118)	0.39 (70)	0.49 (93)
Rain Cl- moles	0.55 (154)	0.67 (119)	0.72 (69)	0.29 (93)
Rain Mg- moles	0.46 (154)	0.65 (119)	0.51 (70)	0.45 (93)
Rain K- moles	0.78 (154)	0.65 (119)	0.67 (70)	0.42 (92)
Rain Na- moles	0.46 (154)	0.57 (118)	0.73 (70)	0.26 (93)
Rain SO_4- moles	0.74 (154)	0.83 (119)	0.75 (70)	0.72 (93)
Rain NO_3- moles	0.78 (154)	0.84 (118)	0.81 (70)	0.75 (93)
Total- moles	0.77 (154)	0.82 (119)	0.81 (70)	0.71 (93)

4.8: Inter-Site Correlations

The Kruskal–Wallis test is a method that does not require a normal distribution for testing whether samples originate from the same distribution. The test at 95% confidence (Table 25) was applied to weekly averaged aerosol concentrations of each site to determine if a site had similar distribution (air mass sources) to another site. The inter-site correlations between Chiricahua and Organ Pipe, resulted in no significant values (p-value has to greater than 0.05 to be significant). This indicates that the aerosol chemistry is not of the same distribution (air mass source). The result makes sense due to large distance between both sites where Chiricahua is the eastern-most site and Organ Pipe is the southwestern-most site (Table 1 and Figure 1). The test applied between Chiricahua and the Grand Canyon, resulted in $PM_{2.5}$ and all aerosol concentrations except SO_4^{2-} were found to be significant. These results suggest that Chiricahua and the Grand Canyon share similar air mass sources. The inter-site correlations between Chiricahua and Petrified NP resulted in similar distributions for coarse mass, PM_{10}, $PM_{2.5}$, fine soil, Cl^-, Mg, K, Na, and NO_3^- aerosol concentrations. Hence, both sites may share similar air mass sources. When comparing Organ Pipe and Petrified NP, no significant values were found (p-value has to greater than 0.05 to be significant). This indicates that the aerosol chemistry is not of the same distribution (air mass source). The same results were

found when comparing Organ Pipe and the Grand Canyon. When comparing the Grand Canyon and Petrified NP, Cl^-, K, Na, and NO_3^- were found to be significant. Hence, both sites may share similar air mass sources. Therefore, by using the Kruskal–Wallis H test, it was determined that Chiricahua, Grand Canyon, and Petrified NP may share similar air mass distributions. Organ Pipe, however, is not related to any site.

Table 25: This table reports the results of the Kruskal–Wallis (2 tailed- 95 % confidence) for weekly averaged aerosol concentration data in Chiricahua National Monument (Chir NM), Grand Canyon, Organ Pipe National Monument (Organ Pipe NM), and Petrified National Park (Petrified NP). Aerosol concentrations are noted in $\mu g\ m^{-3}$ as coarse mass (CM), PM_{10} (MT), $PM_{2.5}$ (MF), fine soil (SOILf), calcium (Ca), chloride (Cl), magnesium (Mg), potassium (K), sodium (Na), sulfate (SO_4), and nitrate (NO_3). The P-value must be greater than 0.05 to be considered significant. If the P-value is significant then the H-value is FALSE, and the distribution is the "same". If the P-value is less than 0.05 (insignificant), then the H-value is 1 and the distribution is "different".

Kruskal-Wallis H-test											
Aerosol concentration data	CM	MT	MF	SOILf	Ca	Cl	Mg	K	Na	SO_4	NO_3
Chiricahua NM vs Grand Canyon											
P-value	2.48E-11	5.22E-06	0.0576	0.0013	0.0652	0.4228	0.096	0.4654	0.2932	1.52E-18	0.1635
H-value	1	1	FALSE	1	FALSE	FALSE	FALSE	FALSE	FALSE	1	FALSE
Same or different distribution?	different	different	same	different	same	same	same	same	same	different	same
Chiricahua NM vs Petrified NP											
P-value	0.5451	0.8543	0.4855	0.1863	0.0259659	0.7099	0.2375	0.652	0.4051	2.67E-10	0.0055
H-value	FALSE	FALSE	FALSE	FALSE	1	FALSE	FALSE	FALSE	FALSE	1	1
Same or different distribution?	same	same	same	same	different	same	same	same	same	different	different
Grand Canyon vs Petrified NP											
P-value	1.47E-09	1.89E-06	0.0032	1.71E-09	1.35E-07	0.161	0.0006	0.7336	0.0537	0.0039	0.1601
H-value	1	1	1	1	1	FALSE	1	FALSE	FALSE	1	FALSE
Same or different distribution?	different	different	different	different	different	same	different	same	same	different	same
Chiricahua NM vs Organ Pipe NM											
P-value	2.28E-13	3.65E-12	1.29E-05	1.21E-07	2.07E-13	3.17E-06	5.14E-06	5.23E-07	8.20E-19	1.64E-13	1.45E-28
H-value	1	1	1	1	1	1	1	1	1	1	1
Same or different distribution?	different	different	different	different	different	different	different	different	different	different	different
Grand Canyon vs Organ Pipe NM											
P-value	6.41E-35	5.48E-28	2.75E-09	1.15E-22	3.51E-26	3.42E-10	1.63E-13	1.54E-11	4.26E-27	1.08E-33	5.25E-29
H-value	1	1	1	1	1	1	1	1	1	1	1
Same or different distribution?	different	different	different	different	different	different	different	different	different	different	different
Petrified NP vs Organ Pipe NM											
P-value	1.95E-15	2.73E-12	3.13E-05	9.06E-08	8.37E-13	4.04E-12	2.24E-06	4.72E-10	8.61E-16	1.81E-26	1.03E-25
H-value	1	1	1	1	1	1	1	1	1	1	1
Same or different distribution?	different	different	different	different	different	different	different	different	different	different	different
All sites											
P-value	5.02E-38	2.12E-28	3.32E-09	1.30E-21	3.05E-27	1.03E-14	2.26E-13	5.30E-12	5.75E-30	7.51E-47	6.68E-40
H-value	1	1	1	1	1	1	1	1	1	1	1
Same or different distribution?	different	different	different	different	different	different	different	different	different	different	different

4.9: Effect of Air Mass Source on Aerosol and Precipitation Chemistry: Case Studies during the Monsoon Period in Chiricahua and Organ Pipe

In this section, the aerosol and precipitation chemistry in Chiricahua and Organ Pipe were compared because the aerosol concentrations were found to have different distributions (Section 4.8). In addition, Organ Pipe is the southwestern-most located site and Chiricahua is the southeastern-most (Table 1 and Figure 1). Based on the results of Jana et al. (2018), in Laveen, Arizona (site located closest to Organ Pipe) most of the air mass sources of moisture originated from the Gulf of California. In the same study, in Red Rock, New Mexico (site located closest to Chiricahua) the moisture pathways originated from both the Gulf of California and Gulf of Mexico. By combining the results in Section 4.8 and Jana et al. (2018), Chiricahua and Organ Pipe can be speculated to come from different air mass sources.

To perform the case studies in this section, the first step was to find the dates of when the backward air mass trajectories at each site (using HYSPLIT Section 2.3) originated from either the Gulf of California or Gulf of Mexico. Next, the aerosol and precipitation data in the same time span as the air mass trajectories were found.

After analyzing an extensive amount of HYSPLIT backward air mass trajectories, it was difficult to find the particular dates in which the air mass source of Chiricahua originated from the Gulf of Mexico and Organ Pipe from the Gulf of California. It can be concluded that although there are different air mass distributions affecting Organ Pipe and Chiricahua (Section 4.8), the origin of air mass for Chiricahua originates mainly from the Gulf of California and at times from both sources. The results of Red Rock, New Mexico by Jana et al. (2018) also report this finding. It is necessary to find a co-located NADP-IMPROVE site that is closer to the east such as in New Mexico where HYSPLIT back trajectories can render more air mass pathways from the Gulf of Mexico. Organ Pipe

in Arizona can be used for similar analysis to represent the site that is characteristic of emissions from the Gulf of California. Then aerosol chemistry and precipitation can be compared between both locations to show whether the moisture pathway originating from the Gulf of California and Gulf of Mexico during the Monsoon plays a role in affecting the aerosol and precipitation chemistry relationships observed within this study.

5. Summary of Results

This study identified the relationships between aerosol and precipitation chemistry during the monsoon season (June 15- September 15) in Arizona by using four co-located IMPROVE and NADP sites. Relationships were determined by using the using a two-tailed student's t-test (95% confidence). The main results of the study are as follows, following the order presented in the results section (Section 4).

The grand annual mean during the monsoon (Section 4.1.1) was calculated to compare the aerosol and precipitation chemistry between sites. Organ Pipe had the highest grand annual mean of coarse mass, PM_{10}, $PM_{2.5}$, fine soil and all aerosol concentrations. This finding was justified by Organ Pipe's low altitude and location where it is situated closer to marine and dust emissions. Chiricahua National Monument (NM) had the highest precipitation amount, most acidic pH, and lowest rain concentrations. In contrast, Petrified National Park (NP) was the site with the lowest rain accumulation, most alkaline pH, and highest rain concentrations. By analyzing the differences in grand annual mean between sites, the relationship where higher rain accumulation results in lower rain concentrations (dilution due to high water amount) and coincides with the most acidic pH is found. This relationship applies in the opposite case and was also observed when considering specific years within each site (Section 4.1.2).

Annual correlations (Section 4.2.1) with respect to aerosol concentrations resulted in significant decreasing trends for SO_4^{2-} in Chiricahua and the Grand Canyon. This is due to air pollution regulations since SO_4^{2-} has been attributed to anthropogenic emissions (Hutchings et al., 2009; Sorooshian et al., 2013). Regarding aerosol mass fractions, there were no major conclusions that could be made. The interrelationships between aerosol concentrations (Section 4.2.2), showed that coarse mass, PM_{10}, $PM_{2.5}$ correlated the highest to fine soil and other crustal emissions (Ca, Mg, K) in all sites except Petrified NP (higher sea salt correlation). This result suggests that the major pollution sources are mostly dust emissions in all sites with contributions of sea salt in Petrified NP. In all sites, Ca and Mg were most related to each other indicating that both are characteristic of the same source (dust emissions). Na and Cl^- were best correlated to each other in all sites except in Chiricahua where Na was found to have higher correlation values to dust concentrations (Ca, Mg). K correlated best with dust emissions except in Petrified NP where due to high correlation with NO_3^-, biomass burning sources for K were speculated (Schlosser et al., 2017). In all sites except in Petrified NP, aerosol concentrations of SO_4^{2-} correlated best with NO_3^-.

The annual correlations regarding rain chemistry (Section 4.3.1) exhibited increasing trends for pH (trend toward alkalinity) in Chiricahua and Grand Canyon. This result can be explained by the reduction of sulfate aerosol concentrations with respect to year (Section 4.2.1). The interrelationships between rain concentrations showed that in all sites rain conductivity was best correlated to SO_4^{2-} and NO_3^-. Rain pH exhibited the highest positive correlation value to Ca^{2+}indicating the role of Ca in acid neutralization. In all sites, rain interrelationships resulted in Ca^{2+}, Mg^{2+}, and K^+ correlating best with one another suggesting that they all originate from crustal emissions. The high correlations found between Na^+ and Cl^- in all sites show that these ions can originate from sea salt emissions. In addition, NO_3^- and SO_4^{2-} correlated best with one another in all sites.

To correlate aerosol and rain data, weekly averages were calculated. The correlation between aerosol and rain concentrations (Section 4.4.1) showed that in all sites, K correlated significantly. The highest correlation value was found in Chiricahua for Ca. In all sites except Organ Pipe, aerosol concentrations of Ca, Cl^-, K, and NO_3^- correlated to their respective rain concentration. These results imply that cloud seeds in these sites can be found in the form of dust emissions (Ca, K), sea salt (Cl^-) and NO_3^-. Cloud seeds in the form of NO_3^- are likely from water soluble dust particles coated with NO_3^-, which are formed by the reactions of precursors of NO_3^- and dust particles (Karydis et al., 2016). Precursors of NO_3^- can also be collected by precipitation via scavenging. The correlations for mass fractions (Section 4.4.2) show that in the Grand Canyon, aerosol and rain mass fractions are negative implying that both are inversely related. In all sites, rain concentrations of Ca^{2+} and Mg^{2+}correlated best with respect to coarse mass, PM_{10}, $PM_{2.5}$, fine soil (Section 4.4.3), indicating that the rain concentrations originate from crustal emissions. In Chiricahua and Grand Canyon, Fine soil correlated with Cl^-, NO_3^-, SO_4^{2-} indicating that acidic gases reacted with crustal particles (Matsuki et al., 2010). Rain pH exhibited significant negative trends (Section 4.4.4) with SO_4^{2-} aerosol mass fraction, demonstrating the acidic profile of SO_4^{2-}.

Correlations between rain accumulation and aerosol and precipitation data were done to analyze the role of precipitation amount on aerosol and precipitation chemistry and relationships. All significant correlations between rain accumulation and aerosol concentrations were negative (Section 4.5.1), demonstrative of the ability of rain to serve as a sink (dilute concentrations). All aerosol mass fractions were negative (Section 4.5.1) except for SO_4^{2-} suggesting that the increase in abundance of SO_4^{2-} in aerosol coincides with an increases of rain accumulation. The significant correlation values between rain concentration and rain accumulation exhibited negative values (Section 4.5.2), which shows the dilution effect by rain. All rain mass fractions exhibited negative trends except NO_3^- and SO_4^{2-}. This result suggests that the abundance of NO_3^- and SO_4^{2-} in rain increases as rain

accumulation increases. This result also coincides with the most acidic pH and it was speculated that the acidity in pH was driven by a combination of the increased abundance of NO_3^- and SO_4^{2-} (provides more acidity) and high precipitation amount (results in lower rain concentrations).

Combining the results of Sections 4.4.2, 4.5.1 and 4.5.2, the observation of an inverse relationship between the air and rain mass fractions of NO_3^- was noted. Based on the results of Section 4.6, it was concluded that air mass fractions of NO_3^- were more alkaline while the rain mass fractions of NO_3^- were more acidic. In the atmosphere, NO_3^- in the form of HNO_3 can react with dust emissions to form compounds that can be alkaline (Karydis et al., 2016). The products of these reactions are highly water soluble and can serve as cloud seeds. Once in rain solution, NO_3^- is acidic. In addition, the correlation values for acidic mass fractions were found to be positive with respect to SO_4^{2-} air mass fractions and rain accumulation and negative for all other aerosol and precipitation data. The opposite case was also observed, and it was concluded that aerosol and rain mass fractions can be used as proxies for acidity and alkalinity. Therefore, the sign of the correlation values of aerosol and rain mass fractions with respect to other aerosol and precipitation data can be used to determine if the fraction is acidic or alkaline.

The results in Section 4.5.2 indicate that the abundance of NO_3^- and SO_4^{2-} increase despite the dilution of rain concentrations by high rain accumulation. It was necessary to determine the absolute amount of rain species to justify the trend of higher rain accumulation coinciding with more acidic rain pH. The amount of moles in rain was calculated (Section 4.7) by multiplying the rain concentration (mg/L) by the reported sample volume. By calculating the grand annual mean during the monsoon of amount of moles in rain, the highest absolute amounts of NO_3^- and SO_4^{2-} were found in Chiricahua than other sites. Using the results of Section 4.1.1, the most acidic rain pH is also found in Chiricahua. This coincides with the highest air mass fraction of SO_4^{2-}, highest rain accumulation, lowest rain concentrations, and highest rain mass fractions of NO_3^- and SO_4^{2-}. Combining these

results, it is apparent that despite the dilution of rain concentrations by high rain accumulation, the abundance and absolute amount of acidic species is high, and this justifies the acidic pH found in that site. The opposite case was analyzed in Petrified NP, where despite the presence of the lowest precipitation amount and higher rain concentrations, the site had the lowest abundance and absolute amount of NO_3^- and SO_4^{2-} resulting in the most alkaline pH being found in this site. This site also had the highest abundance and amount of moles of Ca^{2+} which is alkaline due to its source from dust. Therefore, rain pH was found to be affected by the balance between the abundance and absolute amount of alkaline and acidic rain species. It was noted that the trends in rain concentration were misleading because despite the appearance of low concentrations (due to a high amount of water) there can still be a high absolute amount (moles) and abundance (mass fraction) of other rain ions as observed in Chiricahua and Petrified NP.

The correlation between amount of moles in rain and rain accumulation (Section 4.7.3) resulted in significant positive relationships for all rain species in all sites. In addition, the amount of moles of NO_3^- and SO_4^{2-} have the highest correlation values, suggesting that they increase the most with respect to increased rainfall. This result corroborates the trend that as rain accumulation increases so does the absolute amount of acidic ions and acidity in rain pH. The results of this correlation also serve to explain the full picture behind aerosol scavenging. First based on the results of Section 4.5.1, as rain accumulation increases, all aerosol concentrations decrease. Based on the concept of aerosol scavenging, rain water uptakes aerosols and should be found in rain water. The positive significant correlations between amount of moles in rain and rain accumulation (Section 4.7.3) provides this evidence. The high enhancements of NO_3^- and SO_4^{2-} are most likely due to the high hygroscopicity and ability of acidic precursors to enter precipitation via cloud seeding and scavenging. Rain concentrations decrease with respect to increasing rain accumulation and it is

necessary to find the absolute amount in rain (by looking at moles in rain) to explain the uptake of aerosols by rain.

The Kruskal–Wallis test (Section 4.8) was applied to aerosol concentrations to determine if sites shared the same air mass distribution or not. The results were that Chiricahua, Grand Canyon, and Petrified NP shared aerosol concentrations of the same distribution while Organ Pipe did not share any. In Section 4.9, it was attempted to investigate the effect of air mass location on aerosol and rain chemistry and relationships by comparing Chiricahua and Organ Pipe. However, it was difficult to find dates in which air mass sources in Chiricahua that came from the Gulf of Mexico overlapped with air mass sources in Organ Pipe that came from the Gulf of California.

6. Implications to the Study Area and Future Projections

The rain provided by the North American Monsoon in Arizona is critical to the area's terrestrial and aquatic ecosystems by providing water and essential nutrients such as phosphorus (Eger et al., 2013; Aciego et al., 2017). Arizona is characterized by high dust emissions and it has been shown that NO_3^- and SO_4^{2-} based acids can react with dust to produce highly water-soluble salts that can serve as cloud condensation nuclei (CCN) and ice nuclei (IN) (Matsuki et al., 2010; Karydis et al., 2016). This pathway provides ease for acidic anions to enter rain water which acidifies precipitation chemistry. The inverse relationship between air and rain mass fractions of NO_3^- reported in this study presents evidence of these reactions occurring. In addition, a major result of this study is that as rain accumulation increases, aerosol concentrations decrease and the amount of moles in rain increase. This suggests that the increased precipitation provided by the monsoon results in the uptake of aerosol concentrations by scavenging. The moles of NO_3^- and SO_4^{2-} in rain were found to be the most enhanced in rain due to the high ability of acidic precursors to enter precipitation. Hence at higher rain rates, a high abundance and absolute amount of NO_3^- and SO_4^{2-} in rain and consequently a

highly acidic pH is observed. Therefore, during the monsoon, more acidic rain pH is found in Arizona. In addition, as the aerosol concentrations of dust and precursors of NO_3^- and SO_4^{2-} increase, the rain water pH will continue to increase in acidity, posing a future threat to the ecosystems found in Arizona. However, from 1999 to 2014 in Chiricahua and the Grand Canyon, decreases in SO_4^{2-} aerosol concentrations (most likely due to air regulations) has coincided with an increase in rain alkalinity.

7. Limitations and Future Work

In this study, the correlation between aerosol and rain data was to be used to deduce the composition of the cloud seeds during the monsoon in Arizona. There is a limitation to this where the aerosol data used in this study reports concentrations in the fine mode fraction. Based on previous work, the main condition for an aerosol to serve as a cloud seed is size (Conant et al., 2004; Dusek et al., 2006; Ervens et al., 2007). Hence, it is necessary to use aerosol data that are found in greater size modes and compare these results to the relationships in this study. Another limitation is that the air mass sources that influenced the sites were not determined. It is speculated that air mass source can greatly affect the relationships reported in this work since previous work such as Hutchings et al. (2009) has conducted precipitation studies coupled with long range transport models. The statistical test used within this method can also influence the results. However, in this study the Mann-Kendall test (a non-parametric test) was used to compare the results in Sections 4.1.1 by the student's t-test (95 % confidence) and similar findings were found with a few exceptions (Appendix Table 1).

Future work can consist of re-doing this kind of study by using aerosol concentrations reported for higher size modes. In addition, further work can be conducted to evaluate the effect of air mass source on aerosol and rain chemistry and relationships. A co-located NADP and IMPROVE site can be selected in New Mexico that is affected by the North American Monsoon and its aerosol and rain data can be compared to Organ Pipe.

APPENDIX- SUPPLEMENTARY DATA

Appendix Table 1: This table shows the results of the Mann-Kendall test (95% confidence) between year and aerosol data for Chiricahua National Monument (Chir NM), Grand Canyon, Organ Pipe National Monument (Organ Pipe NM), and Petrified National Park (Pet NP). Aerosol data includes aerosol concentrations and fractions. Values are shown when significant (less than 0.05) and the sample range is shown in parentheses. Aerosol concentrations are noted as coarse mass (CM), PM_{10} (MT), $PM_{2.5}$ (MF), fine soil (SOILf), calcium (Ca), chloride (Cl), magnesium (Mg), potassium (K), sodium (Na), sulfate (SO_4), and nitrate (NO_3). Aerosol mass fractions are noted as Ca frac, Cl frac, Mg frac, K frac, Na frac, SO_4 frac, and NO_3 frac.

	Annual Correlations- Aerosol Data- Mann Kendall test			
	Chir NM	Grand Canyon	Organ Pipe NM	Pet NP
CM	-	-	-	-
MT	-	-	-	-
MF	-	-	-	-
SOILf	-	-	-	-
Ca	-	-	-	-
Cl	-	-	-	-
Mg	-	-	-	-
K	-	-	-	-
Na	-	0.4440 (16)	-	0.0112 (12)
SO_4	0.0428 (16)	0.02738 (16)	-	-
NO_3	-	-	-	0.01117 (12)
Ca frac	-	-	-	-
Cl frac	-	-	-	-
Mg frac	-	-	-	-
K frac	-	-	-	-
Na frac	-	0.0103 (16)	-	0.02364 (12)
SO_4 frac	-	-	-	-
NO_3 frac	-	-	-	-

Appendix Table 2: This table shows the correlation (r-values) for interrelationships between amount of moles in rain in Chiricahua National Monument (Chir NM). The data ranged from 1999-2014.

Amount of moles in rain are noted as Rain Ca-moles, Rain Cl-moles, Rain Mg-moles, Rain K-moles, Rain Na-moles, Rain SO_4-moles, and Rain NO_3-moles. Total-moles corresponds to the sum of all moles in rain. Values are only shown when statistically significant with respect to a two-tailed student's t-test (95% confidence). The values in parentheses indicate the sample range.

	Moles in Rain Interrelationships- Chiricahua NM									
	Rain Conductivity	Rain pH	Rain Ca-moles	Rain Cl-moles	Rain Mg-moles	Rain K-moles	Rain Na-moles	Rain SO_4-moles	Rain NO_3-moles	Total-moles
Rain Conductivity	1.00	-	-	-0.18 (154)	-	-0.16 (154)	-	-0.21 (154)	-0.23 (154)	-0.22 (154)
Rain pH		1.00	0.51 (153)	-	0.47 (154)	0.23 (154)	0.22 (154)	-	-	0.20 (154)
Rain Ca- moles			1.00	0.37 (154)	0.92 (154)	0.41 (154)	0.43 (154)	0.64 (154)	0.65 (154)	0.74 (154)
Rain Cl- moles				1.00	0.46 (154)	0.87 (154)	0.93 (154)	0.58 (154)	0.59 (154)	0.67 (154)
Rain Mg- moles					1.00	0.44 (154)	0.54 (154)	0.70 (154)	0.75 (154)	0.82 (154)
Rain K- moles						1.00	0.85 (154)	0.41 (154)	0.42 (154)	0.52 (154)
Rain Na- moles							1.00	0.53 (154)	0.55 (154)	0.64 (154)
Rain SO_4- moles								1.00	0.89 (154)	0.94 (154)
Rain NO_3- moles									1.00	0.98 (154)
Total- moles										1.00

Appendix Table 3: This table shows the correlation (r-values) for interrelationships between amount of moles in rain for Grand Canyon. The data ranged from 1999-2014. Amount of moles in rain are noted as Rain Ca-moles, Rain Cl-moles, Rain Mg-moles, Rain K-moles, Rain Na-moles, Rain SO_4-moles, and Rain NO_3-moles. Total-moles corresponds to the sum of all moles in rain. Values are only shown when statistically significant with respect to a two-tailed student's t-test (95% confidence). The values in parentheses indicate the sample range.

	Moles in Rain Interrelationships- Grand Canyon									
	Rain Conductivity	Rain pH	Rain Ca-moles	Rain Cl-moles	Rain Mg-moles	Rain K-moles	Rain Na-moles	Rain SO_4-moles	Rain NO_3-moles	Total-moles
Rain Conductivity	1.00	-	-	-	-	-	-	-	-	-
Rain pH		1.00	0.27 (118)	-	0.24 (119)	0.26 (119)	0.22 (118)	-	-	-
Rain Ca- moles			1.00	0.89 (119)	0.97 (119)	0.92 (119)	0.81 (118)	0.86 (119)	0.86 (119)	0.94 (119)
Rain Cl- moles				1.00	0.89 (119)	0.88 (119)	0.97 (118)	0.87 (119)	0.86 (119)	0.91 (119)
Rain Mg- moles					1.00	0.90 (119)	0.81 (118)	0.83 (119)	0.88 (119)	0.92 (119)
Rain K- moles						1.00	0.80 (118)	0.84 (119)	0.85 (119)	0.89 (119)
Rain Na- moles							1.00	0.78 (119)	0.76 (119)	0.82 (119)
Rain SO_4- moles								1.00	0.94 (119)	0.96 (119)
Rain NO_3- moles									1.00	0.99 (119)
Total- moles										1.00

Appendix Table 4: This table shows the correlation (r-values) for interrelationships between amount of moles in rain for Organ Pipe National Monument (Organ Pipe NM). The data ranged from 2003-2014. Amount of moles in rain are noted as Rain Ca-moles, Rain Cl-moles, Rain Mg-moles, Rain K-moles, Rain Na-moles, Rain SO_4-moles, and Rain NO_3-moles. Total-moles corresponds to the sum of all moles in rain. Values are only shown when statistically significant with respect to a two-tailed student's t-test (95% confidence). The values in parentheses indicate the sample range.

	Moles in Rain Interrelationships- Organ Pipe NM									
	Rain Conductivity	Rain pH	Rain Ca-moles	Rain Cl-moles	Rain Mg-moles	Rain K-moles	Rain Na-moles	Rain SO_4-moles	Rain NO_3-moles	Total-moles
Rain Conductivity	1.00	-	-	-0.28 (69)	-	-	-0.25 (70)	-0.31(70)	-0.28 (70)	-0.29 (70)
Rain pH	-	1.00	0.46 (70)	0.25 (69)	0.40 (70)	0.30 (70)	0.24 (70)	-	0.30 (70)	0.31 (70)
Rain Ca- moles			1.00	0.54 (69)	0.92 (70)	0.49 (70)	0.48 (70)	0.74 (70)	0.69 (70)	0.78 (70)
Rain Cl- moles				1.00	0.54 (70)	0.78 (70)	0.98 (70)	0.70 (70)	0.67 (70)	0.80 (70)
Rain Mg- moles					1.00	0.61 (70)	0.70 (70)	0.80 (70)	0.68 (70)	0.83 (70)
Rain K- moles						1.00	0.86 (70)	0.63 (70)	0.61 (70)	0.72 (70)
Rain Na- moles							1.00	0.67 (70)	0.63 (70)	0.78 (70)
Rain SO_4- moles								1.00	0.85 (70)	0.94 (70)
Rain NO_3- moles									1.00	0.96 (70)
Total- moles										1.00

Appendix Table 5: This table shows the correlation (r-values) for interrelationships between amount of moles in rain for Petrified National Park (Petrified NP). The data ranged from 2003-2014. Amount of moles in rain are noted as Rain Ca-moles, Rain Cl-moles, Rain Mg-moles, Rain K-moles, Rain Na-moles, Rain SO_4-moles, and Rain NO_3-moles. Total-moles corresponds to the sum of all moles in rain. Values are only shown when statistically significant with respect to a two-tailed student's t-test (95% confidence). The values in parentheses indicate the sample range.

	Moles in Rain Interrelationships- Pet NP									
	Rain Conductivity	Rain pH	Rain Ca-moles	Rain Cl-moles	Rain Mg-moles	Rain K-moles	Rain Na-moles	Rain SO_4-moles	Rain NO_3-moles	Total-moles
Rain Conductivity	1.00	-	-	-	-	-	-	-	-	-
Rain pH	-	1.00	0.42 (93)	0.25 (93)	0.44 (93)	0.40 (92)	0.29 (93)	-	-	0.21 (93)
Rain Ca- moles			1.00	0.58 (93)	0.94 (93)	0.79 (92)	0.61 (93)	0.76 (93)	0.80 (93)	0.90 (93)
Rain Cl- moles				1.00	0.69 (93)	0.60 (93)	0.99 (93)	0.46 (93)	0.45 (93)	0.58 (93)
Rain Mg- moles					1.00	0.75 (93)	0.71 (93)	0.68 (93)	0.73 (93)	0.83 (93)
Rain K- moles						1.00	0.63 (93)	0.66 (93)	0.64 (93)	0.75 (93)
Rain Na- moles							1.00	0.44 (93)	0.44 (93)	0.57 (93)
Rain SO_4- moles								1.00	0.92 (93)	0.95 (93)
Rain NO_3- moles									1.00	0.97 (93)
Total- moles										1.00

REFERENCES

1. Aciego, S.M.; Riebe, C.S.; Hart, S.C.; Blakowski, M.A.; Carey, C.J.; Aarons, S.M.; Dove, N.C.; Botthoff, J.K.; Sims, K.W.; Aronson, E.L. 2017. Dust outpaces bedrock in nutrient supply to montane forest ecosystems. Natural Communications.
2. *Adams, D. K.; Comrie, A. C.; The north American monsoon. American Meteorological Society. 1997.*
3. Adams, J. L., & Stensrud, D. J. (2007). Impact of tropical easterly waves on the North American monsoon. Journal of Climate, 20(7), 1219–1238. https://doi.org/10.1175/JCLI4071.1
4. American Lung Association Ranking. Available online:http://www.stateoftheair.org/2015/city-rankings/most-polluted-cities.html.
5. Anderson, B. T., Roads, J. O., Chen, S. C., & Juang, H. M. H. (2001). Model dynamics of summertime low-level jets over northwestern Mexico. Journal of Geophysical Research, 106(D4), 3401–3413.
6. Barlow, M., Nigam, S., & Berbery, E. H. (1998). Evolution of the North American monsoon system. Journal of Climate, 11(9), 2238–2257.
7. Baron, J. S., Rueth, H. M., Wolfe, A. M., Nydick, K. R., Allstott, E. J., Minear, J. T., and Moraska, B.: Ecosystem responses to nitrogen deposition in the Colorado Front Range, Ecosystems, 3, 352–368, 2000.
8. Basak, B. and Alagha, O.: The chemical composition of rainwater over Buyukcekmece Lake, Istanbul, Atmos. Res., 71, 275–288, 2004.
9. Carleton, A. M., Carpenter, D. A., & Weser, P. J. (1990). Mechanisms of interannual variability of the southwest United States summer rainfall maximum. Journal of Climate, 3(9), 999–1015.
10. Cayan, D. R., T. Das, D. W. Pierce, T. P. Barnett, M. Tyree, and A. Gershunov (2010), Future dryness in the southwest US and the hydrology of the early 21st century drought, P. Natl. Acad. Sci. USA, 107(50), 21271-21276.
11. Chow, J.C., Lowenthal, D.H., Chen, L.W.A., Wang, X.L., Watson, J.G., 2015. Mass reconstruction methods for PM2.5: a review. Air Qual. Atmos. Health 8, 243–263.
12. Conant, W. C., VanReken, T. M., Rissman, T. A., Varutbangkul, V., Jonsson, H. H., Nenes, A., Jimenez, J. L., Delia, A. E., Bahreini, R., Roberts, G. C., Flagan, R. C., and Seinfeld, J. H.: Aerosolcloud drop concentration closure in warm cumulus, J. Geophys. Res. 109, D13204
13. Crosbie E, Youn JS, Balch B, Wonaschütz A, Shingler T, Wang Z, Conant W, Betterton E, Sorooshian A. On the competition among aerosol number, size and composition in predicting CCN variability: A multi-annual field study in an urbanized desert. Atmos Chem Phys. 2015;15:6943–6958.
14. Csavina, J.; Field, J.; Taylor, M. P.; Gao, S.; Landazuri, A.; Betterton, E. A.; Saez, A. E. A review on the importance of metals and metalloids in atmospheric dust and aerosol from mining operations. Sci. Total Environ. 2012, 433, 58−73.

15. Dadashazar, H., Ma, L., Sorooshian, A., 2019. Sources of pollution and interrelationships between aerosol and precipitation chemistry at a central California site. Sci. Total Environ. 651, 1776–1787
16. DeMott, P.J., D.J. Cziczo, A. J. Prenni, D. M. Murphy, S. M. Kreidenweis, D. S. Thomson, R. Borys, and D.C. Rogers, 2003: Measurements of the concentration and composition of nuclei for cirrus formation. Proceedings of the Nat. Academy of Sciences, 100, No. 25, 14655-14660.
17. Dennison PE, Brewer SC, Arnold JD, Moritz MA. Large wildfire trends in the western United States, 1984–2011. Geophys Res Lett. 2014;41:2928–2933.
18. Diem, J. E. (2000), Comparisons of weekday-weekend ozone: Importance of biogenic volatile organic compound emissions in the semi-arid southwest USA, *Atmos. Environ.*, 34(20), 3445–3451.
19. Diem, J. E., and A. C. Comrie (2000), Integrating remote sensing and local vegetation information for a high-resolution biogenic emissions inventory—Application to an urbanized, semiarid region, *J. Air Waste Manage.*, 50(11), 1968–1979.
20. Dominguez, F., Kumar, P., & Vivoni, E. R. (2008). Precipitation recycling variability and ecoclimatological stability—A study using NARR data. Part II: North American Monsoon region. Journal of Climate, 21(20), 5187–5203. https://doi.org/10.1175/2008JCLI1760.1
21. Dong, C. Y.; Taylor, M. P.; Kristensen, L. J.; Zahran, S. Environmental contamination in an Australian mining community and potential influences on early childhood health and behavioural outcomes. Environ. Pollut. 2015, 207, 345−356.
22. Douglas MW, Maddox RA, Howard K, Reyes S. The Mexican monsoon. J Clim. 1993,6:1665–1677.
23. Douglas, M. W. (1995). The summertime low-level jet over the Gulf of California. Monthly Weather Review, 123(8), 2334–2347.
24. Douglas, M. W., Valdez-Manzanilla, A., & Garcia Cueto, R. (1998). Diurnal variation and horizontal extent of the low-level jet over the northern Gulf of California. Monthly Weather Review, 126(7), 2017–2025.
25. Douglas, M. W., & Leal, J. C. (2003). Summertime surges over the Gulf of California: Aspects of their climatology, mean structure, and evolution from radiosonde, NCEP reanalysis, and rainfall data. Weather and Forecasting, 18(1), 55–74.
26. Draxler, R. R., and G. D. Hess (1997), Description of the HYSPLIT4 modeling system,
27. Draxler, R. R., and G. D. Hess (1998), An Overview of the HYSPLIT_4 Modelling System for Trajectories, Dispersion, and Deposition, Aust. Meteorol. Mag., 47(June 1997), 295–308.
28. Draxler, R. R., B. Stunder, G. Rolph, A. Stein, and A. Taylor (2014), HYSPLIT4 User's Guide Version 4.9, 2009, (September).
29. Dusek, U., Frank, G. P., Hildebrandt, L., Curtius, J., Schneider, J., Walter, S., Chand, D., Drewnick, F., Hings, S., Jung, D., Borrmann, S., and Andreae, M. O.: Size matters more than chemistry for cloud-nucleating ability of aerosol particles, Science, 312, 1375–1378.

30. Erfani, E., & Mitchell, D. (2014). A partial mechanistic understanding of the North American monsoon. Journal of Geophysical Research: Atmospheres, 119, 13,096–13,115. https://doi.org/10.1002/2014JD022038
31. Eger A, Almond PC, Condron LM (2013) Phosphorus fertilisation by active dust deposition in a super-humid, temperate environment–soil phosphorus fractionation and accession processes. Global Biogeochem Cycles
32. Ervens, B., Cubison, M., Andrews, E., Feingold, G., Ogren, J. A., Jimenez, J. L., DeCarlo, P., and Nenes, A.: Prediction of cloud condensation nucleus number concentration using measurements of aerosol size distributions and composition and light scattering enhancement due to humidity, J. Geophys. Res., 112, D10S32, doi:10.1029/2006jd007426, 2007.
33. Fan, Song-Miao, Larry W. Horowitz, Hiram Levy II, and Walter J. Moxim, 2004: Impact of air pollution on wet deposition of mineral dust aerosols. Geophys. Res. Let., 31, L02104, doi:10.1029/2003GL018501.
34. Fernandez DP, Neff JC, Reynolds RL. Biogeochemical and ecological impacts of livestock grazing in semi-arid southeastern Utah, USA. J. Arid. Environ. 2008;72:777–791.
35. Fenn, M. E., Poth, M. A., Aber, J. D., Baron, J. S., Bormann, B. T., Johnson, D. W., Lemly, A. D., McNulty, S. G., Ryan, D. E., and Stottlemyer, R.: Nitrogen excess in North American ecosystems: Predisposing factors, ecosystem responses, and management strategies, Ecol. Appl., 8, 706–733, 1998
36. Field JP, Belnap J, Breshears DD, Neff JC, Okins GS, Whickers JJ, Painter TH, Ravis S, Reheis MC, Reynolds RL. The ecology of dust. Front Ecol Environ. 2010;8:423–430. doi: 10.1890/090050.
37. Gochis D.J., Shuttleworth W.J., Yang Z.L. Sensitivity of the modeled North American monsoon regional climate to convective parameterization. Mon Weather Rev. 2002;130:1282–1298.
38. Guenther, A., T. Karl, P. Harley, C. Wiedinmeyer, P. I. Palmer, and C. Geron (2006), Estimates of global terrestrial isoprene emissions using MEGAN (Model of Emissions of Gases and Aerosols from Nature), *Atmos. Chem. Phys.*, 6, 3181–3210.
39. Harpold, A., Brooks, P., Rajagopal, S., Heidbuchel, I., Jardine, A., and Stielstra, C.: Changes in snowpack accumulation and ablation in the intermountain west, Water Resour. Res., 48, W11501, doi:10.1029/2012wr011949, 2012.
40. Heintzenberg, J., Okada, K., and Strom, J.: On the composition of non-volatile material in upper tropospheric aerosols and cirrus crystals, Atmos. Res., 41, 81–88, 1996
41. Higgins, R. W., Yao, Y., & Wang, X. L. (1997). Influence of the North American monsoon system on the US summer precipitation regime. Journal of Climate, 10(10), 2600–2622.
42. Higgins, R. W., Mo, K. C., & Yao, Y. (1998). Interannual variability of the US summer precipitation regime with emphasis on the southwestern monsoon. Journal of Climate, 11(10), 2582–2606.

43. Higgins, R. W., Chen, Y., & Douglas, a. V. (1999). Interannual variability of the North American warm season precipitation regime. Journal of Climate, 12(3), 653–680.
44. Hutchings, J. W., Robinson, M. S., McIlwraith, H., Kingston, J. T., and Herckes, P.: The chemistry of intercepted clouds in northern Arizona during the North American Monsoon Season, Water Air Soil Poll., 199, 191–202, 2009.
45. Intergovernmental Panel on Climate Change (IPCC) (2013), Climate Change 2013: The Physical Science Basis. Contribution of Working Group I to the Fifth Assessment Report of the Intergovernmental Panel on Climate Change, edited by T. F. Stocker et al., Cambridge Univ. Press, Cambridge, U. K., and New York.
46. Isono K, Ikebe Y. On the ice-nucleating ability of rock-forming minerals and soil particles. J. Meteorol. Soc. Jpn. 1960;38:213–230.
47. Jana, S., Rajagopalan, B., Alexander, M. A., and Ray, A. J.: Understanding the dominant sources and tracks of moisture for summer rainfall in the southwest United States, J. Geophys. Res.-Atmos, 123, 4850–4870, 2018.
48. Karydis, V. A., Tsimpidi, A. P., Pozzer, A., Astitha, M., and Lelieveld, J.: Effects of mineral dust on global atmospheric nitrate concentrations, Atmos. Chem. Phys., 16, 1491–1509, doi:10.5194/acp-16-1491-2016, 2016.
49. Koehler, K. A., Kreidenweis, S. M., DeMott, P. J., Prenni, A. J., and Petters, M. D.: Potential impact of Owens (dry) Lake dust on warm and cold cloud formation, J. Geophys. Res., 112, D12210, doi:10.1029/2007jd008413, 2007.
50. Kumai M. Snow crystals and the identification of the nuclei in the northern United-States of America. J. Meteorol. 1961;18:139–150.
51. Kvaalen, H., Solberg, S., Clarke, N., Torp, T., & Aamlid, D. (2002). Time series study of concentrations of SO_{2-4} SO_4^{2-} and H^+ in precipitation and soil waters in Norway. *Environmental Pollution, 117*, 215–224.
52. Lamb, D., Bowersox, V., 2000. The national atmospheric deposition program: an overview. Atmos. Environ. 34, 1661–1663.
53. Lee, T., Kreidenweis, S. M., and Collett, J. L.: Aerosol ion characteristics during the Big Bend Regional Aerosol and Visibility Observational Study, J. Air Waste Manage., 54, 585–592, 2004.
54. Lee, T., Yu, X. Y., Ayres, B., Kreidenweis, S. M., Malm, W. C., and Collett, J. L.: Observations of fine and coarse particle nitrate at several rural locations in the United States, Atmos. Environ., 42, 2720–2732, 2008
55. Leinen M, Sarnthein M. Paleoclimatology and Paleometeorology: Modern and Past Patterns of Global Atmospheric Transport. Kluwer; Dordrencht, Netherlands: 1989.
56. Levin, Zev, Eliezer Ganor, and Victor Gladstein, 1996: The effects of desert particles coated with sulfate on rain formation in the eastern Mediterranean. J. App. Meteor., 35, 1511-1524

57. Leung, L. R., Qian, Y., & Bian, X. (2003). Hydroclimate of the western United States based on observations and regional climate simulation of 1981–2000. Part I: Seasonal statistics. Journal of Climate, 16(12), 1892–1911.
58. Lopez, D. H.*; Rabbani, M. R.; Crosbie, E.; Raman, A.; Arellano, A.; Sorooshian, A.* Frequency and character of extreme aerosol events in the southwestern United States: A case study analysis in Arizona, Atmos. Basel, 7*(1)*,
59. Malm, W.C.; Sisler, J.F.; Huffman, D.; Eldred, R.A.; Cahill, T.A. Spatial and Seasonal Trends in Particle Concentration and Optical Extinction in the United-States. J. Geophys. Res. 1994, 99, 1347–1370.
60. Malm WC, Sisler JF. Spatial patterns of major aerosol species and selected heavy metals in the United States. Fuel Process Technol. 2000;65–66:473–501.
61. Malm, W. C., Schichtel, B. A., Pitchford, M. L., Ashbaugh, L. L., and Eldred, R. A.: Spatial and monthly trends in speciated fine particle concentration in the United States, J. Geophys. Res., 109, D03306, doi:10.1029/2003jd003739, 2004
62. Matsuki, A., Schwarzenboeck, A., Venzac, H., Laj, P., Crumeyrolle, S., and Gomes, L.: Cloud processing of mineral dust: direct comparison of cloud residual and clear sky particles during AMMA aircraft campaign in summer 2006, Atmos. Chem. Phys., 10, 1057–1069, doi:10.5194/acp-10-1057-2010, 2010.
63. Mejia, J. F., Douglas, M. W., & Lamb, P. J. (2010). Aircraft observations of the 12–15 July 2004 moisture surge event during the North American Monsoon Experiment. Monthly Weather Review, 138(9), 3498–3513.
64. Minoura, H. and Iwasaka, Y. (1996) Rapid change in nitrate and sulphate concentrations observed in early stage of precipitation and their deposition processes. Journal of Atmospheric Chemistry 24, 39—55.
65. National Atmospheric Deposition Program (2012a). NTN Sample Changeout, Aerochem Metrics Bucket Collector, 2012–12 version 1.1. Retrieved from http://nadp.slh.wisc.edu/lib/manuals/NTN_Sample_Changeout_ACM_v_1–1.pdf
66. National Atmospheric Deposition Program (2012b). NTN bag sampling preparation SOP, 2012–06, Version 1.13. Retrieved from http://nadp.slh.wisc.edu/lib/manuals/NTN_bag_sampling_v_1–13.pdf
67. National Atmospheric Deposition Program (2012c). Quality assurance report, May 2014. Retrieved from http://nadp.slh.wisc.edu/lib/qa/cal_qar_2012.pdf
68. National Atmospheric Deposition Program (2013). Sample decanting SOP, NTN, 2013–05, version 1.7. Retrieved from http://nadp.slh.wisc.edu/lib/manuals/NTN_Sample_Decanting_v_1–7.pdf
69. NADP, 2014. Quality Assurance Plan - Central Analytical Laboratory, NADP QA Plan 2014- 01, Version 7. http://nadp.sws.uiuc.edu/lib/qaPlans/qapCal2014.pdf

70. National Atmospheric Deposition Program (2014a). Standard operating procedure for the determination of sample filtration for the NTN,2014-10, Revision 16.
71. National Atmospheric Deposition Program (2014b). Description of parameters included in NADP/NTN report of precipitation-weighted means, 2014–07. Retrieved from http://nadp.slh.wisc.edu/documentation/notes-AvMg.html
72. National Atmospheric Deposition Program (2017). National Trends Network site operations manual. Retrieved from http://nadp.slh.wisc.edu/lib/manuals/NTN_Operations_Manual_v2–4.pdf
73. Neff JC, Reynolds RL, Belnap J, Lamothe P. Multi-decadal impacts of grazing on soil physical and biogeochemical properties in southeast Utah. Ecol. Appl. 2005;15:87–95.
74. Neff JC, Ballantyne AP, Farmer GL, Mahowald NM, Conroy JL, Landry CC, Overpeck JT, Painter TH, Lawrence CR, Reynolds RL. Increasing eolian dust deposition in the western United States linked to human activity. Nat. Geosci. 2008;1:189–195.
75. Nilles, M. A., & Conley, B. E. (2001). Changes in the chemistry of precipitation in the United States, 1981–1998. *Water, Air and Soil Pollution, 130*, 409–414.
76. Okabe, I. T. (1995). The North American monsoon (Doctoral dissertation, University of British Columbia).
77. Ordoñez, P., Nieto, R., Gimeno, L., Ribera, P., Gallego, D., Ochoa-Moya, C. A., & Quintanar, A. I. (2019). Climatological moisture sources for the Western North American Monsoon through a Lagrangian approach: Their influence on precipitation intensity. *Earth System Dynamics,10*(1), 59-72.
78. Park R. J.; Jacob, D. J.; Field, B. D.; Yantosca, R. M.; Chin, M. Natural and transboundary pollution influences on sulfate-nitrate-ammonium aerosols in the United States: Implications for policy. J. Geophys Atmospheres. 2004, 109.
79. Perry, Kevin D., Steven S. Cliff, and Michael P. Jimenez-Cruz, 2004: Evidence for hygroscopic mineral dust particles from the Intercontinental Transport and Chemical Transformation Experiment. J. Geophys. Res., 109, D23S28
80. Ponette-González, A.G., Collins, J.D., Manuel, J.E., Byers, T.A., Glass, G.A., Weathers, K.C., Gill, T.E., 2018. Wet dust deposition during the 2012 US drought: an overlooked path- way for elemental flux to ecosystems. J. Geophys. Res.-Atmos. 123, 8238–8254.
81. Prabhakar, G.; Sorooshian, A.; Toffol, E.; Arellano, A. F.; Betterton, E. A. Spatiotemporal distribution of airborne particulate metals and metalloids in a populated arid region. Atmos. Environ. 2014, 92, 339−347.
82. Raman A, Arellano AF, Brost JJ. Revisiting haboobs in the southwestern United States: An observational case study of the 5 July 2011 Phoenix dust storm. Atmos Environ. 2014;89:179–188.
83. Raman, A., Arellano AF and Sorooshian, A., (2016), Decreasing Aerosol Loading in the North American Monsoon Region, *Atmosphere, 7*, 24,

84. Rosenfeld, D. and Givati, A.: Evidence of orographic precipitation suppression by air pollution-induced aerosols in the western United States, J. Appl. Meteorol. Clim., 45, 893–911, 2006
85. Seager, R., et al. (2007), Model projections of an imminent transition to a more arid climate in southwestern North America, Science, 316(5828), 1181-1184.
86. Seager, R. and Vecchi, G. A.: Greenhouse warming and the 21st century hydroclimate of southwestern North America, P. Natl. Acad. Sci. USA, 107, 21277–21282, doi:10.1073/pnas.0910856107, 2010.
87. Schlesinger WH, Reynolds JF, Cunningham GL, Huenneke LF, Jarrell WM, Virginia RA, Whitford WG. Science. 1990 Mar 2; 247(4946):1043-8.
88. Schlosser, J.S., Braun, R.A., Bradley, T., Dadashazar, H., MacDonald, A.B., Aldhaif, A.A., et al., 2017. Analysis of aerosol composition data for western United States wildfires be- tween 2005 and 2015: dust emissions, chloride depletion, and most enhanced aerosol constituents. J. Geophys. Res.-Atmos. 122, 8951–8966.
89. Sheppard, P. R., Comrie, A. C., Packin, G. D., Angersbach, K., & Hughes, M. K. (2002). The climate of the US Southwest. Climate Research, 21(3), 219–238.
90. Sicard, P., Coddeville, P., Sauvage, S., & Galloo, J. C. (2007). Trends in chemical composition of wet-only precipitation at rural French monitoring stations over the 1990–2003 period. Water, Air and Soil Pollution: Focus, 7(1–3), 49–58.
91. Solomon, P.A., Crumpler, D., Flanagan, J.B., Jayanty, R.K.M., Rickman, E.E., McDade, C.E., 2014. US National $PM_{2.5}$ Chemical Speciation Monitoring Networks-CSN and IMPROVE: description of networks. J. Air Waste Manage. Assoc. 64, 1410–1438.
92. Sorooshian, A., Wonaschutz, A., Jarjour, E. G., Hashimoto, B. I., ¨ Schichtel, B. A., and Betterton, E. A.: An aerosol climatology for a rapidly growing arid region (southern Arizona): Major aerosol species and remotely sensed aerosol properties, J. Geophys. Res., 116, 19205, doi:10.1029/2011jd016197, 2011.
93. Sorooshian, A.; Shingler, T.; Harpold, A.; Feagles, C. W.; Meixner, T.; Brooks, P. D. Aerosol and precipitation chemistry in the southwestern United States: spatiotemporal trends and interrelationships. *Atmos. Chem. Phys.* 2013, *13*, (15), 7361-7379.
94. Stein, A.F., Draxler, R.R, Rolph, G.D., Stunder, B.J.B., Cohen, M.D., and Ngan, F., (2015). NOAA's HYSPLIT atmospheric transport and dispersion modeling system, Bull. Amer. Meteor. Soc., 96, 2059-2077
95. Stensrud, D. J., Gall, R. L., & Nordquist, M. K. (1997). Surges over the Gulf of California during the Mexican monsoon. Monthly Weather Review, 125(4), 417–437.
96. Taylor, M. P.; Mould, S. A.; Kristensen, L. J.; Rouillon, M. Environmental arsenic, cadmium and lead dust emissions from metal mine operations: Implications for environmental management, monitoring and human health. Environ. Res. 2014, 135, 296−303.

97. Teixeira, E. C., Migliavacca, D., Pereira, S., Machado, A. C. M., and Dallarosa, J. B.: Study of wet precipitation and its chemical composition in South of Brazil, An. Acad. Bras. Cienc., 80, 381– 395, 2008.
98. Twohy, Cynthia H., Sonia M. Kreidenweis, Trude Eidhammer, Edward V. Browell, Andrew J. Heymsfield, Aaron R. Bansemer, Bruce E. Anderson, Gao Chen, Syed Ismail, Paul J. DeMott, and Susan C. Van Den Heever, 2009: Saharan dust particles nucleate droplets in eastern Atlantic clouds. Geophys. Res. Lett., 36, L01807.
99. Van den Heever, Susan C., Gustavo G. Carrio, William R. Cotton, Paul J. DeMott, and Anthony J. Prenni, 2006: Impacts of nucleating aerosol on Florida storms. Part I: Mesoscale simulations. J. Atmos. Sci, 63, 1752-1775
100. Vera, C., Higgins, W., Amador, J., Ambrizzi, T., Garreaud, R., Gochis, D., et al. (2006). Toward a unified view of the American monsoon systems. Journal of Climate, 19(20), 4977–5000.
101. Westerling AL, Bryant BP. Climate change and wildfire in California. Clim Chang. 2008;87:231–249.
102. Wiacek, A., T. Peter, and U. Lohmann, 2010: The potential influence of Asian and African mineral dust on ice, mixed-phase and liquid water clouds. Atmos. Chem. Phys. Discuss., 10, 4027–4077.
103. Wolfe AP, Van Gorp AC, Baron JS. Recent ecological and biogeochemical changes in alpine lakes of Rocky Mountain National Park (Colorado, USA): a response to anthropogenic nitrogen deposition. Geobiology. 2003;1:153–168.
104. Woodhouse CA, Mekob DM, MacDonald GM, Stahled DW, Cook ER. A 1,200-year perspective of 21st century drought in southwestern North America. Proc Natl Acad Sci U S A. 2010;107:21,283–21,288. doi: 10.1073/pnas.0911197107.
105. Youn JS, Wang Z, Wonaschutz A, Arellano A, Betterton EA, Sorooshian A. Evidence of aqueous secondary organic aerosol formation from biogenic emissions in the. North Am. Sonoran Desert. Geophys. Res. Lett. 2013;40:3468–3472.
106. Youn, J. S.; Csavina, J.; Rine, K. P.; Shingler, T.; Taylor, M. P.; Saez, A. E.; Betterton, E. A.; Sorooshian, A. Hygroscopic Properties and Respiratory System Deposition Behavior of Particulate Matter Emitted By Mining and Smelting Operations. Environ. Sci. Technol. 2016, 50 (21), 11706−11713.
107. Zhao Z, Pritchard MS, Russell LM. Effects on precipitation, clouds, and temperature from long-range transport of idealized aerosol plumes in WRF-Chem simulations. J Geophys Res Atmos. 2012:117
108. Zimmermann F, Weinbruch S, Schutz L, Hofmann H, Ebert M, Kandler K, Worringen A. Ice nucleation properties of the most abundant mineral dust phases. J. Geophys. Res. 2008;113:D23204. doi:10.1029/2008jd010655